Cell impedance of cancer cells: towards novel diagnostic and therapeutic selection methods

By Wei Duan

A thesis submitted for the degree of Master of Philosophy

School of Life Sciences

University of Sussex

January 2013

I hereby declare that this thesis has not been and will not be, submitted in whole or in part to another University for the award of any other degree.

Signature:…….

Acknowledgments

The most important, I would like to deeply and sincerely thank my first supervisor Professor Alison Sinclair for her extremely patient and professional supervision on my research, training me thinking and writing scientifically, correction of my thesis, encouraging me, helping me to bail out depression, and guidance on my future life. Thank her very much indeed for giving me this opportunity. I also need to thank Dr Wei Wang for his great support, funding my study, helping me to start over my new life in Brighton, and also providing me with the opportunity to work part-time as a clinic assistant in Oxford. I strongly appreciate Dr Helen Prance and Prof Chris Chatwin helping me to amend my thesis and give me many valuable academic advices on engineering. It is hard to finish my research without their support.

I am very grateful to Dr Guofeng Qiao for his collaboration on operating the cell impedance system, data acquisition and data analysis. Tremendous thanks to Dr Julian Thorpe for his great effort on taking TEM photos. He patiently taught me every step of preparation cells for TEM and he did the section and photographing. Thank Dr Questa Karlsson, Dr Kirsty Flower, Dr Natalie Braithwaite and Jamie Heather for helping me to fit in a totally different culture in both academia and life from the first day I was in the lab. I also would like to deeply thank Lina Chen for her remarkable friendship and support. My time in the lab would be less enjoyable without her. Thank you Nick Balan, Dr Kay Osborn, Dr Sharada Ramasubramanyan, Dr David Wood, Dr Andrea Gunnell, Dr Michelle West, Xiaolin Zhang, Dr Yang Song and Dr Guangfu Zhang for the support, advices, unforgettable lunchtimes, amazing dinners, yummy cakes and snacks, and also funny lab tricks.

Finally, I would like to say thank you to my parents, grandparents and my boyfriend Liang. I cannot imagine what my life would be without your endless love, missing, encouragement and support. Liang has relocated three times just for me. Thank you so much for everything you did for me. My landlady Mrs Patricia Norman also deserves my sincere thanks for concerning about me especially when I had illness.

UNIVERISTY OF SUSSEX

WEI DUAN MPhil BIOCHEMISTIRY

Cell impedance of cancer cells: towards novel diagnostic and therapeutic selection methods

Summary

Cancer is caused by genetic damage to DNA, this mutant cell then grows in an uncontrolled manner in the organism. Breast cancer is a one of most common cancers among women. Early detection of breast cancer is the most important way to reduce the mortality rate. Impedance measure is one of the methods for breast cancer detection.

Apoptosis is programmed cell death and plays an essential role in protection of both tissues and organisms. There are many ways to detect apoptosis such as flow cytometry of PI stained cells, caspase assays and impedance measurements.

The aim of this project is to use cell impedance system (CIS) to ask whether breast cancer cell lines and a normal breast cell line can be distinguished. Furthermore, whether cells undergoing apoptosis in response to the chemotherapy reagent Etoposide can be identified using CIS.

Table of Contents

List of Figures

List of Tables

List of Abbreviations

Ac-DEVD-AMC	(N-acetyl)-(Asp-Glu-Val-Asp)-(7-amino-4-methylcoumarin)
Apaf-1	Apoptotic protease activating factor 1
CARD	Caspase recruitment domains
Caspase	Cysteine-aspartic acid protease
CIS	Cell impedance system
CO_2	Carbon dioxide
CT	Computational tomography
DD	Death domains
DED	Death effector domains
DMEM	Dulbecco modified eagle's minimal essential medium
DMSO	Dimethyl sulphoxide
DNA	Deoxyribonucleic acid
DPBS	Dulbecco's phosphate buffered saline
DTT	Dithiothreitol
EDTA	Ethylene diamine tetraacetic acid
EIM	Electrical impedance mammography
EIT	Electrical impedance tomography
FACS	Fluorescent activated cell sorting
FBS	Foetal bovine serum
GF	Growth factor
MRI	Magnetic resonance imaging

NaCl	Sodium chloride
PCV	Packed cell volume
PDGF	Platelet-derived growth factor
PI	Propidium iodide
PO	Propylene oxide
pRb	Retinoblastoma protein
PSG	Penicillin streptomycin glutamine
RNA	Ribonucleic acid
RNase	Ribonuclease
RPMI	Roswell park memorial institute medium
TEM	Transmission electrode microscope
TNF	Tumour necrosis factor
v/v	Volume to volume
w/v	Weight to volume

List of Publication

Qiao, G., **Duan, W.**, Chatwin,C., Sinclair, A.J. and Wang, W. (2010) Electrical properties of breast cancer cells from impedance measurement of cell suspensions. *Journal of Physics: Conference Series* 224

Qiao, G., Wang, W., **Duan, W**., Zheng, F., Sinclair, A.J. and Chatwin, C. R. (2012). "Bioimpedance analysis for the characterization of breast cancer cells in suspension." *IEEE Trans Biomed Eng* 59(8): 2321-2329

1 Introduction

1.1 Cancer

Cancer arises from normal cells. It is an accumulation of genetic errors and genetic damages in cells (King, 2000). The cell's fate to develop cancer is dependent upon its exposure to DNA damaging factors, both endogenous (oxygen species *etc.*) and exogenous (X-rays, some chemicals and viruses *etc.*) and responses to DNA damage (Lutz and Fekete, 1996; Weinberg, 1998; Kastan and Bartek, 2004).

The possibility of tumour development is reduced by the efficient repair of DNA damage. However, genomic abnormalities will be increased by mutations in DNA-damage response and checkpoint signalling pathways. The DNA damages can make cells arrest or not to survive. But mutations in apoptosis pathway or cell-cycle checkpoints will allow cell division with the abnormal genes. This increases the cells proneness to cancer (Figure 1.1) (Kastan and Bartek, 2004). The six hallmarks in cell physiology that can generate malignant growth (Figure 1.2) will be discussed in detail in the following sections.

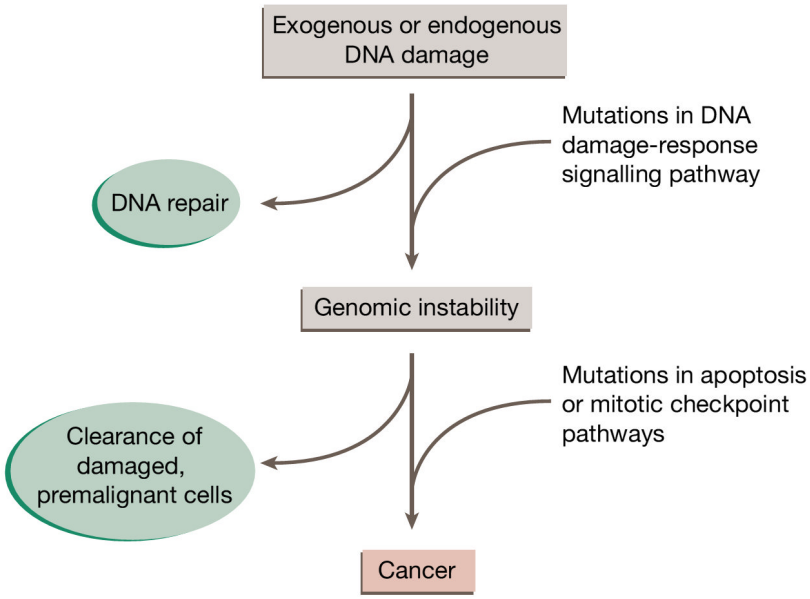

Figure 1.1 The progress of cancer development (Kastan and Bartek, 2004).

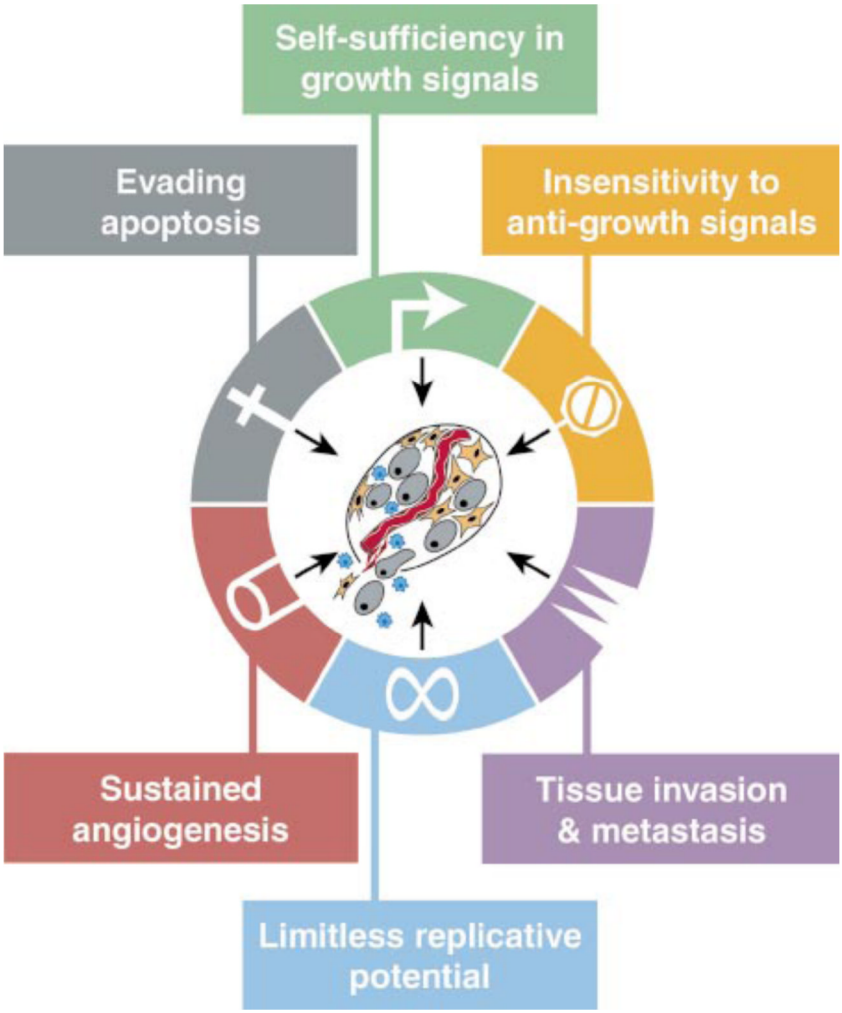

Figure 1.2 Six hallmarks of cancer (Hanahan and Weinberg, 2000).

1.1.1 Self-sufficiency in growth signals

Normal cells need mitogenic growth signals, and then they can go into a proliferative state from quiescence. Transmembrane receptors transmit these signals into the cell. Mitogenic growth signals bind a specific group of signalling molecules, which are growth factors, extracellular matrix components, and cell-to-cell interaction molecules (Figure 1.3). In contrast with normal cells, cancer cells are less dependent on exogenous growth signals (Hanahan and Weinberg, 2000) .

There are three common molecular strategies found in cancer that increase growth signals.

The change in extracellular growth signals: in normal cells, mitogenic growth factors are made by cells to stimulate surrounding cell growth. However, cancer cells are able to synthesize growth factors and response to these factors creating a positive feedback signalling loop (Fedi, 1997). The ability of manufacture of growth factors by cancer cells makes them less dependence on other surrounding cells. The glioblastomas can produce platelet-derived growth factor (PDGF) and sarcomas also are able to create tumour growth factor α,TGFα, which are evident (Fedi *et al.*, 1997).

The increase in transmembrane receptors: the transmembrane receptors on cell surface which transfer the growth signals into the cell are overexpressed in cancer cells. The receptor overexpression makes cancer cell very sensitive to the growth factors. Cancer cells are responsive to the low level of growth factors which would not trigger growth (Fedi, 1997). For example, the upregulation of the epidermal GF receptor (EGF-R/erbB) in breast and brain tumours have been identified (Slamon *et al.*, 1987; Yarden and Ullrich, 1988).

The changes of intracellular circuits which are responsible for signal transduction and action. The Ras proteins aid to transfer signals from outside to inside cells (Alberts, 2008). The structure of Ras proteins changes in about 25%-30% of human cancers. The mutated Ras proteins remain in a hyperactive state, which allows the mitogenic signals into cells without the stimulation by normal upstream regulators (Medema and Bos, 1993; Rowinsky *et al.*, 1999).

Therefore, cancer cells do not need to depend on mitogenic growth signals (Hanahan and Weinberg, 2000).

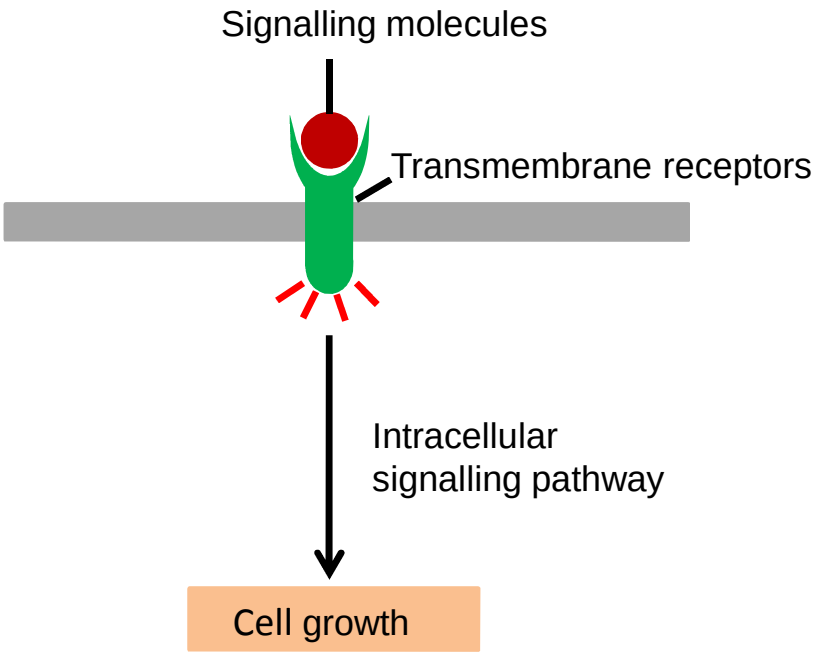

Figure 1.3 Transmembrane receptors transmit growth signals into the cell. Mitogenic growth signals bind a specific group of signalling molecules and result in cell growing (Alberts, 2010).

1.1.2 Insensitivity to antigrowth signals

The function of multiple antigrowth signals in a normal tissue is to keep cells in quiescence and tissue homeostasis. These signals contain both growth inhibitors and cell-to-cell communication inhibitors in the extracellular matrix and on the surface of surrounding cells. The transmembrane cell surface receptors receive these growth-inhibitory signals and couple to intracellular signalling circuits (Hanahan and Weinberg, 2000).

Antigrowth signals can stop cell proliferation in two ways. Cells are forced to withdraw from the active proliferative state in the cell cycle to the quiescence G_0 phase. Alternatively, cell are induced to stop proliferative potential permanently by being induced to move to postmitotic state (Hanahan and Weinberg, 2000). Cancer cells have to avoid the antiproliferative signals if they are to proliferate. The retinoblastoma protein (pRb) is missing in a children eye tumor, *Retinoblastoma* (Alberts, 2010). pRb is an cell cycle progress inhibitor (Alberts, 2002). E2F is a transcription factors governing the genes which are key to the progress from G1 to S phase of the cell cycle. In a

hypophosphorylated state, the pRb blocks cell growth by the function change of E2F (Weinberg, 1998). In cancer cells, pRb is missing (Alberts, 2002), which allows them going through the cell cycle inappropriately (Harrington, 2008).

1.1.3 Evading apoptosis

All cell types have the program of apoptosis in the form of latency. Cancer cell population expanding is determined not only by the rate of cell growth, but also the rate of cell death. Resistance to apoptosis is a hallmark of all type of cancer (Hanahan and Weinberg, 2000).

The Caspase (cysteine-aspartic acid protease) family has 14 members (Thornberry and Lazebnik, 1998), most of which contribute to apoptosis. The effectors and executors of apoptosis such as Caspases are present but not active. Once induced by some physiologic signals, the apoptotic program develops by following steps. Cellular membrane, nuclear skeletons and the chromosomes are all broken down and degraded. The nucleus is fragmented. Finally, the apoptotic body is engulfed by nearby cells and disappears (Wyllie *et al.*, 1980).

The machinery of apoptosis is divided into two types: the sensors and the effectors. The sensors are responsible for observing the extracellular and intracellular conditions which is normal or abnormal. This impacts whether a cell is going to survive or not. Many signals which induce apoptosis affect the mitochondria. Mitochondria respond to proapoptotic signals with the release of cytochrome C. The Bcl-2 family proteins function as either proapoptosis or antiapoptosis, which have an effect on the mitochondria death signalling by the cytochrome C release. When the DNA is damaged, the p53, the tumour suppressor protein, is able to induce apoptosis by upregulating expression of proapoptotic Bax. The Bax can stimulate the mitochondria to release the cytochrome C, which can consequently activate the effectors of apoptosis - Caspase 8 and 9 to co-operate with Caspase 3 leading apoptosis (Hanahan and Weinberg, 2000).

Apoptosis will be introduced in detail in the ‘1.3 Apoptosis’ section.

1.1.4 Limitless replicative potential

All types of mammalian cells have cell-autonomous programs, which can limit the multiplication. The cell-autonomous program works independently. Cells stop doubling when the population expand to a certain number. However, in cancer cells, this program is interrupted leading to a clone of cancer cells expanding oversize, which constitutes a macroscopic (Hanahan and Weinberg, 2000).

Generating growth signals, insensitivity to antigrowth signals, and resistance to apoptosis still cannot ensure vast cancer cells growth. Many of types of cancer cells are immortalized in culture, which means cancer cells acquired the limitless replicative potential *in vivo* during the proliferative progression. The limitless replicative potential is crucial for the development to the malignant state (Hayflick, 1997).

Furthermore, telomeres, thousands of repeats of a short 6bp sequence element, at the end of chromosomes play a role as a counter in the cell replication. During each phase of cell cycle, the 50-100bp of telomeric DNA is missing from the end of the chromosome, because the DNA polymerases are not able to entirely replicate the 3’ ends of DNA in S phase. Eventually, the telomeres cannot protect the end of DNA leading the end-to-end chromosomal fusions causing cell death (Counter *et al.*, 1992). However, cancer cells can upregulate expression of the telomerase to repair the telomeric DNA making the telomeres maintained at a certain length, which permit cancer cell limitless replication (Bryan *et al.*, 1995; Bryan and Cech, 1999).

1.1.5 Sustained angiogenesis

The vasculature is responsible to supply the oxygen and nutrients, which are very important to cell survival and function. The cells in a tissue are located in within 100μm of a capillary blood vessel. Normally, angiogenesis is transitory and under carefully control when a tissue has been formed (Bouck *et al.*, 1996; Hanahan and Folkman, 1996). Cancer cells must gain angiogenic ability which allows them to get adequate oxygen and nutrients to develop (Alberts, 2008).

1.1.6 Invasion and metastasis

Many types of human cancer cells can invade tissue and go to distant locations where they may establish new colonies. The metastasis of cancer cells causes 90% human cancer death (Sporn, 1996). Some cancer cells lack the cell-adhesion molecules. For example, cadherin , which is a protein mediating cell-cell adhesion and holding normal cells at the place where they should be (Alberts, 2010). So they can invade surrounding tissue and blood vessels. When the invasive cancer cells cross the blood stream and reach a new site, they escape from the vessels. At the new site, these cancer cells survive and proliferate, depending on the interaction with other five hallmark abilities (Hanahan and Weinberg, 2000; Alberts, 2008) (Figure 1.4).

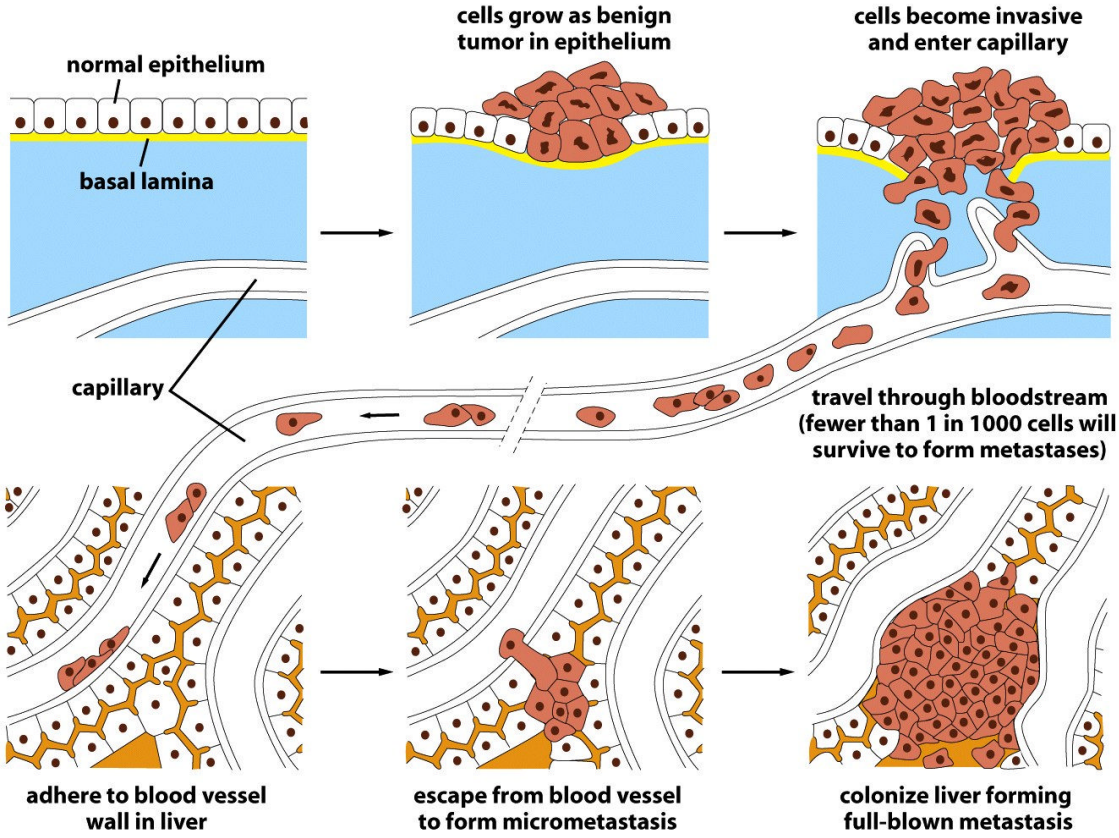

Figure 1.4 The process of cancer cells metastasis (Alberts, 2008).

1.2 Breast cancer and representative cell lines

The normal breast is composed of lobules, ducts and stroma. Most breast cancers start in the ducts or lobules (Sariego *et al.*, 1995).Breast cancer is one of the most common types of cancer of women in the world. In 2012, it is predictable that more than 39,920 of patients will die from breast cancer and there will be another 229,060 new cases in the US alone (Siegel *et al.*, 2012). The established risk factors of breast cancer are age, weight, childbearing and family *etc..* (Hoogstraten and McDivitt, 1981; Gibson *et al.*, 2010) There is no effective methods of avoiding breast cancer, but women can prevent the risk factors for breast cancer such as smoking, alcohol drinking, diet *etc.*. Women in high risk of breast cancer also can take medical or surgical preventive measures (Vogel, 2000).

The mortality rate of breast cancer can be reduced by early detection. At present, X-ray mammography is the most common technique used to detect breast cancer (Elmore *et al.*, 1998; Simonetti *et al.*, 1998). But, the limitations includes the reduced ability to detect cancer in a thick layer of breast tissue (Zou and Guo, 2003). Another two techniques, ultrasound and magnetic resonance imaging (MRI) also can be used to diagnose breast cancer. However, breast MRI is very expensive and cannot be used to diagnose the patient under a certain circumstances such as patient with a pacemaker (Edell and Eisen, 1999; NHS, 2011).

In this project, one type of human breast tissue cell line and two breast cancer cells are used. The MCF-10A cell line is human epithelial breast cell line. The MCF-7 is early-stage human breast adenocarcinoma cell line. The MDA-MB-231 cell line is invasive human breast adenocarcinoma cell line (Han *et al.*, 2007).

1.3 Apoptosis

Apoptosis defines the morphological progression leading to controlled cellular self-destruction (Kerr *et al.*, 1972). The word, apoptosis, is a Greek word meaning petals falling off from flowers and leaves dropping off from trees, which are no longer needed (Fadeel and Orrenius, 2005). Apoptosis is strictly

regulated program of cell death and plays a crucial role in the development and the maintenance of multicellular organisms or cell populations in tissues (Leist and Jaattela, 2001). Apoptosis is an established program in nearly all cells and can be induced by many internal and external factors (Fadeel and Orrenius, 2005).

1.3.1 Morphological features of apoptosis

Apoptotic cells have many morphological changes. As described in ‘Evading apoptosis’ section, the cell shrinking indicates deformation and loose contact to surrounding cells. The chromatin condenses along the nuclear membrane. The plasma membrane blebs occur. In the end, the cell is fragmented into apoptotic bodies containing cytosol. The neighbour cells engulf the apoptotic bodies (Saraste and Pulkki, 2000).

1.3.2 Molecular mechanisms of apoptosis

1.3.3 Death signals activate signalling pathways

Apoptosis requires the interaction of numbers of factors. The apoptotic signals encoded by genes are going to be activated by a death-inducing stimulus (Ishizaki *et al.*, 1995; Weil *et al.*, 1996). A lot of stimuli from intracellular or extracellular can trigger apoptosis such as, DNA damage due to faults in DNA repair mechanisms, cytotoxic treatments or radiation treatment, lacking of survival signals, or the death signal ligation of the cell surface receptor (Fadeel and Orrenius, 2005).

1.3.4 Caspases are central executioners of apoptosis

In cells, caspases are in the form of procaspases, which are inactive zymogens. The proapoptotic caspases is classified into two groups: initiator caspases such as procaspases-2, -8, -9 and -10, and executioner caspase such as procaspases-3, -6 and -7. The initiator caspases contain death effector domains (DED) for example procaspases -8 and -10, or caspase recruitment domains (CARD) such as procaspase-9 and procaspase-2 (Denault and

Salvesen, 2002). The activated initiator caspases are response to either extrinsic apoptosis pathways or intrinsic apoptosis pathways as below.

In extrinsic apoptosis pathways, the death-inducing stimuli from outside of the cell are ligation to the death receptor on cell membrane; and then the death receptor recruits adaptor molecules by containing cytoplasmic death domains (DD). The adaptors also contain DEDs which can recruit procaspase-8 by its own death effector domains (DEDs). Procaspse-8 is activated by proteolytic reaction and forms the active caspase-8, a heterotetramer of two large and two small subunits. The caspse-8 proteolytically cleaves and activates other caspases for the execution of apoptosis (Figure 1.5) (Denault and Salvesen, 2002).

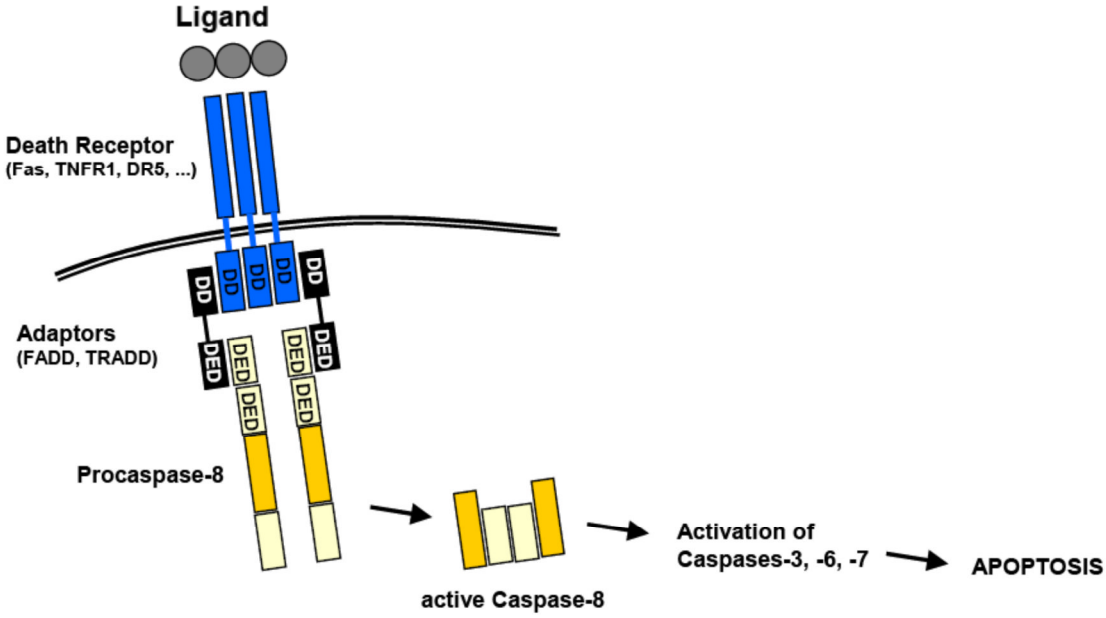

Figure 1.5 In extrinsic apoptosis pathways (Denault and Salvesen, 2002).

In intrinsic apoptosis pathways, the release of cytochrome C from inner membrane of mitochondria is triggered by apoptotic stimulus. Apoptosome is formed when cytochrome C is released from the mitochondria. Apoptotic protease activating factor 1 (Apaf-1) is the core of the apoptosome. The cytochrome C and Apaf-1 protein forms a heptameric, wheel-like structure which is apoptosome. Apoptosome can activate initiator protocaspase such as procaspase-9 by binding them to a heptamer (Figure 1.6) (Acehan *et al.*, 2002).

Once the initiator caspases have been activated, they can proteolytically activate the executioner caspase including caspases-3, -6 and -7 resulting in apoptosis (Earnshaw *et al.*, 1999).

In some cells, the intrinsic pathway is needed to amplify the extrinsic pathway of apoptotic signals (Alberts, 2008). Caspase 8 can mediate the cleavage of the proapoptotic protein Bid, one of the Bcl-2 family members, which results in the release of cytochrome C from mitochondria (Fadeel *et al.*, 1999; Wang and Youle, 2009). So there are sufficient signals to trigger apoptosis.

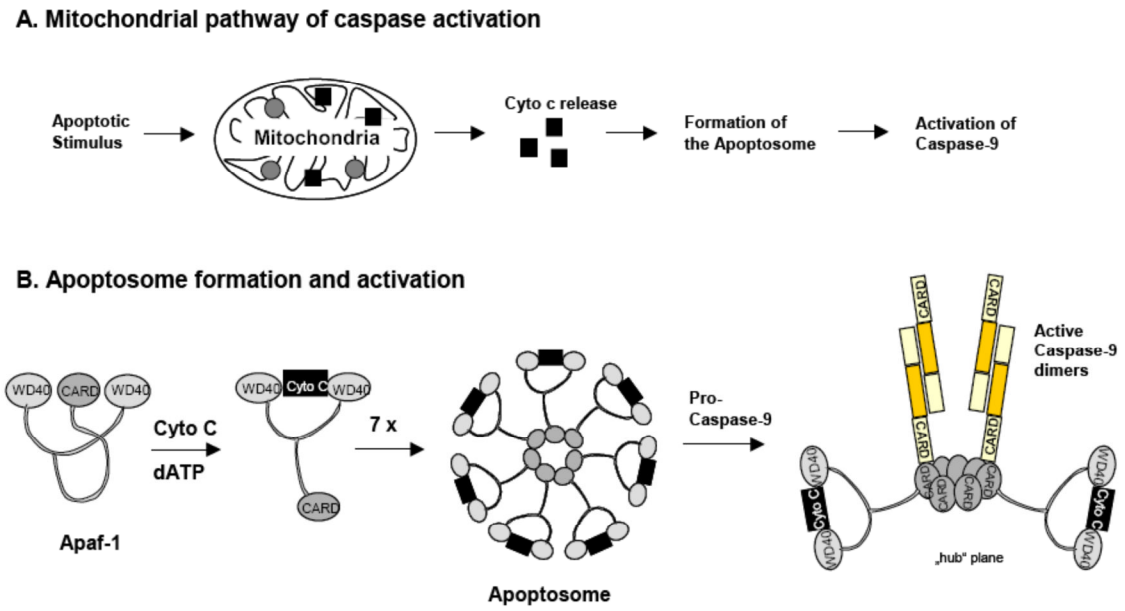

Figure 1.6 In intrinsic apoptosis pathways (Acehan *et al.*, 2002).

1.3.5 p53

Tumour suppressor protein p53 is encoded by tumour suppressor gene p53. The p53 is able to response to the irreparable DNA damage etc. (Alberts, 2008). p53 also can induce the expression of proapoptotic proteins such as Bax, Apaf-1 etc., and inhabit the expression of antiapoptotic proteins Bcl-2 (Wu *et al.*, 2001; Hoffman *et al.*, 2002; Vousden and Lu, 2002). Moreover, p53 protein can

translocate to the mitochondria and suppress antiapoptotic gene Bcl-X_L release of cytochrome C (Mihara *et al.*, 2003).

1.3.6 Methods of cell apoptosis detection

Apoptosis occurs by complicated signalling cascade. When, where and what kind of proteins involved are tightly regulated. It is important to detect the initiators, the effectors and executioners at right time point. Moreover, multi ways of detection can be used to observe apoptosis. For example, use a first assay to detect early apoptosis and a second one to observe the late apoptosis. Two ways based on different principles can confirm apoptosis (Watanabe *et al.*, 2002; Otsuki *et al.*, 2003; Elmore, 2007).

Early apoptosis detection

AlamarBlue Assay

AlamarBlue is a real-time and nontoxic assay to indicate the viability and cytotoxicity of cells. The damaged and nonviable cells generate lower intensity of fluorescence than healthy cells (LifeTechnologies, 2012). AlamerBlue will be introduced in detail in ‘5.3 Using AlamarBlue assay to indicate apoptosis’ section.

Caspase Assay

Caspase assay is caspase substrates. Caspases such as caspase-3 can cleave the non-fluorescent substrates to generate fluorescent amino acid peptides. The intensity of fluorescence indicates the quantity of caspases (Millipore, 2012).

Phosphatidylserine (PS)

Phosphatidylserine (PS) transfer from the inner cell membrane to the outside of cell membrane in early apoptosis. AnnexinV is a protein can specifically bind with the exposed PS in outer membrane, which can be detected by a fluorescent microscopy or a fluoremeter (Kylarova *et al.*, 2002).

Glutathione (GSH)

Glutathione (GSH) is very important in cells as it can remove the toxic oxides within the cells. When the level of mitochondrial GSH reduces, it will lead to the cytochrome C transferring from the inner membrane of mitochondria to the cytoplasm. Then, apoptosis will be triggered (Circu *et al.*, 2008). Therefore, GSH could be a target to detect early apoptosis.

Cytochrome C

Cytochrome C plays a key role in apoptosis. As described before, it exists in the inner membrane of mitochondria. The apoptotic stimuli will make it released outside mitochondria. Then caspase cascade reaction will start. So using antibody to mark the position of cytochrome C can determine apoptosis (Terauchi *et al.*, 2005).

Mitochondrial membrane potential

Mitochondrial membrane potential changes in early apoptosis, when the morphology of mitochondrial has not changed. The mitochondrial membrane potential changes result in the alteration of the permeability. By using a cationic dye which is very sensitive to the mitochondrial permeability changes, cell undergoing apoptosis can be detected by fluorescent microscopy or by flow cytometry (Scarlett *et al.*, 2000).

Late apoptosis detection

PI staining

Propidium iodide (PI) can intercalate DNA double-stranded becoming strongly fluorescent. As PI cannot pass through live cell membrane, it only can stain dead or dying cells. PI can be detected by a fluorescence microscopy and flow cytometry and indicate the DNA content in cell cycle (LifeTechnologies, 2012). So apoptotic cells can be differentiated from the normal cells.

TUNEL

In late apoptosis, endonuclease cut nuclear DNA into a large number of 180-200 bp in length of DNA fragments. Terminal deoxynucleotidyl transferase mediated dUTP nick end labelling is a method to detect DNA fragments through

labelling the terminal end of nucleic acids. The nicks of DNA can be identified by the terminal deoxynucleotidyl transferase which will catalyse the addition of dUTPs labelled with a marker (Kylarova *et al.*, 2002).

Telomere length detection

Telomere is a thousand repeats of 6 bp TTAGGG at the end of chromosome. In each time of cell division, chromosome telomeres will shorten. Without the protection of telomeres, chromosome becomes unstable and the chromosomal ends will get fusion. This will make cells having a limited life span. So telomere length can indicate senescence or apoptosis (Millipore, 2005; Bermudez *et al.*, 2006).

1.3.7 Apoptosis and disease

In the human body, thousands of cells are generated by mitosis and a similar number of cells undergo apoptosis in every second for maintenance of homeostasis and regulation of immune cell selection (Fadeel *et al.*, 1999). Dysregulation of apoptosis will lead to various disease such as cancer, due to cell accumulation, resistance to therapy (Reed, 2002). Cancer cells resist to the chemotherapeutic drugs and irradiation because of its apoptosis resistance (Fulda and Debatin, 2004).

1.4 Bio-impedance techniques for breast cancer detection

1.4.1 What is bio-impedance

Bio impedance is a measure of how much cells or tissue impede the flow of electric current. Impedance is measured in ohms, symbol Ω (Dean *et al.*, 2008). Bio-impedance varies with the cell structure. This can be used to distinguish normal tissue from cancerous tissue in various organs, including breast, cervix, skin, bladder and prostate (Halter *et al.*, 2007). The cellular components, the diameters, and the cellular internal structure determine the electrical properties of cells over different frequency ranges. So, different

cellular structures of cells will have characteristic impedance spectra (Halter *et al.*, 2007).

1.4.2 The application of bio-impedance in breast cancer

The different bio-impedance of tissue depends on their structures. The cell membrane, cytoplasm *etc*. are capacitive and resistive (Zou and Guo, 2003). In the 1920s, Frick and Morse firstly found the significant difference of capacitance between breast cancers and normal tissues in various types of breast tissue (Fricke H, 1926). This was the first time that bio-impedance was applied to biology (Zou and Guo, 2003).

From 1920, various *in vitro* impedance measurement results have shown significant differences between malignant tumours and breast tissues (Zou and Guo, 2003). In contrast to surrounding normal tissues, malignant tumours displayed lower impedance (Jossinet *et al.*, 1985). The electrical properties of malignant tissue changes because there is an increase in cellular water and salt contents which alters the membrane permeability, there is also changed packing density, and orientation of cells (Scholz, 2000).

1.5 Bio-impedance of cells

As addressed before, bio-impedance can be used to distinguish tissue and carcinoma in many organs (Halter *et al.*, 2007). Also it has been widely applied to measure the conditions of animal tissues *in vivo* and *in vitro* (Bauchot *et al.*, 2000; Kerner *et al.*, 2002). Bio-impedance is a useful method to determine the cellular changes quantitatively (McRae *et al.*, 1999; Soley *et al.*, 2005). Bio-impedance of cells over a range of frequencies can estimate cell population, the electric property of the cell membrane and the intercellular and intracellular conductivity (Dean *et al.*, 2008).

In addition, bio-impedance is a non-invasive diagnostic technique (Gersing, 1998; Kerner *et al.*, 2002). In 1998, it had been used to determine whether a canine heart muscle and a porcine liver can recover or not from

ischemia (Gersing, 1998). In 2002, the investigation of the bio-impedance of 26 women's breasts was carried out by Kerner (Kerner *et al.*, 2002). In 2005, the growing yeast cells were observed using bio-impedance (Soley *et al.*, 2005). In 2007 bio-impedance was used to distinguish normal and carcinoma prostate tissue (Halter *et al.*, 2007).

Bio-impedance can be applied to wider areas such as the food industry, and other commercial uses (Spreekens and Stekelenburg, 1986; Varshney and Li, 2008).

1.5.1 Electrical properties of cells

Ions in cells allow electrical conduction (Dean *et al.*, 2008). In an electric field, current flows due to the movement of ions in the medium and cells. Different cells have their particular ionic content and mobility. This can be characterised by a combination of cell conductivity, σ (Pethig, 1987; Dean *et al.*, 2008) and permittivity ε. Conductivity is a measure of the ability of a material conducting the electric current. Permittivity describes the ability of a material to resist the electric current (Grimnes and Martinsen, 2008). Conductivity and permittivity vary between different cells according to equation 1.1 (Pethig, 1987).

$$\varepsilon = \varepsilon_r \varepsilon_0 + j * \frac{\sigma}{\omega} \tag{1.1}$$

Where: ε_r is relative permittivity due to different materials,

ε_0 =8.85× 10^{-12} F/m, it is the vacuum permittivity,

σ = electrical conductivity,

ω is angular frequency = 2 π f. f is frequency,

j is complex number, $j = \sqrt{-1}$.

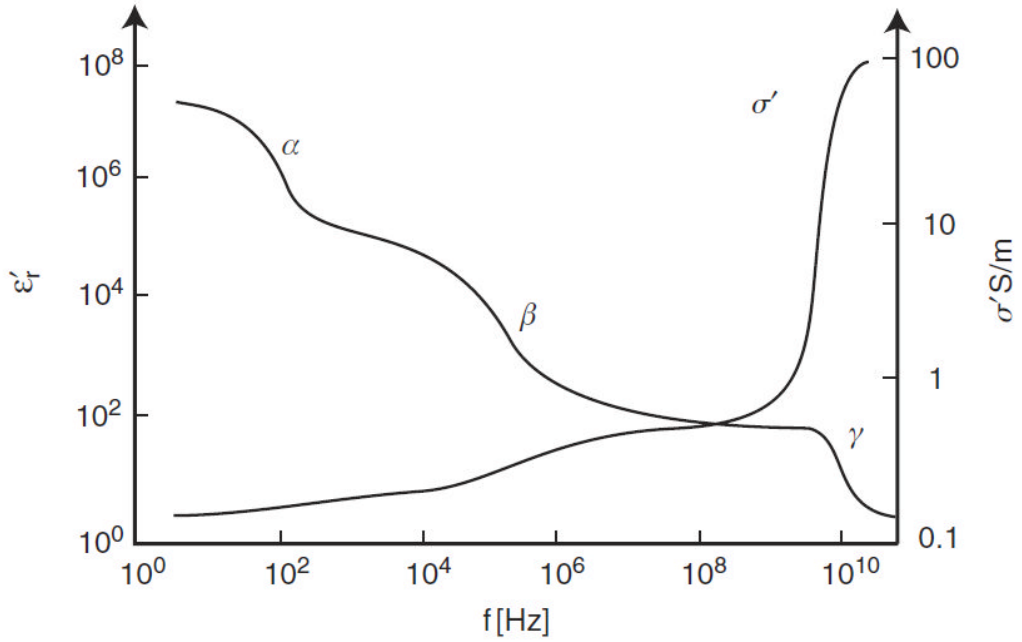

Figure 1.7 Three dispersions of cells (Schwan, 1993; Grimnes and Martinsen, 2008).

The permittivity and conductivity are both are frequency dependent. With the increasing frequency, permittivity falls, whilst conductivity increases. The three dispersions vary with frequency according to the electric properties of the cell suspensions (Schwan, 1957). According to Schwan' theory, there are three dispersion mechanisms α, β, γ of the electric properties of cell suspensions (Schwan, 1957)(Figure 1.7). The α-dispersion is significant over the frequency range of 10 Hz–10 kHz. This is influences the ions or intercellular factors outside cells. From 0.1MHz to 10 MHz, the flow of current is able to pass through the cell membrane and cytoplasm because the cell membrane acts as a capacitor, which causes the β-dispersion to occur. β-dispersion is affected by the impedance changes of the cell membrane. When the frequency is between 100MHz to some GHz, γ-dispersion occurs due to the internal structure of the cells that is the nuclear envelope, membrane of organelles and water concentration in each cell (Schwan, 1993; Tacconi *et al.*, 2004; Grimnes and Martinsen, 2008) (Table 1.1).

Table 1.1 Dispersions of cells (Grimnes and Martinsen, 2008).

Type	Characteristic frequency	Mechanism
α	mHz–kHz	Counterion effects (perpendicular or lateral) near the membrane surfaces, active cell membrane effects and gated channels, intracellular structures (e.g. sarcotubular system.), ionic diffusion, dielectric losses (at lower frequencies the lower the conductivity).
β	0.001–100 MHz	Maxwell–Wagner effects, passive cell membrane capacitance, intracellular organelle membranes, protein molecule response.
γ	0.1–100 GHz	Dipolar mechanisms in polar media such as water, salts and proteins.

1.6 Aims of this project

This project aims to use the cell impedance system (CIS)

to distinguish breast cancer cell lines from a normal breast cell line;

to investigate whether undergoing apoptosis could be detected by CIS.

2 Materials and methods

2.1 Cell culture

Jurkat 6 and DG75 cell lines were cultured in RPMI media (Invitrogen) supplemented with 10% heat-inactivated fetal bovine serum, 2 mmol/L L-glutamine, 100 IU/mL penicillin, 100 µg/mL streptomycin (Invitrogen). The cells were maintained in an incubator at 37°C with 5% CO_2. Cells were split 2 to 3 times every week. For storage, cells were frozen in freezing media which is composed of 85% fetal bovine serum and 15% DMSO (Sigma).

Human breast cancer cell lines MDA-MB-231 and MDA-MB-7 (CLS-Cell lines service, Germany), and human breast tissue cell line MCF-10A (American Type Culture Collection, USA) were cultured in DMEM/F12 media (Invitrogen) supplemented with 10% heat-inactivated fetal bovine serum, 2 mmol/L L-glutamine, 100 IU/mL penicillin, 100 µg/mL streptomycin (Invitrogen), 20 ng/mL epidermal growth factor (Invitrogen), 500 ng/mL hydrocortisone (Sigma), 100 ng/mL cholera toxin (Sigma) and 10 µg/mL bovine insulin (Sigma). The cells were maintained in an incubator at 37°C with 5% CO_2. Cells were split 2 to 3 times every week. For storage, cells were frozen in freezing media which is composed of 85% fetal bovine serum and 15% DMSO (Sigma).

2.2 Cell viability measurement

To wash cells from the media, they were pelleted by centrifugation at 1300 rpm for 5 minutes and the supernatant was retained as conditioned media. Cells were re-suspended in 4°C DPBS and pelleted as above. Then cells were re-suspended in DPBS or DPBS with serum replacement, respectively. 1ml of $3X10^5$ cells/ml cells was placed in each well of 12-well plate. At 0 minute, 30 minutes, 60 minutes and 120 minutes cells were counted. To count cells, 100ul of cells were placed in a 1.5ml tube at 20°C, mixed with an equal volume of Trypan Blue (Invitrogen) and vortexed. Then 10ul of cells were added to a haemocytometer. The approximate number of cells was determined using a 16 square haemocytometer, under microscope. The white cells were alive the blue

ones were dead. The number of live cells was recorded and the curves of viability were drawn.

Cell viability was also measured by AlamarBlue assay (Invitrogen). A 96-well plate contained cells at different densities of 0, 80, 400, 2000, 10000 and 50000 cells per 100µL and then incubated at 37°C and 5% CO_2 for 24 hours. 10µL of AlamarBlue assay were added into each well. A fluorometer was used to measure the fluorescent intensity of the plate at each time point.

2.3 Cell diameters measurement

Cells were in suspension placed into a 24-well plate. The Olympus optical microscope with a DMK 31BF03 camera was used to observe cells at 10 times magnification. The camera was linked to a PC via an IEEE 1394 interface. A software named SCIght was used to analyse cells, which can measure the number of pixels between 2 points on the image. 50 µm is equal to 106 pixels; hence, 1 pixel is equal to 0.47 µm. 50 cells of each cell lines were measured without bias.

2.4 Fluorescent Activated Cell Sorting (FACS)

Etoposide was prepared at 10mg/ml in DMSO and added directly to the cells in culture media to give a final concentration of 10µg/ml. Control cells contained an equivalent volume of DMSO. Cells were incubated for 0h, 24h, 48h and 72h, washed with DPBS, fixed with 80% ethanol and kept at 4°C for 1 hour. Then ethanol was removed after cells were pelleted by centrifugation at 1300 rpm for 5 minutes. 1 ml Propidium Iodide (PI) Stain and 5ul RNase A were added to a cell pellet and kept at 4°C for 1 hour. FACS CANTO flow cytometry was used to analyse cells.

2.5 AlamarBlue assay detecting apoptosis

MCF-10A, MCF-7 and MDA-MB-231 cells were trypsinazed. Cells were placed in a 96-well plate at the density of $2X10^5$ cells/ well. After being added 10µL AlamarBlue (Invitrogen), the plate was incubated for 5 hours and then

measured fluorescent intensity by using fluorometer (Promega GloMax-Multi Detection System).

2.6 Caspase assay detecting apoptosis

At 4h, 8h, 24h each time point, 1.5 $X10^6$ cells with Etoposide or with DMSO were spun down and washed with DPBS. Then DPBS were removed and cells pellet were frozen at -80°C. $1X10^7$ cells/ml cells were lysed on ice, in 150µL Caspases Lysis Buffer with adding protease inhibitor cocktail. Cells were vortexed and debris pelleted by centrifugation in a micro-centrifuge at 13000rpm for 10 seconds. The supernatant containing the lysed cells was frozen at -80°C. The assays were carried out in 96-well plate by mixing 50µl of cell lysate with 200µl of Caspase Reaction Buffer containing 5µg of the Ac-DEVD-AMC Caspase-3 Fluorogenic Substrate. Controls were performed using 50µl of Caspase Lysis Buffer. The plate were incubated at 37°C for 60 minutes and the fluorescence produced by AMC release was visualized using a fluorometer with an excitation wavelength of 380nm and an emission wavelength of 440nm.

Caspase Lysis Buffer

1 ml of 1 M Tris pH 7.5	(10 mM final)
10 ml of 100 mM NaH_2PO_4/Na_2HPO_4 pH 7.5	(10 mM final)
6.5 ml of 2M NaCl	(130 mM final)
1 ml of 100% triton-x100	(1% final)
10 ml of 100 mM $Na_4P_2O_7$	(10 mM final)

Add water to 100 ml and store at 4°C.

Caspase Reaction Buffer

10 ml of 200 mM Hepes, pH 7.5	(20 mM final)
20 ml of 50% glycerol	(10 % final)
0.2 ml of 1 M DTT	(2 mM final)

Add water to 100 ml and store at 4°C.

2.7 Cell impedance measurement

Cells were in suspension and washed with DPBS. Cells were measured in 50% DPBS and 50% sterile water with 2% serum replacement at 25°C or 37°C. Before and after each measurement, viability, density testing and volume fraction were measured. Each time, 180μL cells suspensions were loaded into the chamber.

The cell impedance system was set up with using impedance analyser Agilent 4194A controlled by a laptop through GPIB-USB cable for data acquisition. The measurement device was plugged into Agilent 4194A directly by four BNC connectors. Three breast cell lines were measured and compared with conditions control.

2.8 Transmission electron micrographs

Preparation for TEM

Cells were pelleted in the culture media by centrifugation at 2000 rpm in eppendorfs.

Fixation

0.1ml of 25% glutaraldehyde was added to each eppendorf. The eppendorfs were rotated over night at room temperature

Rinsing and staining

The supernatants were removed and the pellets were washed with fresh media. The eppendorfs were rotated for 10 minutes then the media was removed, five times repeated. 1 ml of osmium tetroxide was added to each eppendorf and left in a hood for 2 hours, then removed. The pellets were rinsed with deionised water and kept in it for 20 minutes. The deionised water was removed. These steps were repeated three times. The eppendorfs were kept overnight in a 4°C cold room.

Dehydration

The eppendorfs were taken out from the cold room. The deionised water was removed. 1.5 ml of 50% ethanol were added into each eppendorf, left for 20 minutes, and removed. 1.5 ml of 75% ethanol were added into each eppendorf, left for 20 minutes, and removed. 1.5 ml of absolute ethanol were added into each eppendorf, left for 20 minutes, and removed. This step was three times repeated. 1.5 ml of Propylene oxide (PO) were added into each eppendorf, left for 20 minutes, and removed. 0.75ml of PO and resin were added into each eppendorf (PO: resin=50:50). The eppendorfs were rotated overnight at room temperature.

The mixture of PO and resin was removed then 1 ml of resin was added into each eppendorf. The eppendorfs were rotated overnight at room temperature.

The resin was removed. 1ml of fresh resin was added into each eppendorf. The eppendorfs were rotated overnight at a 4°C cold room.

Section and photographing

Thanks Dr Julian Thorpe for the TEM section and TEM photographing.

3 Testing conditions design and the performance

3.1 Introduction

The study of applying Cell Impedance System (CIS) for distinguishing cells will be discussed in the following three chapters. This chapter aims to investigate the testing conditions and their performance. Chapter Four will ask whether different pathologies of breast cancer cells can be differentiated from breast tissue cells by Cell Impedance System (CIS). Moreover, Chapter Five will focus on whether cells undergoing apoptosis and normal growing cells also can be distinguished by CIS.

Breast tissue cells and breast cancer cells are adherent cells growing in DMEM/F12 media with fetal bovine serum and other supplements as discussed in Chapter Two. The impedance measurement device is a cylindrical chamber into which cell suspension is loaded. Cells will be kept in suspension during the process of impedance measurement. Fetal bovine serum (FBS) is the portion of plasma remaining after centrifugation of blood. It is variable from batch to batch in composition. Culture media has complex supplements including FBS, which may influence impedance measurements and repeatability. Dulbecco's Phosphate Buffered Saline (DPBS) will be used as an alternative to culture media. DPBS, one kind of isotonic solution, is widely used in washing cells and able to maintain cell tonicity and survival for a limited period of time. The serum replacement is also designed to aid cell viability, which may lengthen survival time in DPBS. Moreover, in the process of impedance measurement, cells will be taken out from the incubator and cell impedance will be measured at the room temperature of approximately 20°C. Each cell line will take not more than 120 minutes to be measured. So these conditions all need to be tested before the impedance measurement.

3.2 Cell survival in DPBS with serum replacement

To question whether cells are healthy while cells are in the conditions, DG 75 and Jurkat 6 cells viability will be evaluated in DPBS at 4°C, 20°C and 37°C to find out which is the best suitable temperature. 4°C is used for slowing

down cell division and preventing over-heating as current flows will generate heat when they pass through electrodes. 20°C and 37°C are the temperatures for room temperature and cell native growing environment, respectively. The serum replacement is less complex than FBS and designed for long-term growth of human cells and only contains human serum albumin, human transferrin, and human recombinant insulin (Sigma-Aldrich, 2010). These proteins play roles as growth factors in cell culture. So the serum replacement may aid cell survival and is used to replace fetal bovine serum (FBS) as it is more reproducible.

Cell suspensions in DPBS with or without the serum replacement were placed in a 24-well plate, incubated for 0~120 minutes and live cells were counted with a haemocytometer. Figure 3.1 shows that in DPBS DG 75 cell population dramatically reduced in the first 30 minutes at indicated three different temperatures. And also Figure 3.2 shows Jurkat 6 cell in DPBS nearly died out within 120 minutes. Compared with cells without serum replacement, cell densities of DG 75 and Jurkat 6 cells in DPBS with serum replacement remained stable over 120 minutes at three different temperatures. At 20°C, room temperature, cell survival was more stable than at other two temperatures. With aid of serum replacement, cells can survive at least 120 minutes. So the optimal conditions are room temperature, 20°C, and cells in DPBS with serum replacement.

During the measurement of impedance, cells will be exposed in air rather than at 5% CO_2. So whether cells can survive exposure in air also needs to be measured. Cells suspension in DPBS with serum replacement were placed in 24-well plate and incubated at 20°C with covering or not. Figure 3.3 shows that covering or not did not affect the viability of DG 75 and Jurkat 6 cells. After 120 minutes, cells densities were the same as at the beginning. So DG 75 and Jurkat 6 cells can survive in DPBS with serum replacement without covering for 120 minutes.

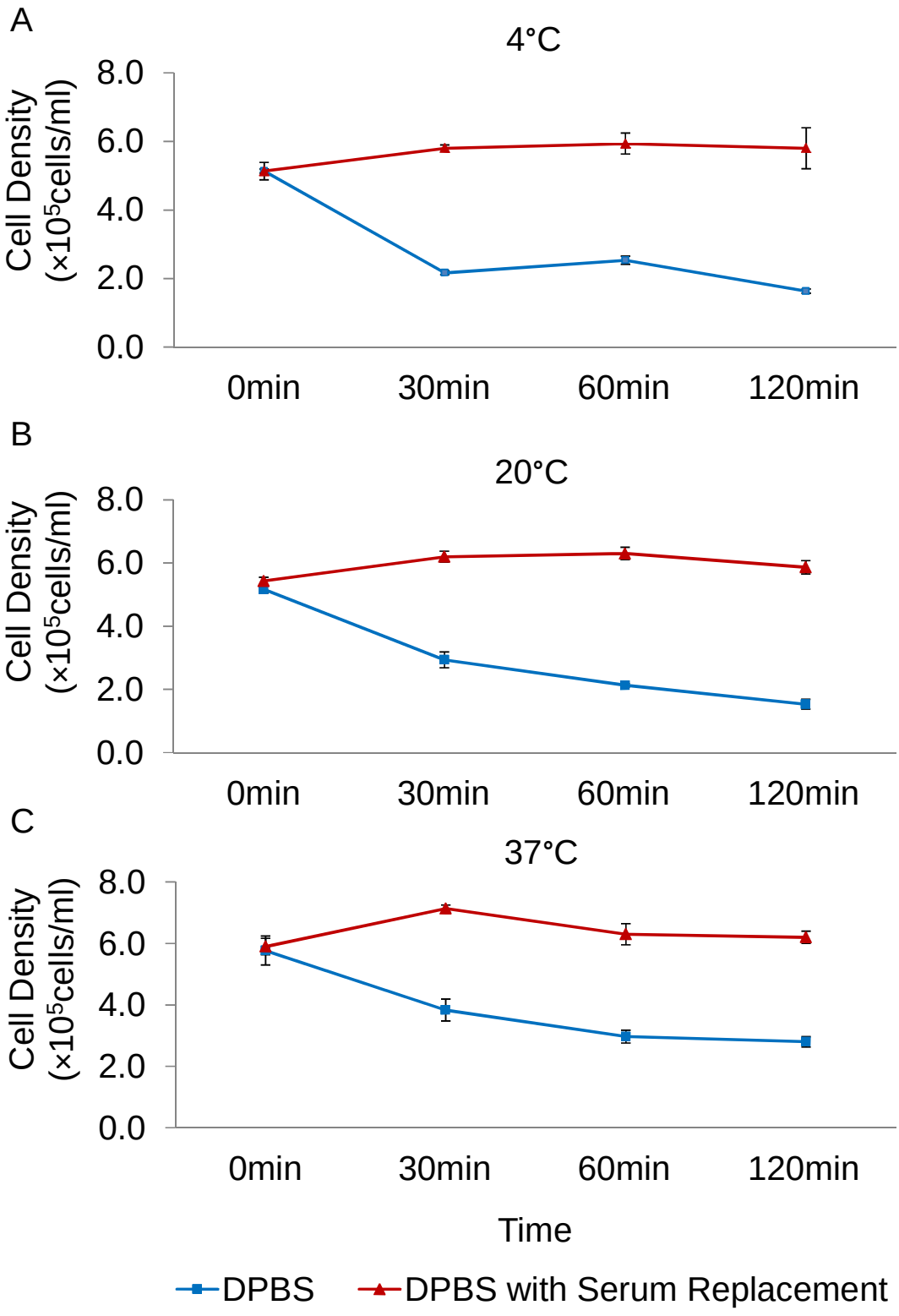

Figure 3.1 DG75 viability test at different temperature with or without serum replacement. Lymphoma cells DG75 were incubated in DPBS or DPBS with serum replacement for 0~120 minutes at the indicated temperature. Cells were dyed with Trypan Blue assay. The number of viable cells was determined using a haemocytometer in triplicate from three wells and error bars represent standard deviation.

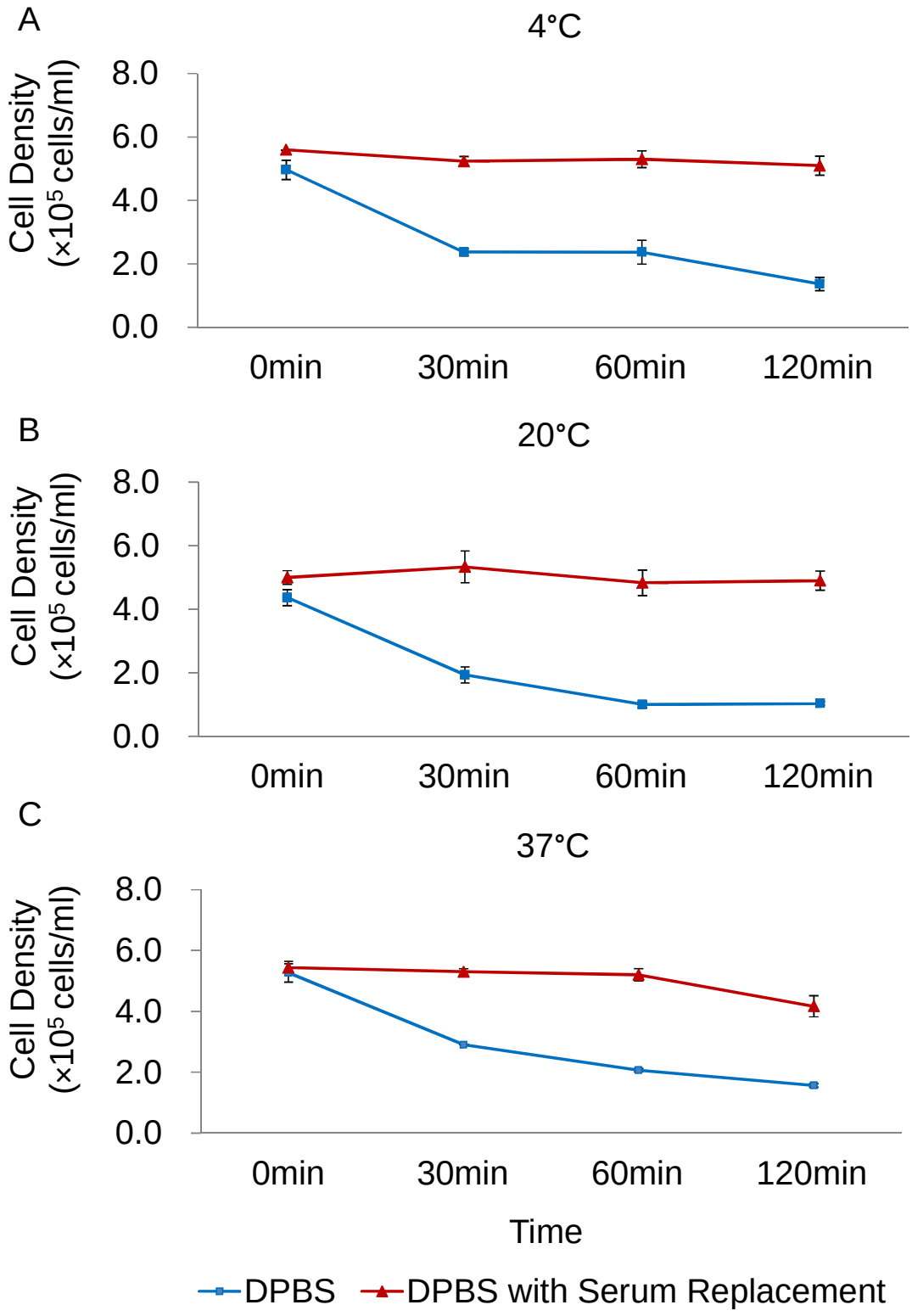

Figure 3.2 Jurkat 6 viability test at different temperature with or without serum replacement. Lymphoma cells Jurkat 6 were incubated in DPBS or DPBS with serum replacement for 0~120 minutes at the indicated temperature. Cells were dyed with Trypan Blue assay. The number of viable cells was determined using a haemocytometer in triplicate from three wells and error bars represent standard deviation.

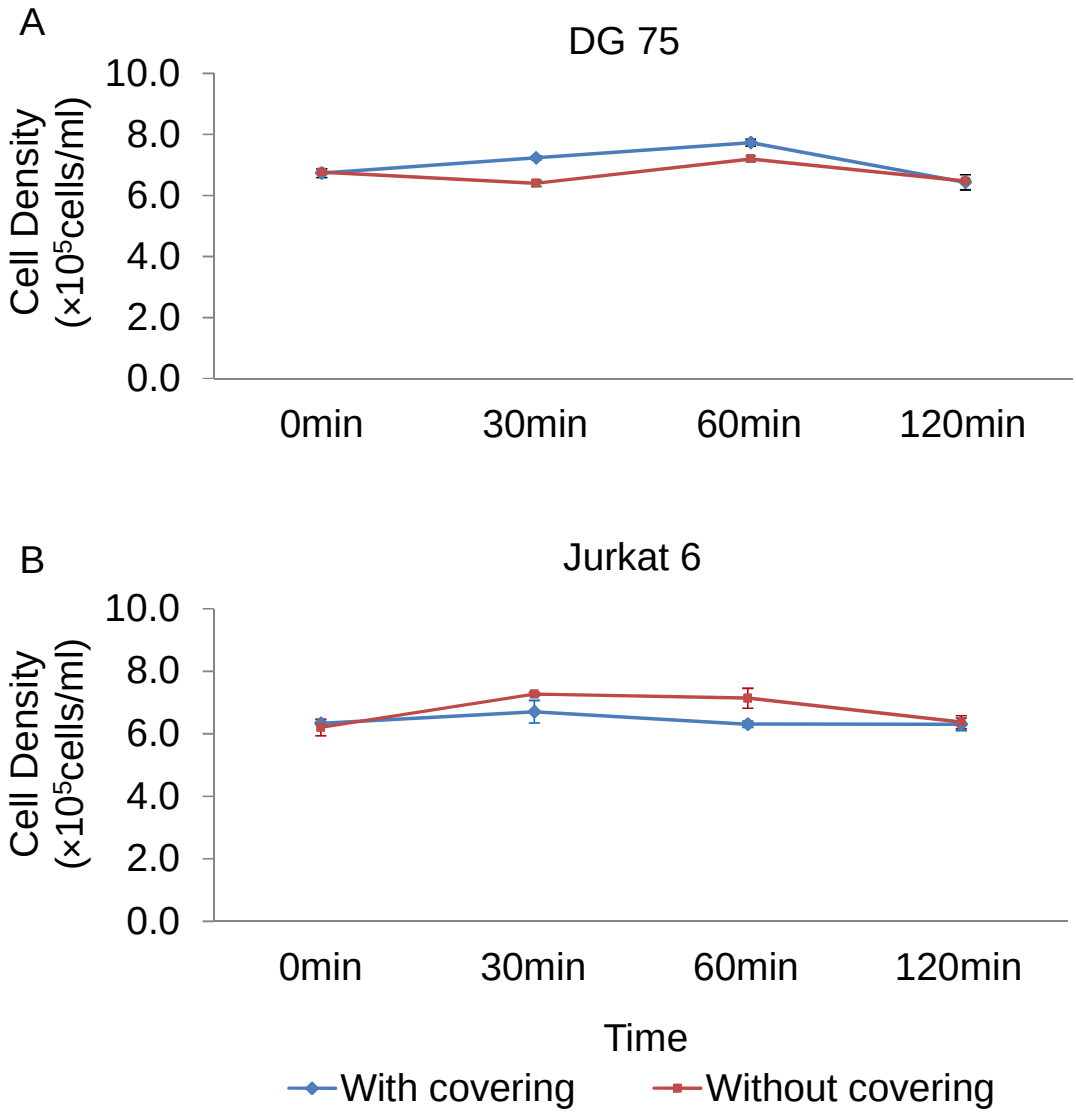

Figure 3.3 DG 75 and Jurkat 6 viability test with or without covering. Lymphoma cells DG75 and Jurkat 6 were incubated in DPBS with serum replacement with covering or without covering for 0~120 minutes at 20°C. Cells were dyed with Trypan Blue assay. The number of viable cells was determined using a haemocytometer in triplicate from three wells and error bars represent standard deviation.

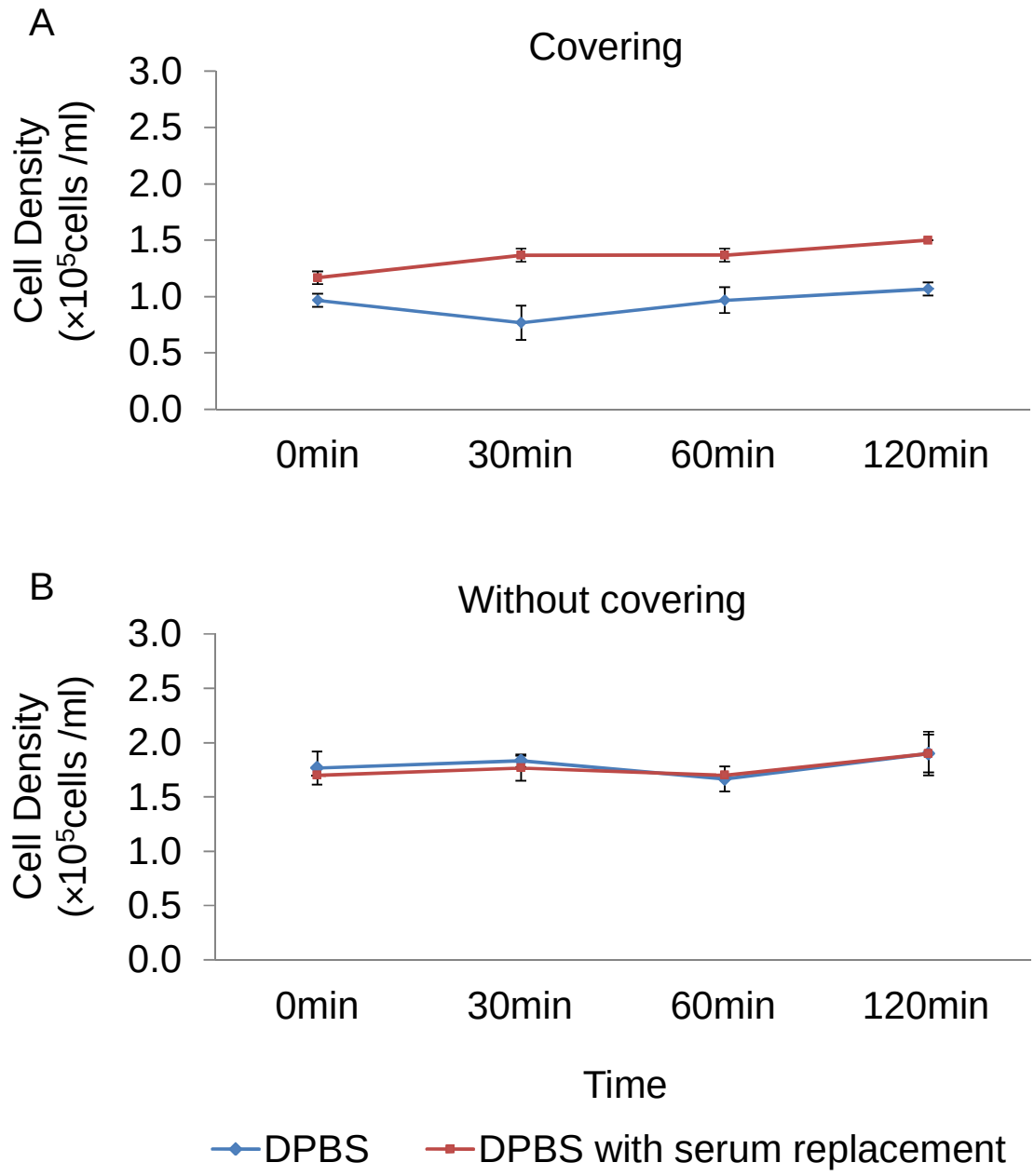

Figure 3.4 MCF-10A viability test with or without covering. Breast tissue cells MCF-10A were incubated in DPBS or DPBS with serum replacement for 0~120 minutes at 20°C. The number of viable cells was determined in triplicate from three wells and error bars represent standard deviation.

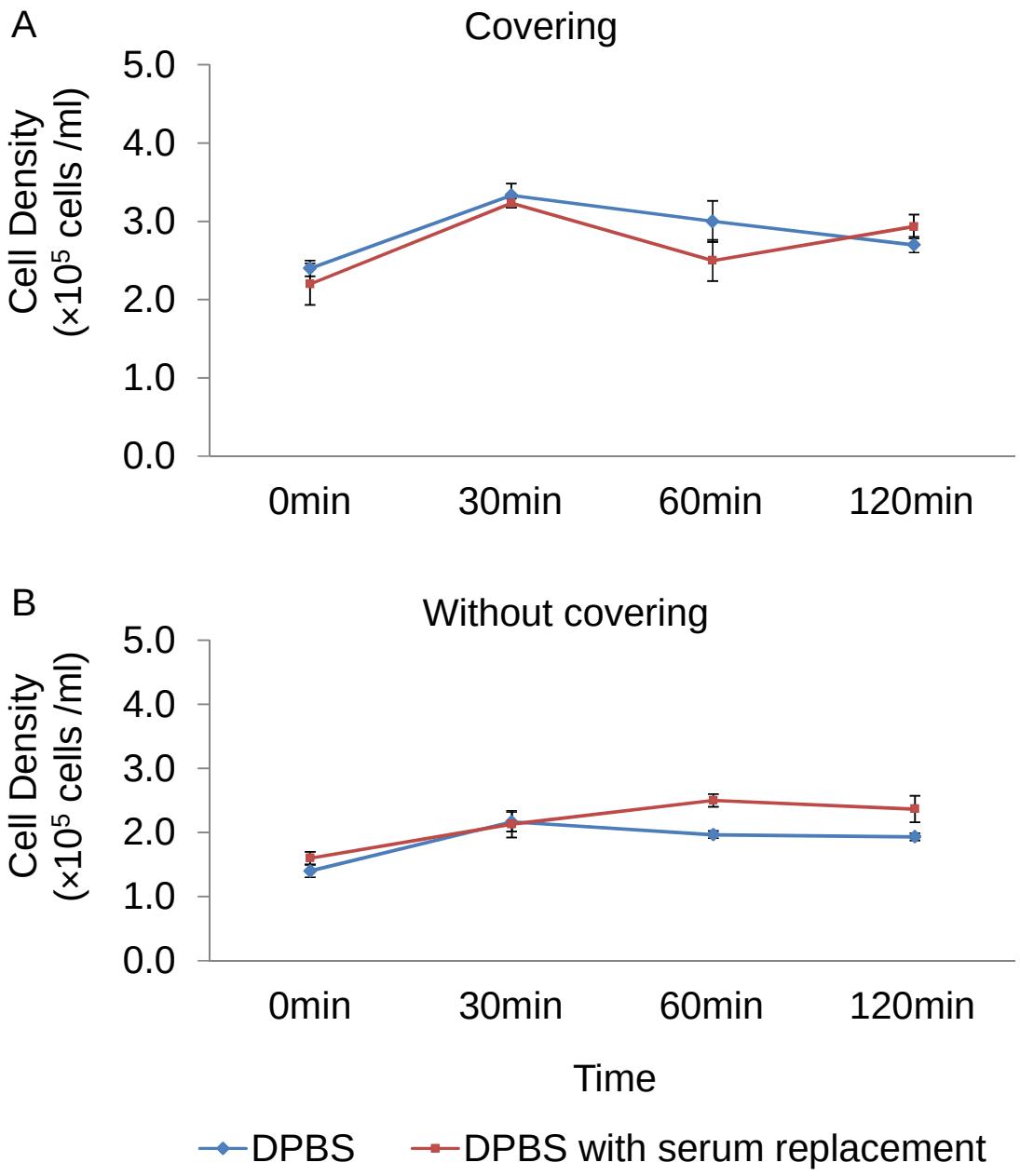

Figure 3.5 MCF-7 viability test with or without covering. Early breast cancer cells MCF-7 were incubated in DPBS or DPBS with serum replacement for 0~120 minutes at 20°C Cells were dyed with Trypan Blue assay. The number of viable cells was determined using a haemocytometer in triplicate from three wells and error bars represent standard deviation.

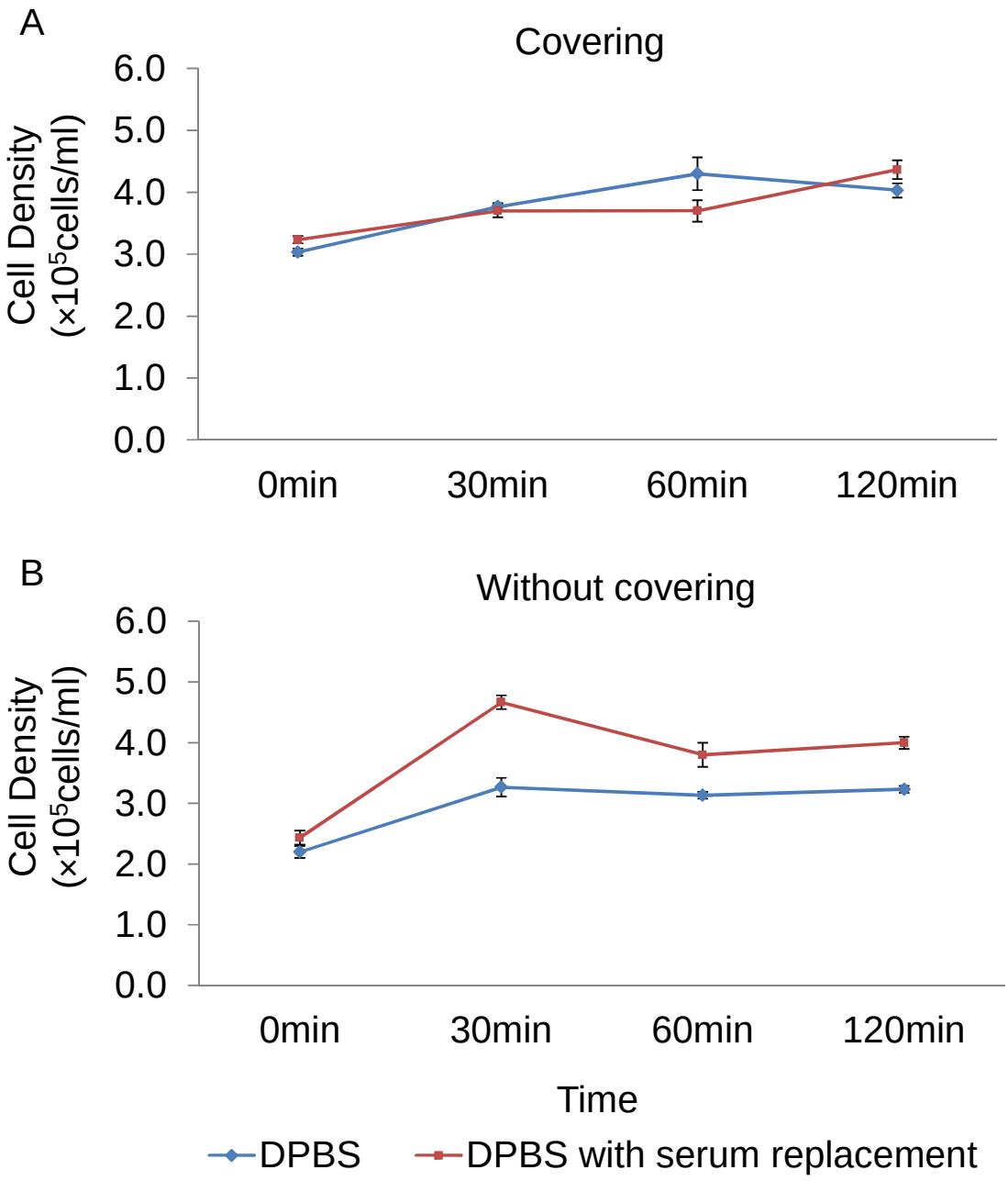

Figure 3.6 MDA-MB-231 viability test with or without covering. Invasive breast cancer cells MDA-MB-231 were incubated in DPBS or DPBS with serum replacement for 0~120 minutes at 20°C. Cells were dyed with Trypan Blue assay. The number of viable cells was determined using a haemocytometer in triplicate from three wells and error bars represent standard deviation.

Human breast cell line MCF-10A and human breast cancer cell lines MCF-7, and MDA-MB-231, were placed in suspension in 24-well plates and incubated at 20°C for 0~120 minutes conditions I found optimal for lymphoid cells. Figure 3.4-Figure 3.6 show that in two hours time period, regardless of covering or not, cells can survive in both DPBS or DPBS with serum replacement.

3.3 Cell morphology

Human breast cell line MCF-10A and human breast cancer cell lines MCF-7, and MDA-MB-231 can be differentiated by morphology. Cells were cultured adhered to plastic dishes and photographed. Figure 3.7 shows the morphology of three breast cell lines.

After trypsinization, cells were in suspension and photographed at the indicated densities. Figure 3.8 demonstrate MCF-10A cells were quite uniform, but there were variations on MCF-7 or MDA-MB-231 cells.

3.4 Differences in cell volume

In order to know the accurate impedance of cells, the total volume of cells must be the same, but from the cell morphology photographs of breast cancer cells and breast tissue cells, the diameters did not look the same. In order to ask how variable the diameter is, after trypsinization, 50 cells of each cell line were measured under microscope by using IC Imaging Control 3.0 software. Figure 3.9A displays that there is a great variation in diameters of MDA-MB-231 cells and also variation in others. In Figure 3.9B, the size of error bar shows that MCF-7 and MDA-MB-231 cells display greater variation than others.

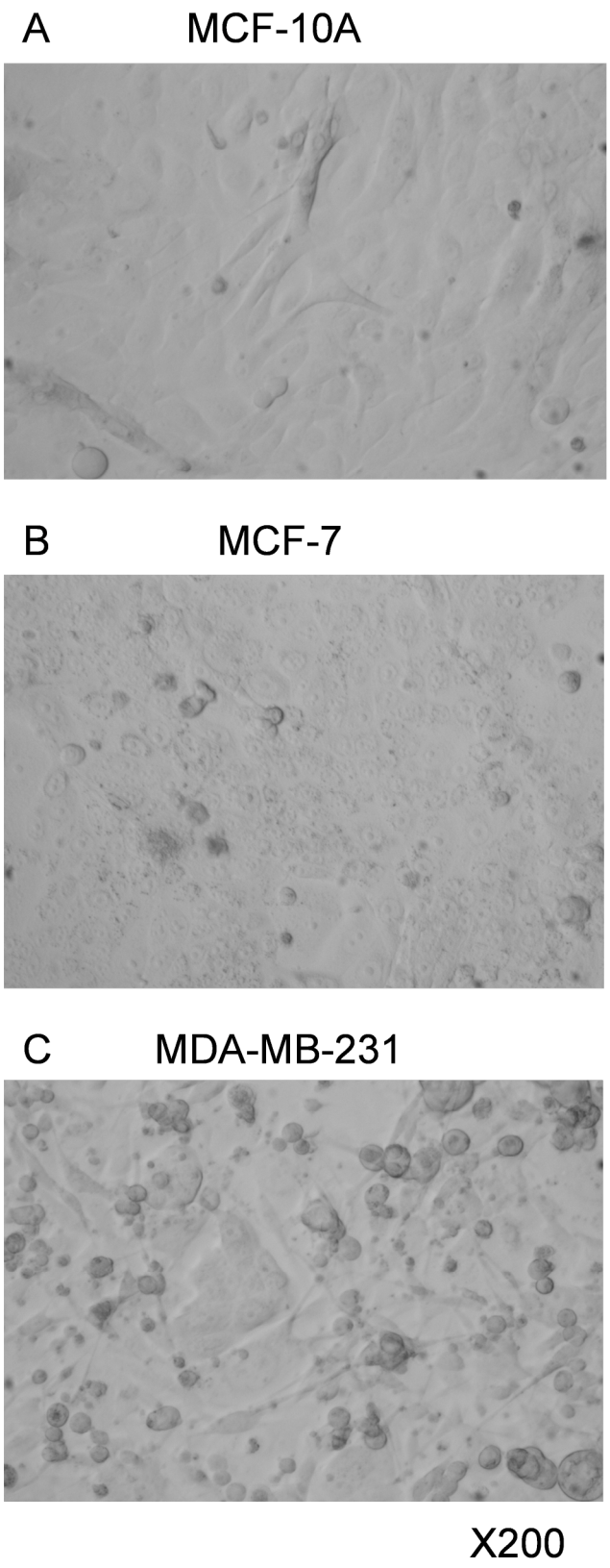

Figure 3.7 Morphology of MCF-10A, MCF-7, and MDA-MB-231 cells. Cells were cultured adhered to plastic dishes. Cells were plated at density of $2X10^5$ cells/ml and photographed.

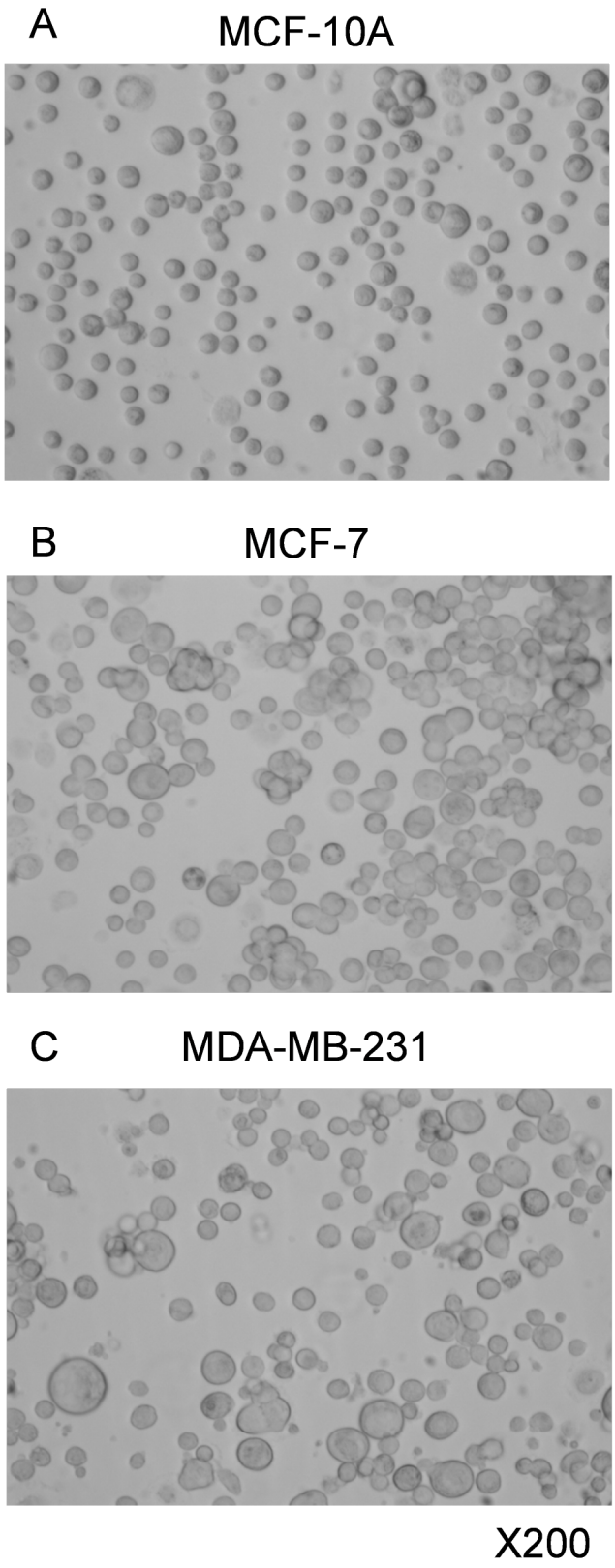

Figure 3.8 Morphology of MCF-10A, MCF-7, and MDA-MB-231 cells in suspension. The three breast cell lines were removed from culture plates by trypsinization and photographic images taken. The density of the cells is $2X10^5$ cells /ml.

A

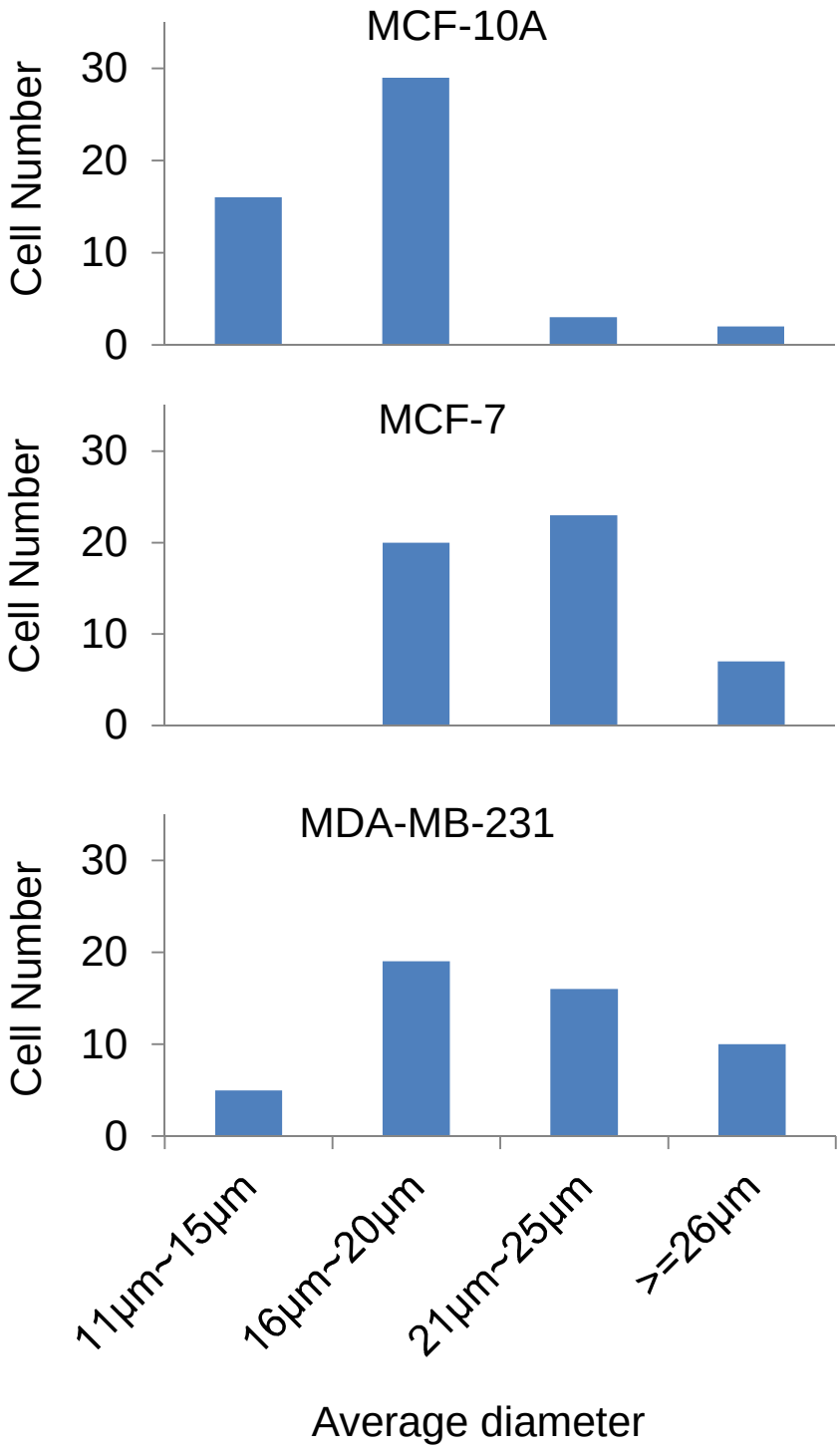
MCF-10A
Cell Number
30
20
10
0
MCF-7
Cell Number
30
20
10
0
MDA-MB-231
Cell Number
30
20
10
0
11μm~15μm
16μm~20μm
21μm~25μm
>=26μm
Average diameter

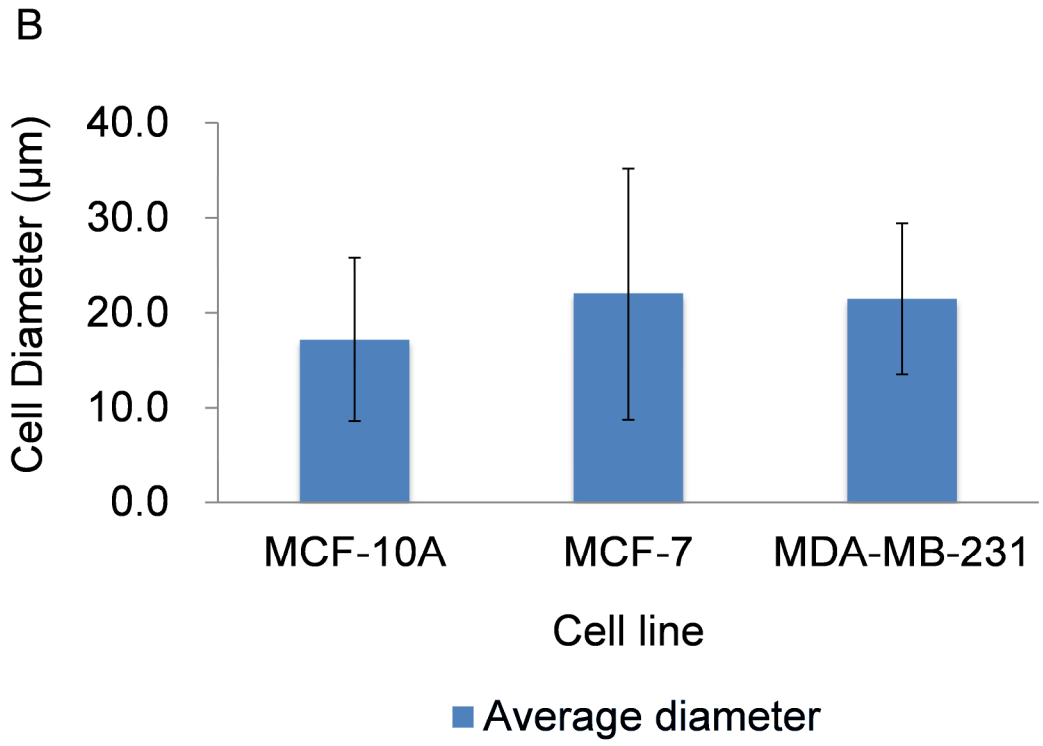

Figure 3.9 These three breast cell lines were removed from culture plates by trypsinization. The diameters of 50 cells were measured in suspension. Figure A is the cell number at different diameters. The X axis is the diameters of three cell lines and Y axis is the number being measured. Figure B is the average diameter of each cell line.

3.5 Cell survival in modified DPBS buffer

As described before, cells can survive up to 120 minutes in DPBS. However, a problem is that DPBS is much more conductive than cells. The impedance of cells at the density of 3~6X10^7 cells/ml cannot be observed in DPBS. To solve this problem, deionised water which is non-conductive was added into DPBS to reduce the conductivity. A series of modified buffers were made with different volume ratio of deionised water and DPBS, which are from 10% DPBS with 90% deionised water with serum replacement to 50% DPBS with 50% deionised water with serum replacement. Unfortunately, cells cannot survive with less than 50% DPBS with 50% deionised water. Figure 3.10 shows MCF-10A, MCF-7 and MDA-MB-231 cells can survive over 60 minutes in 50% DPBS with 50% deionised water at 20°C.

3.6 Cell survival in isotonic media

The Isotonic media was composed of 8.5% (w/v) sucrose (Fisher) and 0.3% (w/v) dextrose (Fisher) was used for preparing cell suspensions (Gascoyne *et al.*, 1997). The Dulbecco's Phosphate Buffered Saline (DPBS) (Invitrogen) was used to adjust the conductivity of the isotonic media to 9 mS/cm (Labeed *et al.*, 2006). The viability of three cell lines in the 9 mS/cm conductivity isotonic media was tested to ensure cells would survive in the media for at least 1 hour during the impedance measurement. Cells in the isotonic media at 37°C are to mimic the cells native growing environment. Figure 3.11 shows within 60 minutes, three cell lines all can survive in the isotonic media.

3.7 Cell volume estimate

Because some cell lines had variable diameters, it was important to determine cell volume (Figure 3.12). Before impedance measurement, the cell volume of each cell line was measured by Packed Cell Volume counting tubes (PCV tubes). 10µl of cell suspensions were loaded into a PCV tube and then centrifuged at 5000rpm for 1 minute. The packed cell volume in µl can be read from the PCV tubes (Figure 3.13).

Cells were re-suspended at a density that resulted in them occupying 20% of the volume with remaining 80% consisting of buffer. Figure 3.14 represents the cell density at which 20% packed cell volume is generated, because the small average diameters, MCF-10A cells were at density at $6X10^7$ cells/ml. However, the densities of MCF-7 and MDA-MB-231 cells were only around $3X10^7$ cells/ml.

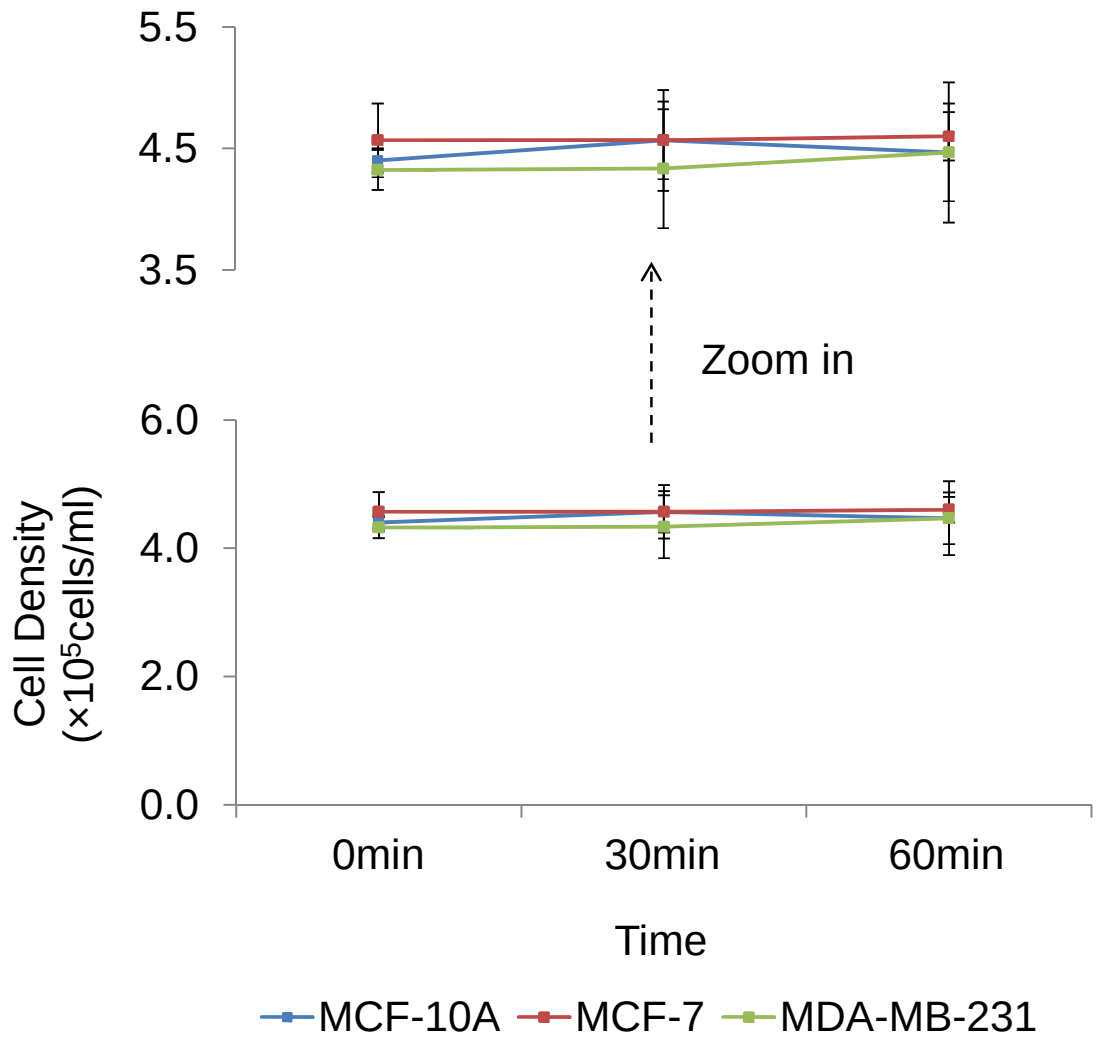

Figure 3.10 Cell viability tests. Cells were incubated in buffer which is 50% DPBS and 50% sterile water with 2% serum replacement for 0~60 minutes at 20°C. Cells were dyed with Trypan Blue assay. The number of viable cells was determined using a haemocytometer in triplicate from three wells and error bars represent standard deviation.

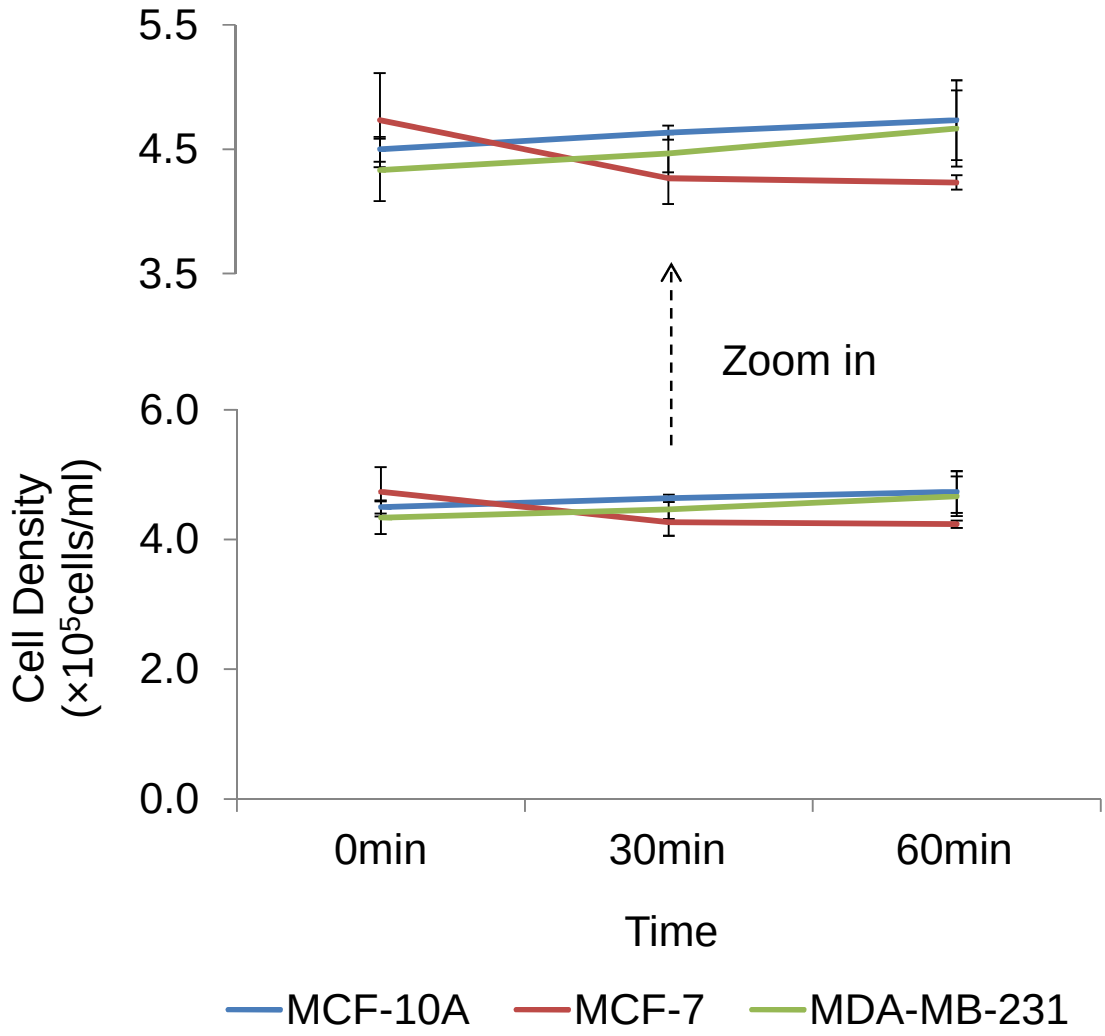

Figure 3.11 Cell viability tests. Cells were incubated in isotonic media for 0~60 minutes at 37°C. Cells were dyed with Trypan Blue assay. The number of viable cells was determined using a haemocytometer in triplicate from three wells and error bars represent standard deviation.

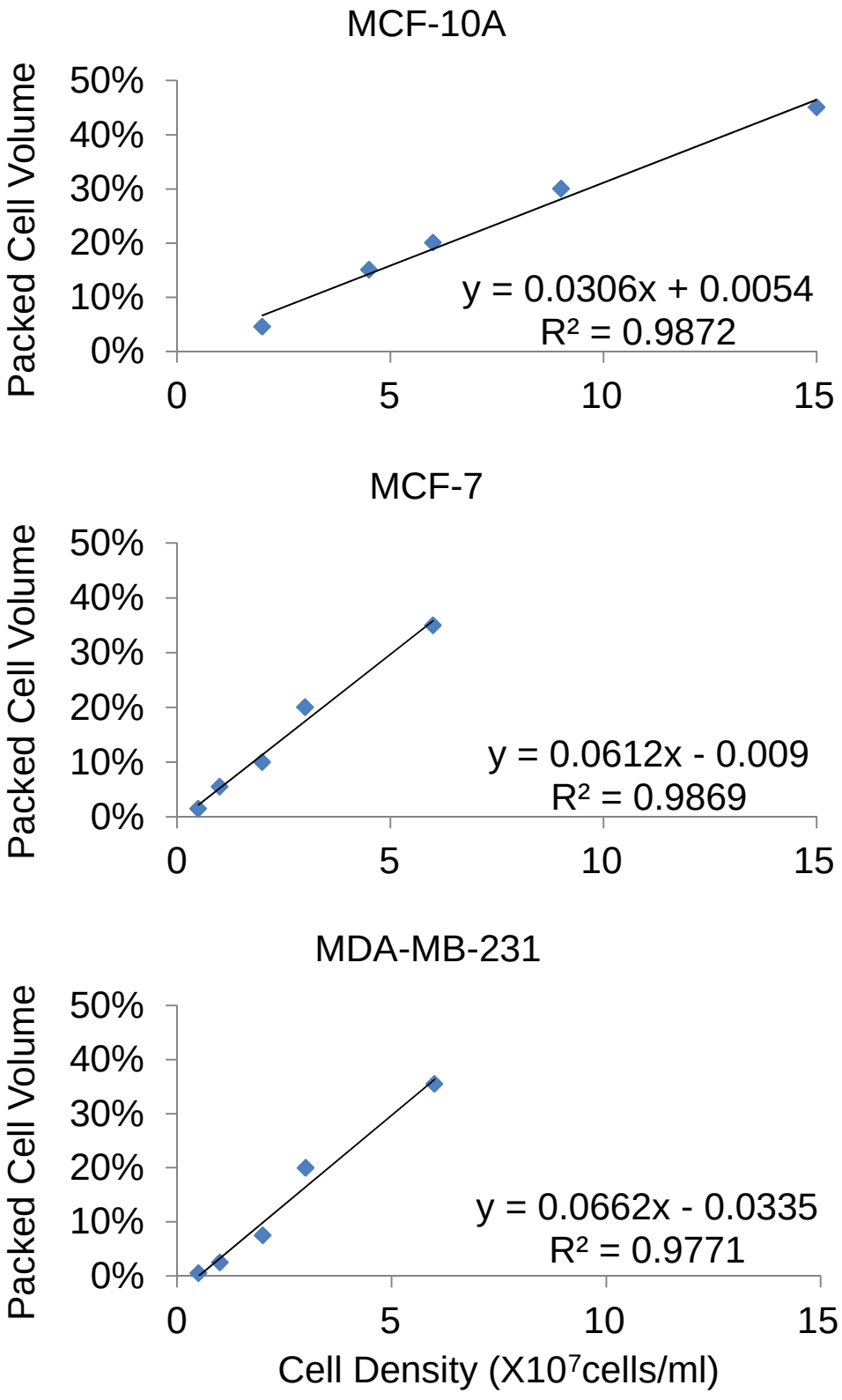

Figure 3.12 the standard curve of MCF-10A, MCF-7 and MDA-MB-231 packed cell volume with corresponding cell density. The number of cells was determined by Trypan Blue Assay. 10µl of cell suspensions in culture media were loaded into a PCV tube and then centrifuged at 5000rpm for 1 minute. The packed cell volume in µl can be read from the PCV tubes. The X axis is cell density; the Y axis is packed cell volume.

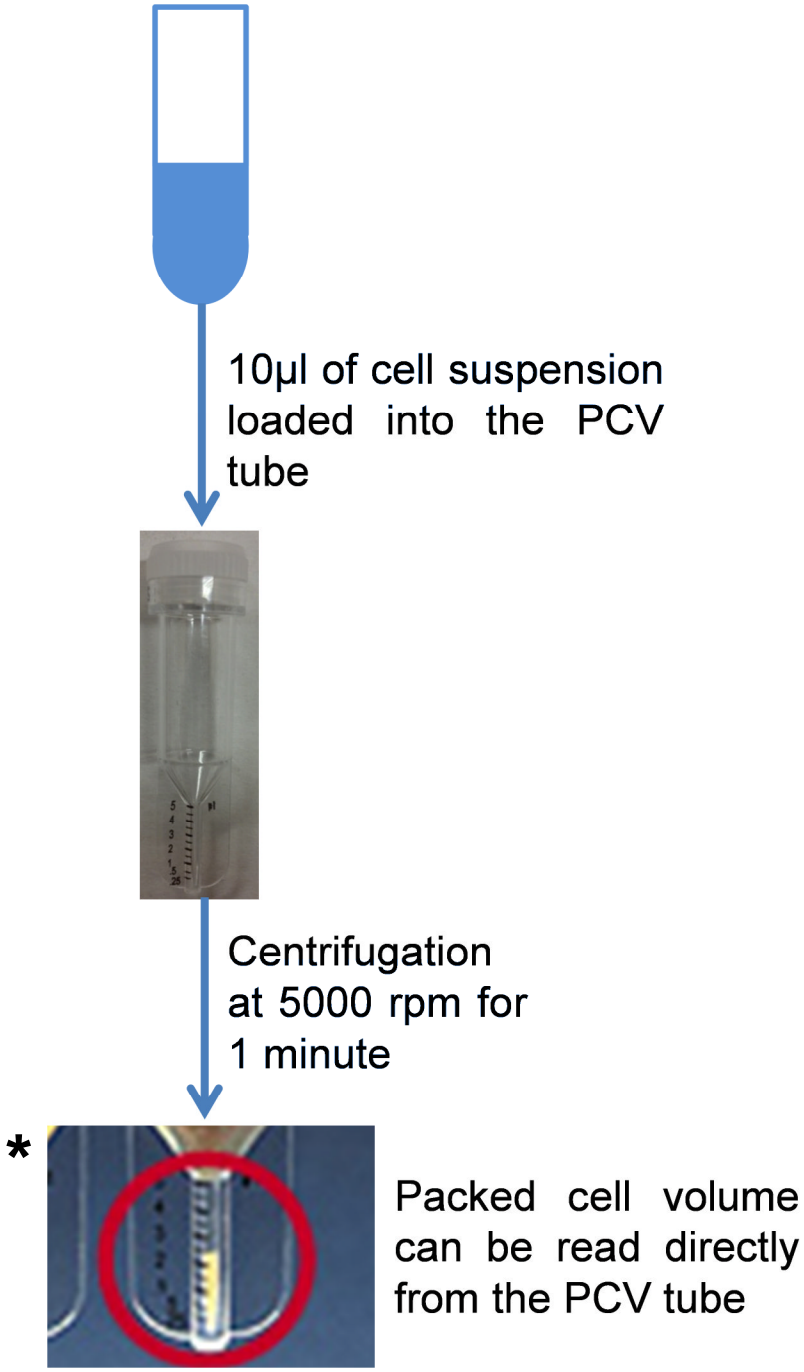

Figure 3.13 the schematic of determine packed cell volume. (The picture with the asterisk was from http://www.tpp-us.com/docs/products/pcv_biomass_cell_counters.html)

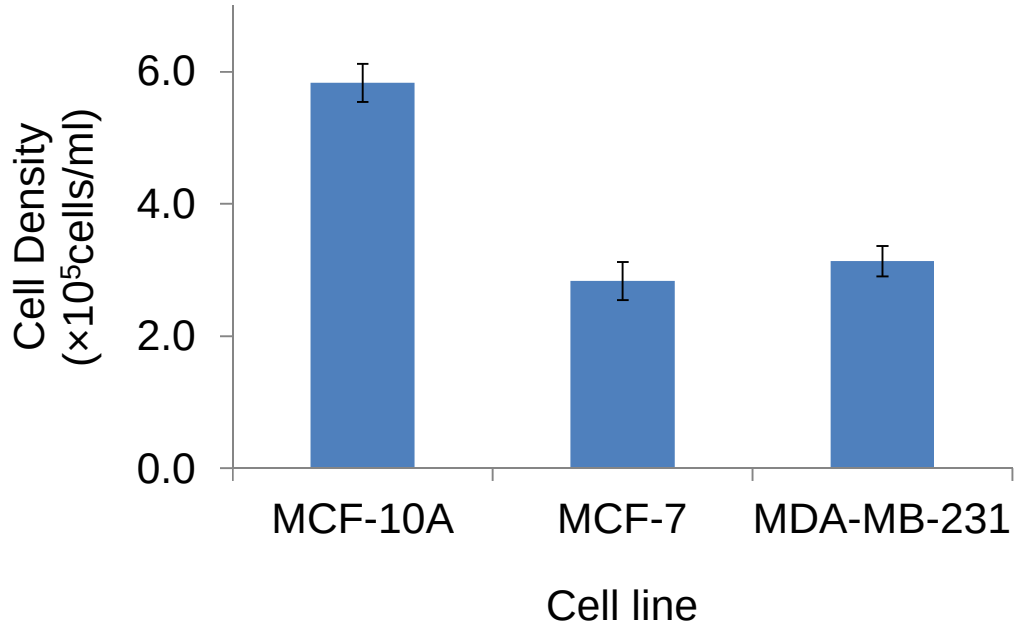

Figure 3.14 cell density at 20% packed cell volume of each cell line. After trypsinization, 10µl cell suspensions were loaded into a PCV tube and then centrifuged at 5000rpm for 1 minute. The packed cell volume in µl can be read from the PCV tubes. Cells were re-suspended at a density that resulted in them occupying 20% of the volume with remaining 80% consisting of buffer. Error bars represent standard deviation.

4 Bio-Impedance of cancer cell suspension for breast cancer cell identification

4.1 Introduction

In this chapter, whether different pathologies of breast cancer cells can be differentiated from breast tissue cells by Cell Impedance System (CIS) will be investigated.

4.2 Bio-Impedance measurement process

Breast tissue cell line MCF-10A, early breast cancer cell line MCF-7 and invasive breast cancer cell line MDA-MB-231 were cultured in several large flasks until at around 70% confluence. After cells were in suspension by trypsinization, cells were washed with DPBS and then removed. The modified buffer, 50%DPBS and 50% sterile water with 2% serum replacement, or isotonic media was used to re-suspend cells. Then cell suspensions were loaded into chambers and cell density, packed cell volume (PCV) were detected before and after each impedance measurement, as showed in Figure 4.1.

The cell impedance system was set up using an impedance analyser, Agilent 4194A controlled by a laptop through a GPIB-USB cable for data acquisition. The 4-terminal measurement device was plugged into the Agilent 4194A directly by four BNC connectors as shown in Figure 4.2. The 4-terminal measurement device was composed of two parts: the cylindrical chamber and the adapter. Two Platinum plated disc electrodes in the cylindrical chamber provided the current and another two Platinum needle electrodes were used for the voltage measurement. At the top of the cylindrical chamber, two holes were made for loading cell suspension.

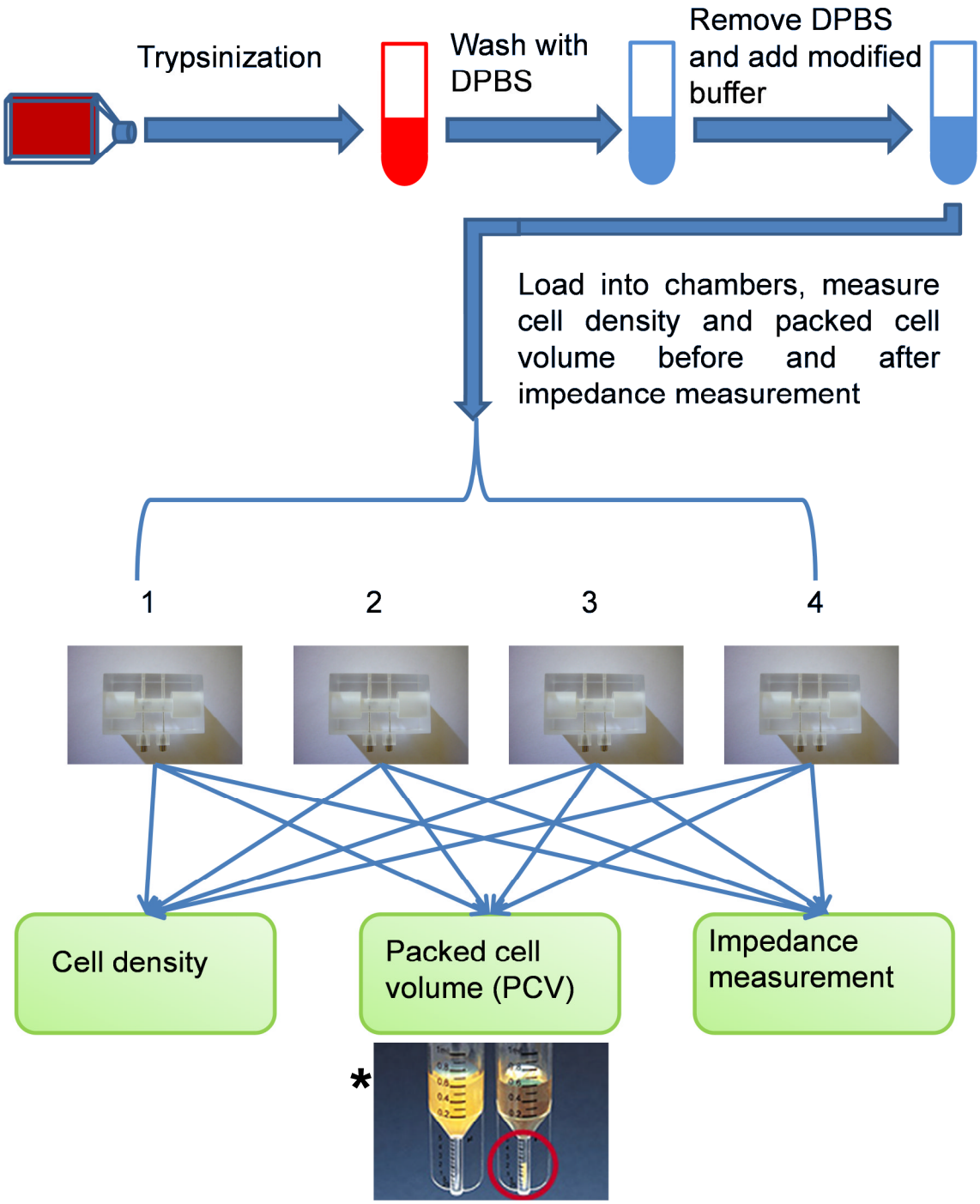

Figure 4.1 the schematic of experiments: every breast cell line was removed from culture plates by trypsinization, and then washed with DPBS and modified buffer or isotonic media, respectively. Cells were re-suspended with modified buffer and loaded into the chamber followed by cell density, packed cell volume and impedance measurement. (The picture with the asterisk was from http://www.tpp-us.com/docs/products/pcv_biomass_cell_counters.html)

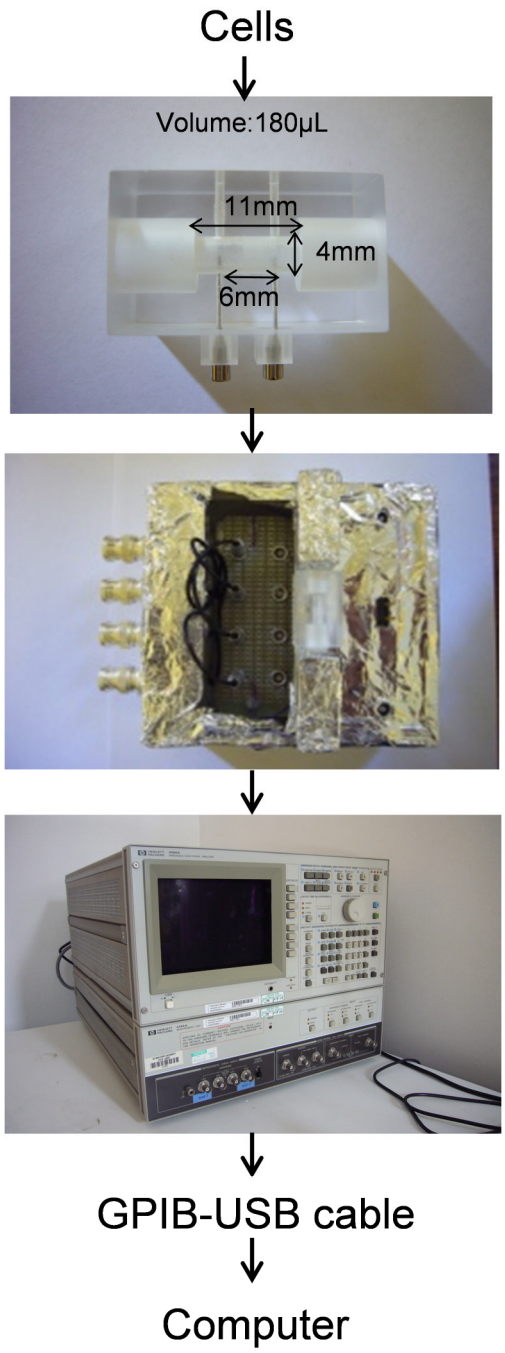

Figure 4.2 Cell impedance system. Cell impedance system is composed of the cylindrical chamber, the adapter with four BNC connectors and the impedance analyser controlled by a computer.

4.3 Cell density before and after each impedance measurement

Before and after each impedance measurement, cell density was measured to question whether cells were recovered. Figure 4.3 represents that the density of MCF-10A cells reduced by around 42%. It could be due to cells stuck onto the inner surface of the measurement cylindrical chamber or cell death. However, cell density of MCF-7 and MDA-MB-231 were almost the same as before impedance measurement. The small increase in cell density of MDA-MB-231 is due to variation in the experiment. In the isotonic media, cell density also varies in the three cell lines because of the same reason (Figure 4.4).

4.4 Electric model of cell suspension

In the study of cell impedance, a classic equivalent circuit model called the Cole-Cole model is used to reveal the alteration of cells. Membrane capacitance is an important electric property of cell membranes, where the impedance decreases with increasing frequency (Cole and Cole, 1941). A pure conductive solution shows a direct relationship between impedance and frequency between 1 kHz to 10 MHz.

According to the electric equivalent model (Cole and Cole, 1941), at low frequency (1kHz-20kHz) range the cell membrane performs as a pure resistor, the R_m (Membrane resistance) as shown in Figure 4.5A and the total measurement impedance is made up of R_b (Resistance from buffer) in the parallel with the sum of R_i (intra-cellular resistance) and R_m. This arises over low frequencies, with a small flow of current passed through cell membranes, the impedance of membrane capacitance C_m is very high. So cell membranes were considered as a good resistor and a part of current passed cell membrane R_m and intracellular R_i; the other part of current went through buffer R_b directly.

Due to the frequency dependence of the membrane capacitance C_m, when the frequency increases the membrane starts to be more conductive, which makes the total impedance decrease (Cole and Cole, 1941). Over high frequency range, greater than 1.5MHz, the membrane capacitance, C_m,

becomes a good conductor over high frequencies, which little impedes the flow of current and the capacitive impedance can be neglected compared to the resistance of the membrane R_m. In this case, the entire impedance is contributed only by the parallel combination of R_b and R_i.

Each type of cell has a specific combination of those parameters, R_i, R_m, C_m, which has been treated as a unique signature of cells for the identification of normal and cancer cells (Cole and Cole, 1941).

4.5 Bio-Impedance of breast cells

The impedance measurement of breast cell suspension were carried out in two different conditions which were in 50%DPBS and 50% sterile water with 2% serum replacement at 20°C, or in isotonic media at 37°C. The curve data shown in Figure 4.5B and 4.5C were calibrated. The raw data were read directly from the impedance analyser contained system errors. The calibration can remove those system errors.

Figure 4.5B shows that in 50%DPBS and 50% sterile water with 2% serum replacement at 20°C, normal breast cell line MCF-10A has lower impedance than other two breast cancer cell lines over all frequencies. There was no overlap between each cell line over low frequencies. The impedance of MDA-MB-231 cells has large error bars may be due to variation in size. It was clearly displayed that three cell lines can be differentiated by impedance. Over the middle range of frequencies, the dispersion phenomenon is the drop of impedance against frequency, thought to be caused by double layer structure of cell membranes acting as an capacitor (Cole and Cole, 1941). The membrane capacitance Cm was starting to become as a good conductor from a resistor as illustrated before, which dominated the impedance changes.

Over low frequency of Figure 4.5B, 1 kHz~30 kHz 10 values of each cell lines are used to calculate significance of the data. All the P Values are less than 0.05, which means that there is significant difference among impedance of three cell lines (Table 4.1). Membrane capacitance of each cell line also was calculated as Table 4.2 shown. Cell impedance, cell diameter and packed cell volume were very important factors in calculations. MCF-10A cells have highest

membrane capacitance. MDA-MB-231 cells have lowest C_m among three cell lines. The equations were provided by Dr Guofeng Qiao (Qiao, 2011).

Table 4.1 Student Ttest of 10 impedance values at low frequency (in modified buffer at 20°C)

Test	P Value
MCF-10A against MCF-7	1.1E-15
MCF-10A against MDA-MB-231	2.5E-19
MCF-7 against MDA-MB-231	7.2E-18

Table 4.2 Membrane capacitance of cells from the equivalent circuit model (in modified buffer at 20°C)

	Cm (μF/ cm^2)	SD
MCF-10A	3.0	0.4
MCF-7	1.1	0.1
MDA-MB-231	0.9	0.1

*The results were calculated from a series of equations which were provided by Dr Guofeng Qiao (Qiao, 2011).

Figure 4.5C indicates that in the isotonic media at 37°C, normal breast cell line MCF-7 has lower impedance than other two breast cancer cell lines at all frequencies. MDA-MB-231 cells still have the highest impedance among three cell lines. Also, the dispersion can be observed at middle range frequency.

Over low frequency of Figure 4.5C, 1 kHz~30 kHz 10 values of each cell lines are used to calculate significance of the data. Though the error bars are overlapping, all the P Values are still less than 0.05, which shows the significant difference among impedance of three cell lines (Table 4.3). Membrane capacitance of each cell line also was calculated as Table 4.4 shown. MCF-10A cells have highest membrane capacitance. MCF-7 cells have lowest C_m among three cell lines.

Table 4.3 Student Ttest of 10 impedance values at low frequency (in isotonic media at 37°C)

Test	P Value
MCF-10A against MCF-7	9.1E-18
MCF-10A against MDA-MB-231	7.5E-10
MCF-7 against MDA-MB-231	2.7E-16

Table 4.4 Membrane capacitance of cells from the equivalent circuit model (in isotonic media at 37°C)

	Cm (μF/ cm^2)	SD
MCF-10A	4.3	0.2
MCF-7	3.7	0.5
MDA-MB-231	0.9	0.5

*The results were calculated from a series of equations which were provided by Dr Guofeng Qiao (Qiao, 2011).

4.6 Transmission electron micrographs of breast cells

To investigate what may cause the impedance difference in different pathologies of breast cells, the transmission electron micrographs were taken. Figure 4.6 clearly show that MCF-10A cells had spherical nuclear envelope. However, for MCF-7 cells nuclear envelope were not as circular as MCF-10A. MDA-MB-231cells had nuclear envelope irregular.

The nuclear circularity of TEM photos of each cell line were analysed by using the Image J software. The nuclear circularity of MDA-MB-231 had significant difference compared to MCF-10A and MCF-7, respectively (Figure 4.7). Thanks Dr Julian Thorpe for the TEM section and TEM photographing.

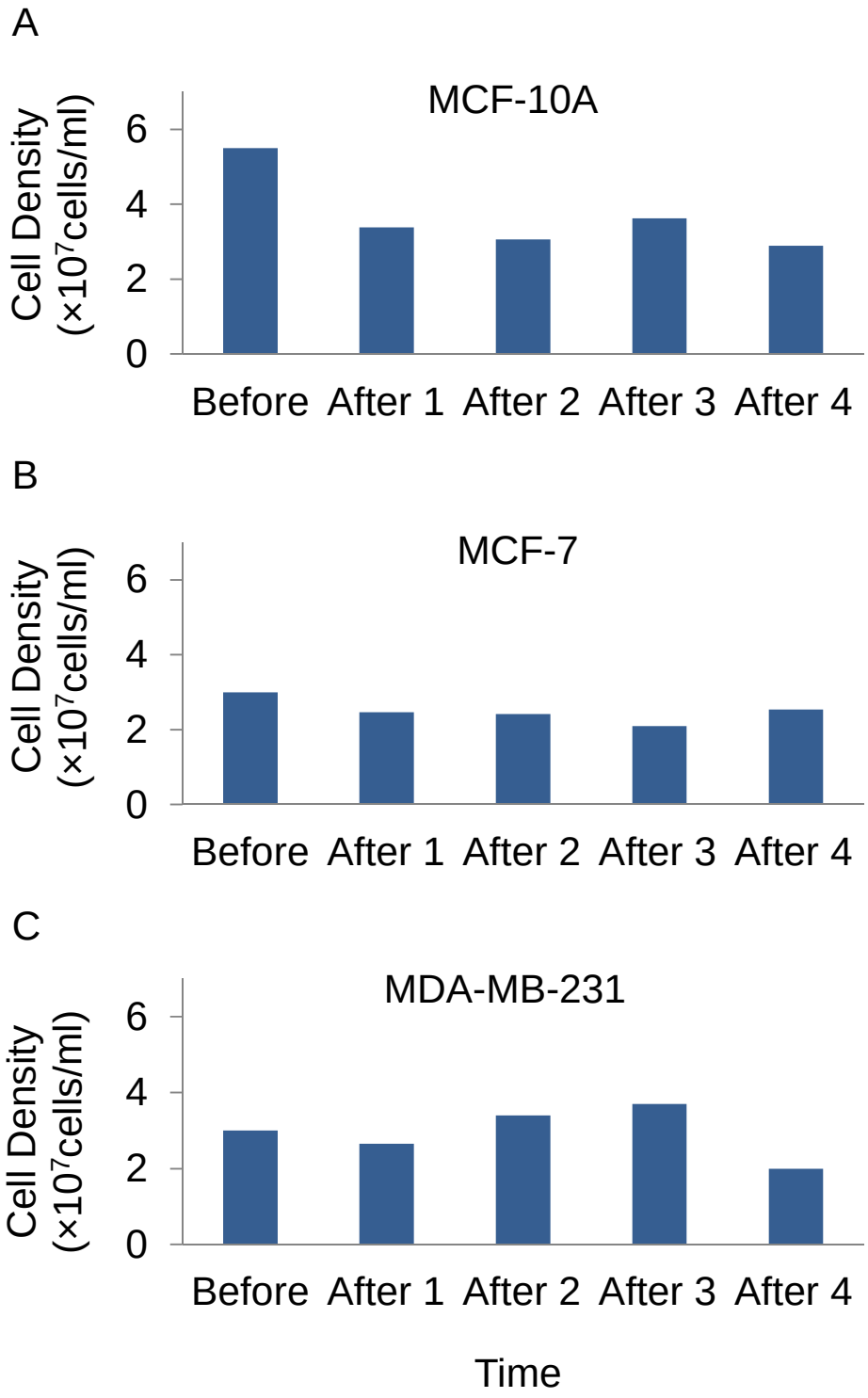

Figure 4.3 Cells viability test before or after four impedance measurement. Cells were incubated in 50% DPBS and 50% sterile water with 2% serum replacement. Cell densities were measured after each measurement.

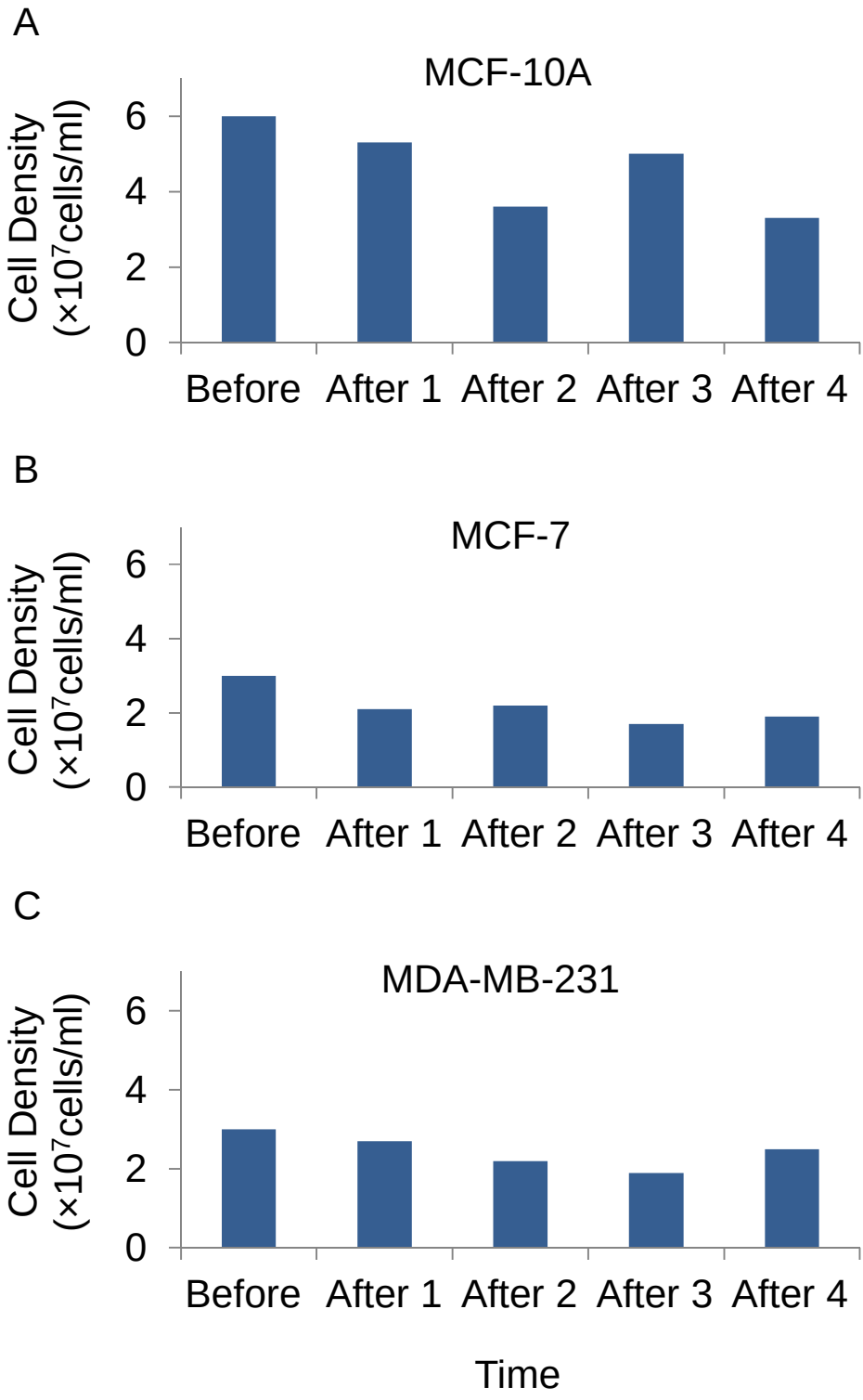

Figure 4.4 Cells viability test before or after four impedance measurement. Cells were incubated in isotonic media. Cell densities were measured after each impedance measurement. Cell densities were measured after each measurement.

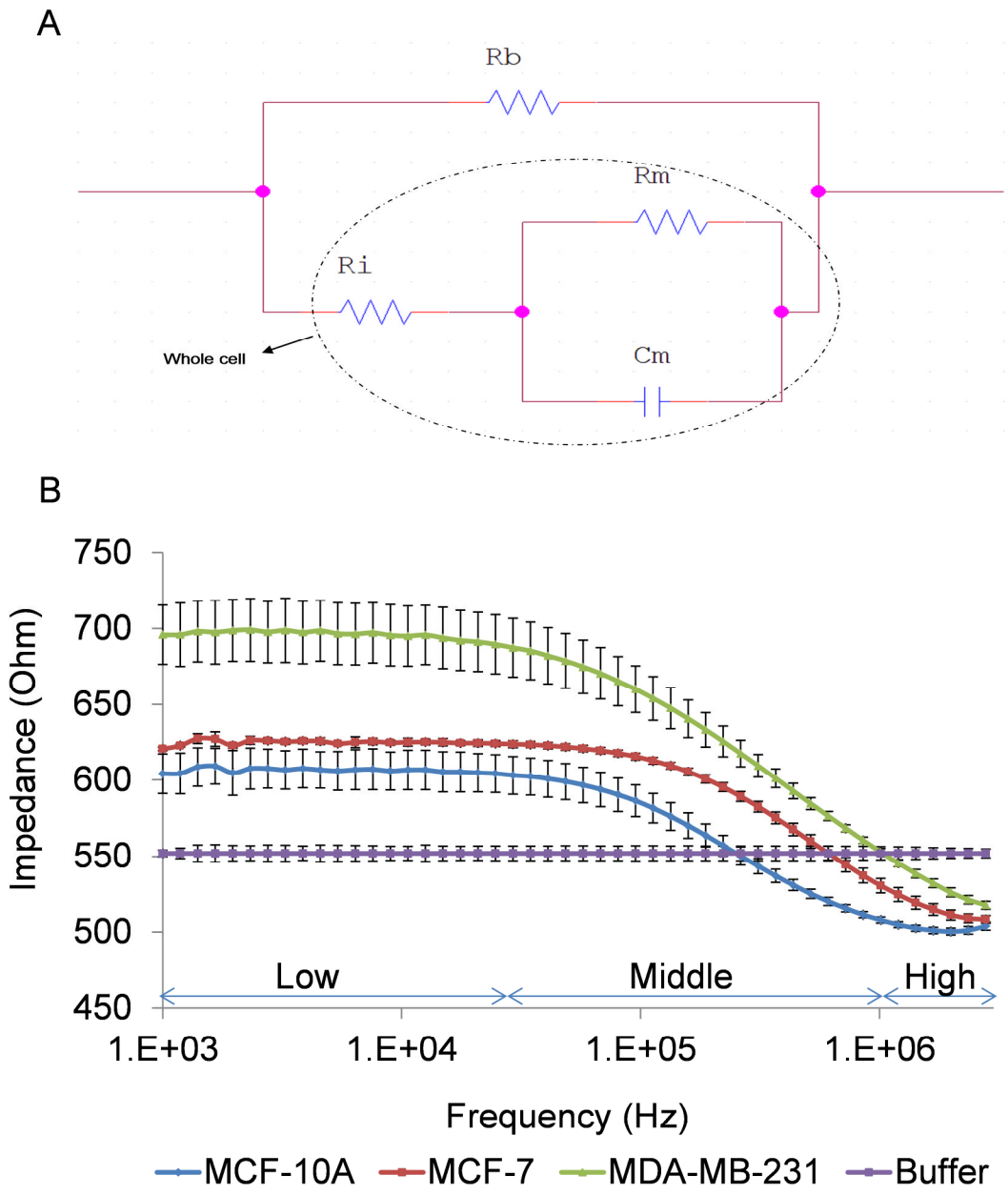
A
Rb
Rm
Ri
Cm
Whole cell
B
Impedance (Ohm)
750
700
650
600
550
500
450
Low
Middle
High
1.E+03
1.E+04
1.E+05
1.E+06
Frequency (Hz)
MCF-10A
MCF-7
MDA-MB-231
Buffer

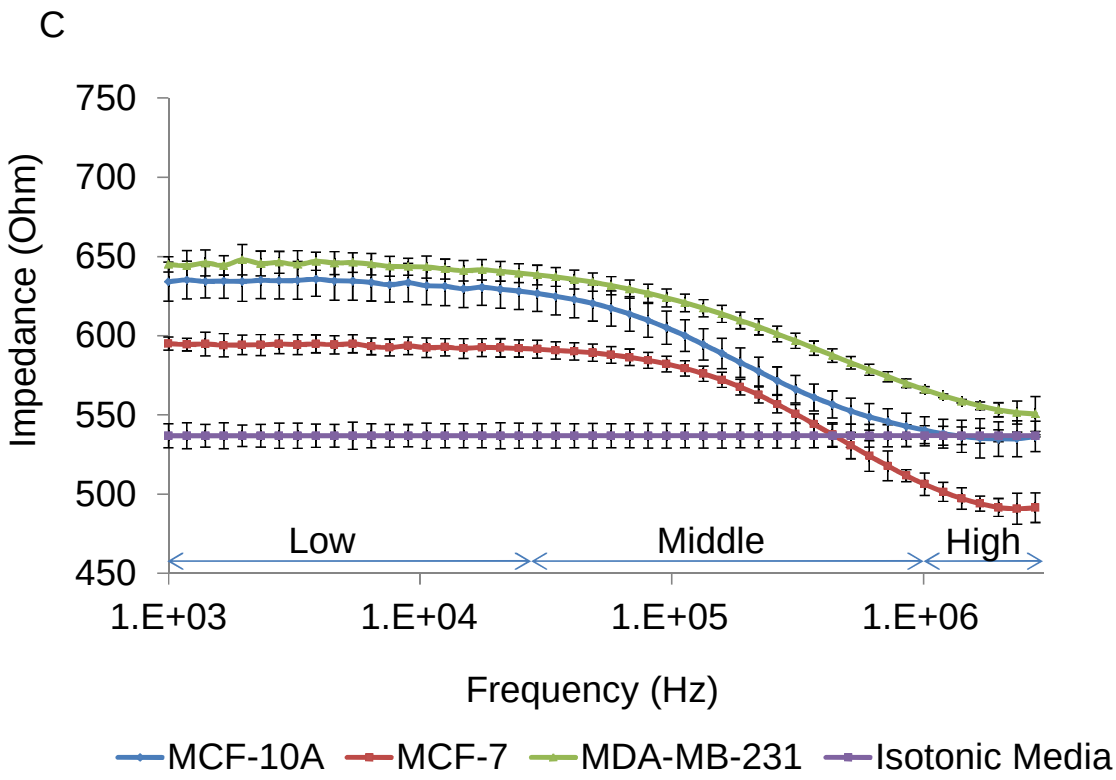

Figure 4.5 A is an electric equivalent circuit model for cell impedance analysis of a cell. R_b is the resistance from buffer, R_i is the intra-cellular resistance. R_m and C_m are the membrane resistance and capacitance, respectively. B represents that the impedance of four breast cells lines measured using an Impedance Analyser at same volume ratio 20%(v/v) at 20°C. The buffer is 50% sterile water and 50% DPBS with 2% serum replacement. C was measured in the isotonic media at 37°C. X axis is frequency and Y axis is impedance. Error bars represent standard deviation from four impedance measurements.

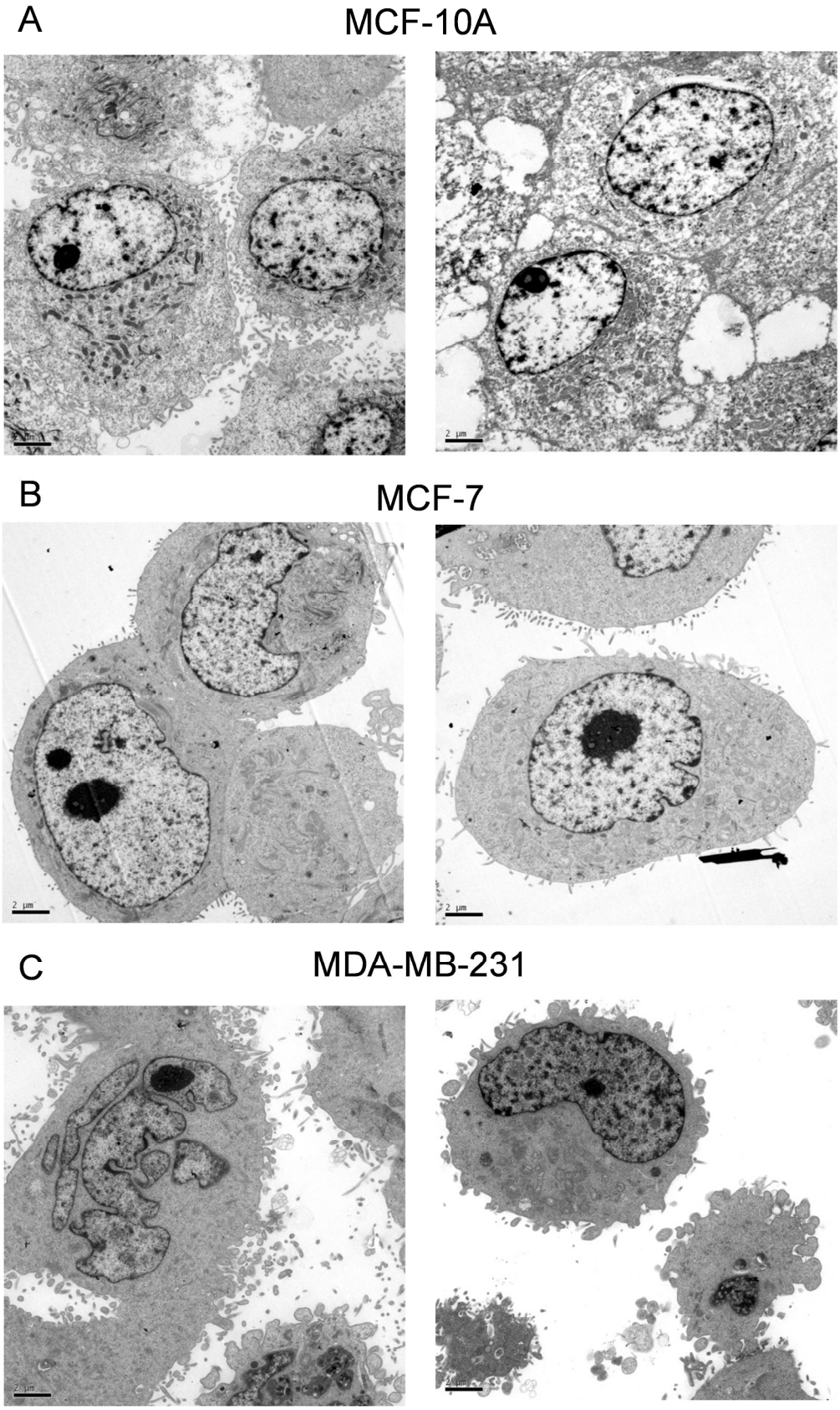

Figure 4.6 Transmission electron micrographs of MCF-10A, MCF-7 and MDA-MB-231 cells. Cells were removed from culture plates by trypsinization. The scale bar is 2 nm. Thanks Dr Julian Thorpe for the TEM section and TEM photographing.

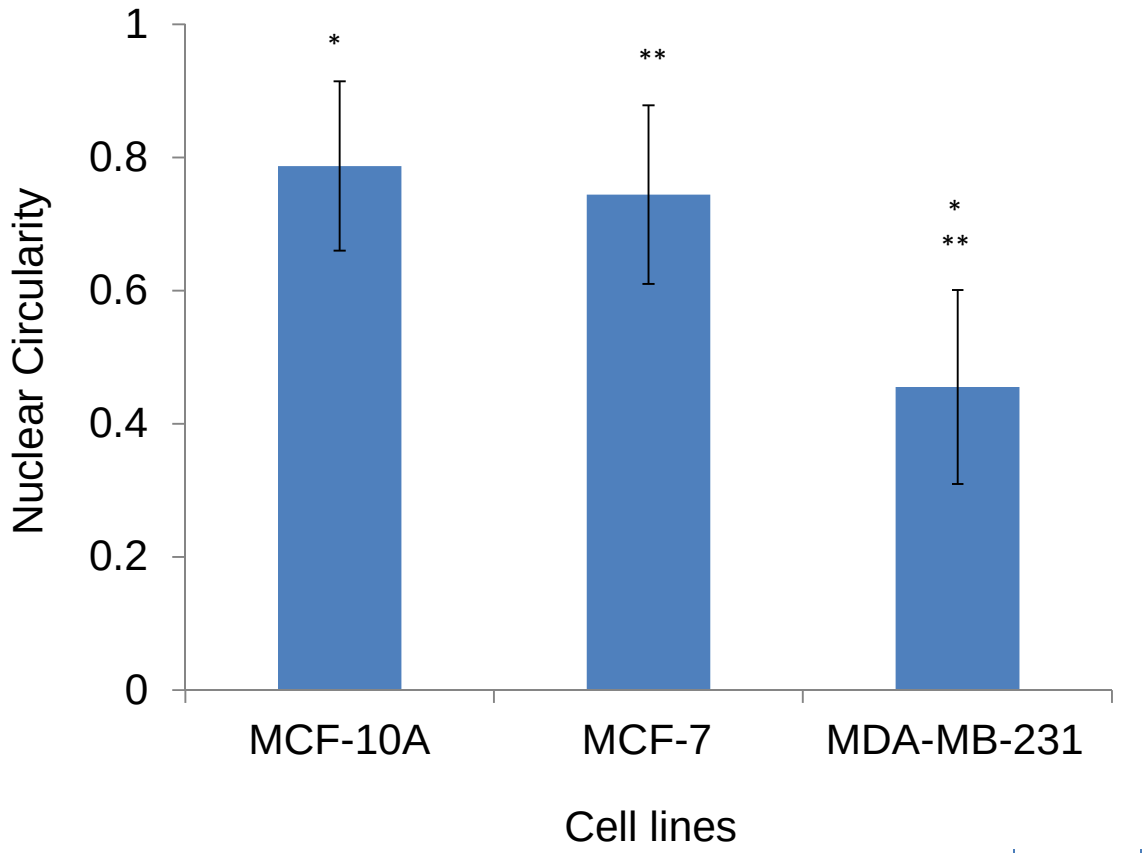

Figure 4.7 Nuclear circularity of MCF-10A, MCF-7 and MDA-MB-231cells. The TEM micrographs were analysed by using Image J. The circularity of a circle is 1. X axis is cell lines and Y axis is nuclear circularity. The student Ttest as indicated (*,**) shows p value <0.05. Error bars represent standard deviation.

5 Bio-impedance of Jurkat 6 cell suspension for apoptosis identification

5.1 Introduction

As described in Chapter Four, CIS can distinguish breast cancer cell from breast tissue cells. Another question will be investigated in depth is whether cell undergoing apoptosis and normal growing cells also can be distinguished by CIS.

Cancer cells contain more apoptotic cells (Holland and Frei, 2000). The application of chemotherapy reagent will induce cells apoptosis (Hannun, 1997). To question whether cell impedance is able to differentiate cells apoptosis or normal growth cells, Etoposide, a chemotherapy reagent, is used to induce apoptosis (Kaufmann, 1989). It is widely used to treat many types of cancer including breast cancer and lymphoma. In cell division, the topoisomerases II is needed to unwind the DNA helix. The topoisomerases II can cut both strands of the DNA helix. Cancer cells grow fast so they need more the topoisomerase II than normal cells. Etoposide inhibits the topoisomerase II. If the topoisomerase II is inhibited, cells stop dividing (Kellner *et al.*, 2002) .

5.2 Fluorescent Activated Cell Sorting (FACS)

Four phases are consisted of cell cycle G1 phase, S phase, G2 phase and M phase. In G1 phase, cells increase size and are ready for synthesis; DNA replicate in S phase; Cells complete synthesis and are ready to divide in G2 phase; in M phase, cells split.

Fluorescent activated cell sorting is a method to observe cell cycle profile by a Flow cytometry. A distribution of cell in Sub G1, G1, S and G2 phase can be plotted. Sub G1 is fractional DNA content, which are apoptotic cells. The cleavage of chromosome DNA into fragments is one of the features of apoptosis.

DMSO treatment cells were measured as control cells as Etoposide is dissolved in DMSO. Cells were analysed by a FACS CANTO flow cytometry which shows DNA contents in cells. Figure 5.1 and Figure 5.2 shows that compared with DMSO and Etoposide treated DG75 cells, from 24 hours cell cycle changes occurred and more than 60% of cells accumulate in G2 phase. Similarly, Figure 5.3 and Figure 5.4 represent that around 30% of Jurkat 6 cells apoptosis. Etoposide induced DG 75 and Jurkat 6 cells apoptosis.

Different from lymphoma cells, with the same dose of Etoposide treatment, cell cycle profile of G2 phase almost doubled as that at 0 hour time point in MCF-10A cells (Figure 5.5 and Figure 5.6). Figure 5.7 and Figure 5.8 display that Etoposide did not influence MCF-7 cells. Around 25% cells apoptosed in MDA-MB-231 cells and the percentage of cells in S phase increased from 6.5% to 23.3% (Figure 5.9 and Figure 5.10). Etoposide can slightly change cell cycle of breast cells

5.3 Using AlamarBlue Assay to indicate apoptosis

AlamarBlue Assay is another method to indicate cells apoptosis. AlamarBlue is a proven indicator of cell viability. The living cells can reduce resazurin to resorufin, the fluorescent molecule. The alamarBlue is a blue, nontoxic, virtually non-fluorescent cell permeable compound. In the living cells, resazurin is reduced to resorufin, which generates high intensity of red fluorescence (LifeTechnologies, 2012). The higher florescent intensity indicates healthy cells. The amount of resorufin decreased in cells apoptosis. So the intensity of fluorescence declines.

After incubation with 10μL AlamarBlue for 5 hours, Jurkat 6 cells measured fluorescent intensity by using fluorometer (Promega GloMax-Multi Detection System). The florescent intensity of DMSO treated Jurkat 6 cells increased at 24 hours, which indicates cells were growing. However, there was a dramatically drop in Etoposide treatment from 24 hours. Even at 72 hours the florescent intensity cannot be observed as shown in Figure 5.11.

MCF-10A, MCF-7 and MDA-MB-231cells were trypsinazed and placed in 96-well plate at density of $2X10^5$ cells/well. After added 10μL AlamarBlue, the

plate was incubated for 5 hours and then measured fluorescent intensity by using fluorometer. Figure 5.12 shows that with the increasing time, the florescent intensity of Etoposide groups were as high as control groups in all three cell lines, which is unexpected.

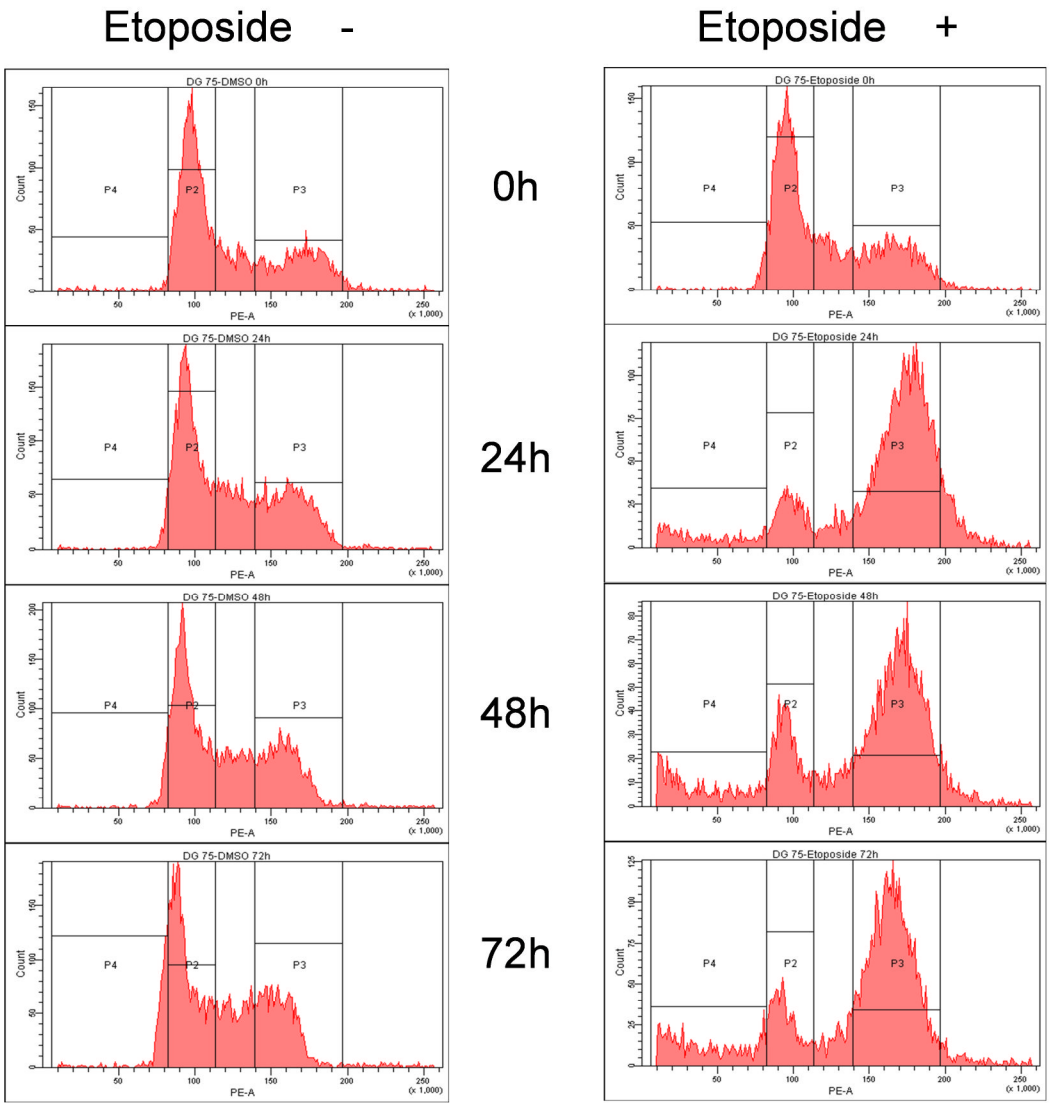

Figure 5.1 Effect of Etoposide on cell cycle profile of DG75 cells. Lymphoma cells DG75 were treated with or without Etoposide, harvested at 0h, 24h, 48h and 72h and dyed by Propidium Iodide (PI) Stain. Cells were analysed by FACS CANTO. The graphs show DNA changes in cell cycle. The relative DNA content is shown on the X axis and the number of cells containing that content on the Y axis. Cell with a G1 (P2), G2/ M (P3) or apoptotic content of DNA are shown.

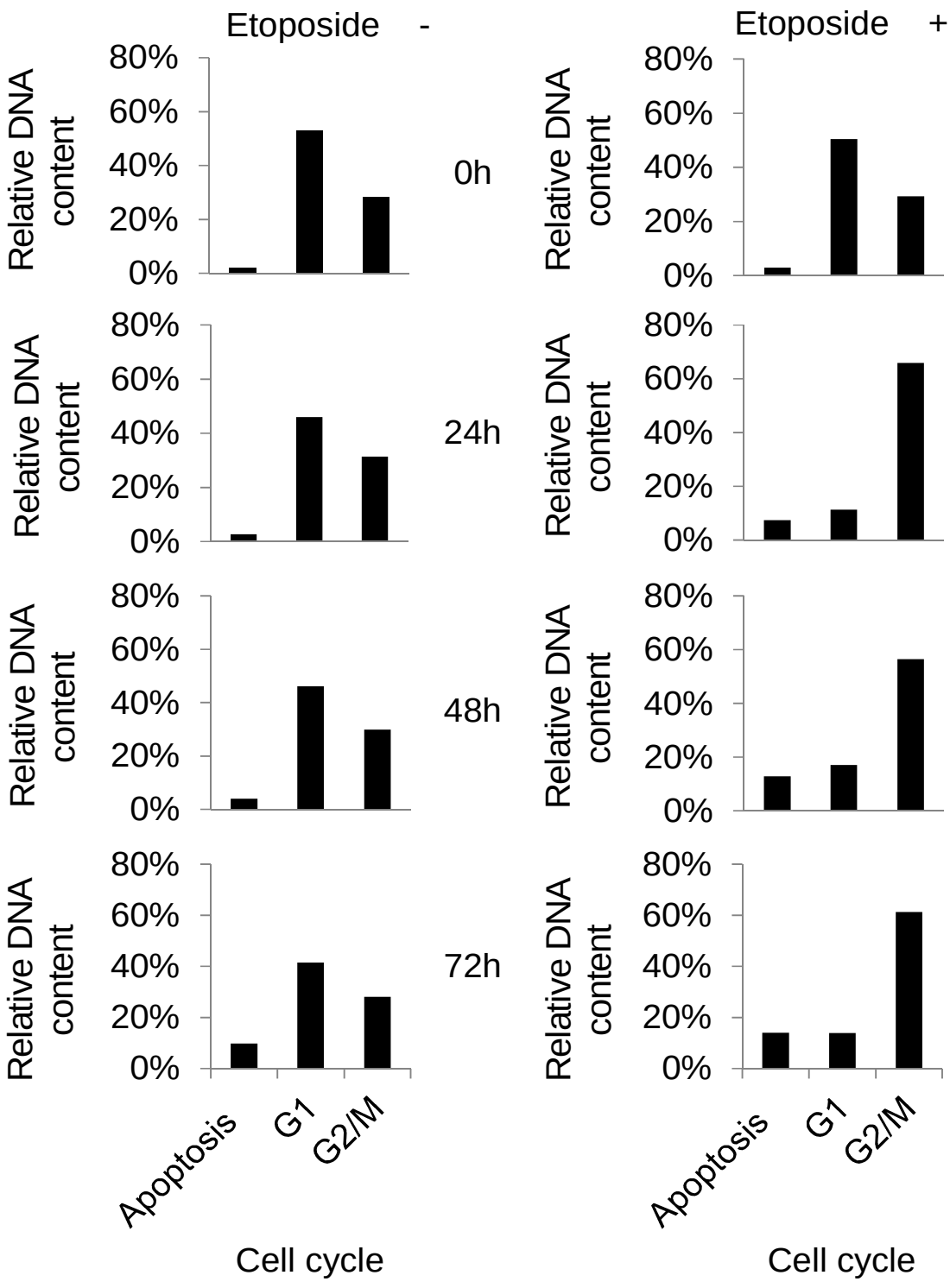

Figure 5.2 The histograms of FACS.results of DG75. X axis is cell cycle and Y axis is the relative DNA content.

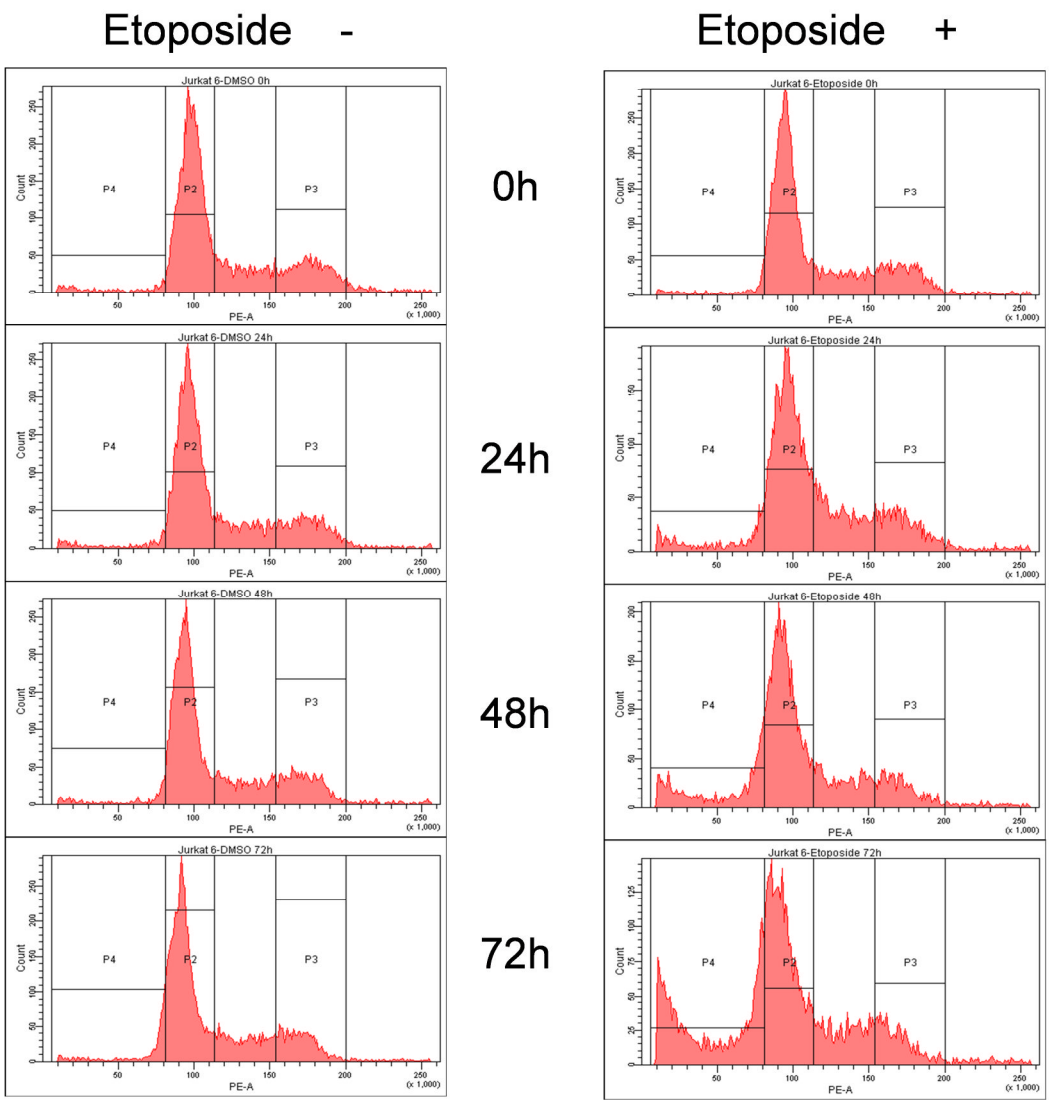

Figure 5.3 Effect of Etoposide on cell cycle profile of Jurkat 6 cells. Lymphoma cells Jurkat 6 were treated with or without Etoposide, harvested at 0h, 24h, 48h and 72h and dyed by Propidium Iodide (PI) Stain. Cells were analysed by FACS CANTO. The graphs show DNA changes in cell cycle. The relative DNA content is shown on the X axis and the number of cells containing that content on the Y axis. Cell with a G1 (P2), G2/M (P3) or apoptotic content of DNA are shown.

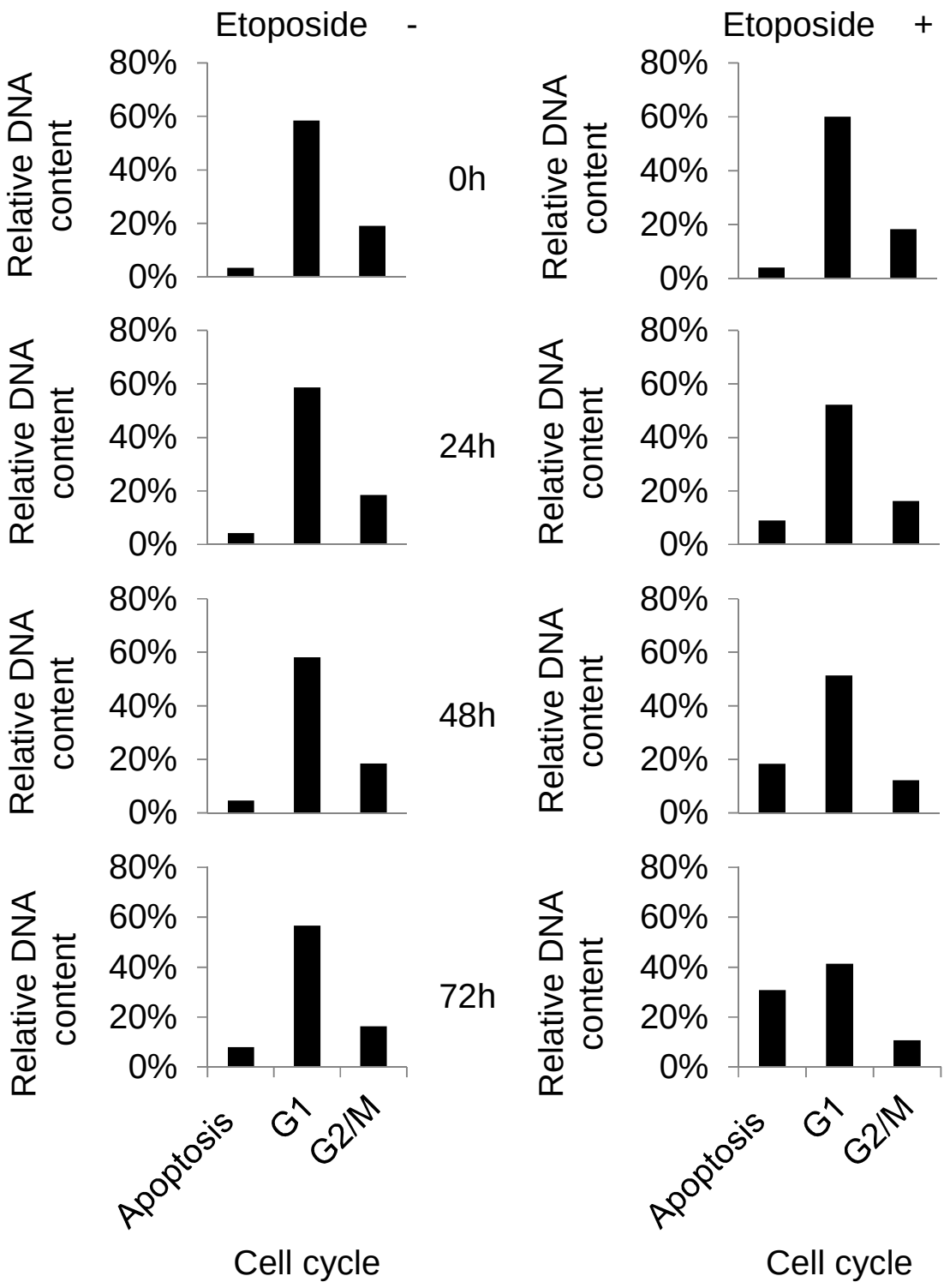

Figure 5.4 The histograms of FACS.results of Jurkat 6. X axis is cell cycle and Y axis is the relative DNA content.

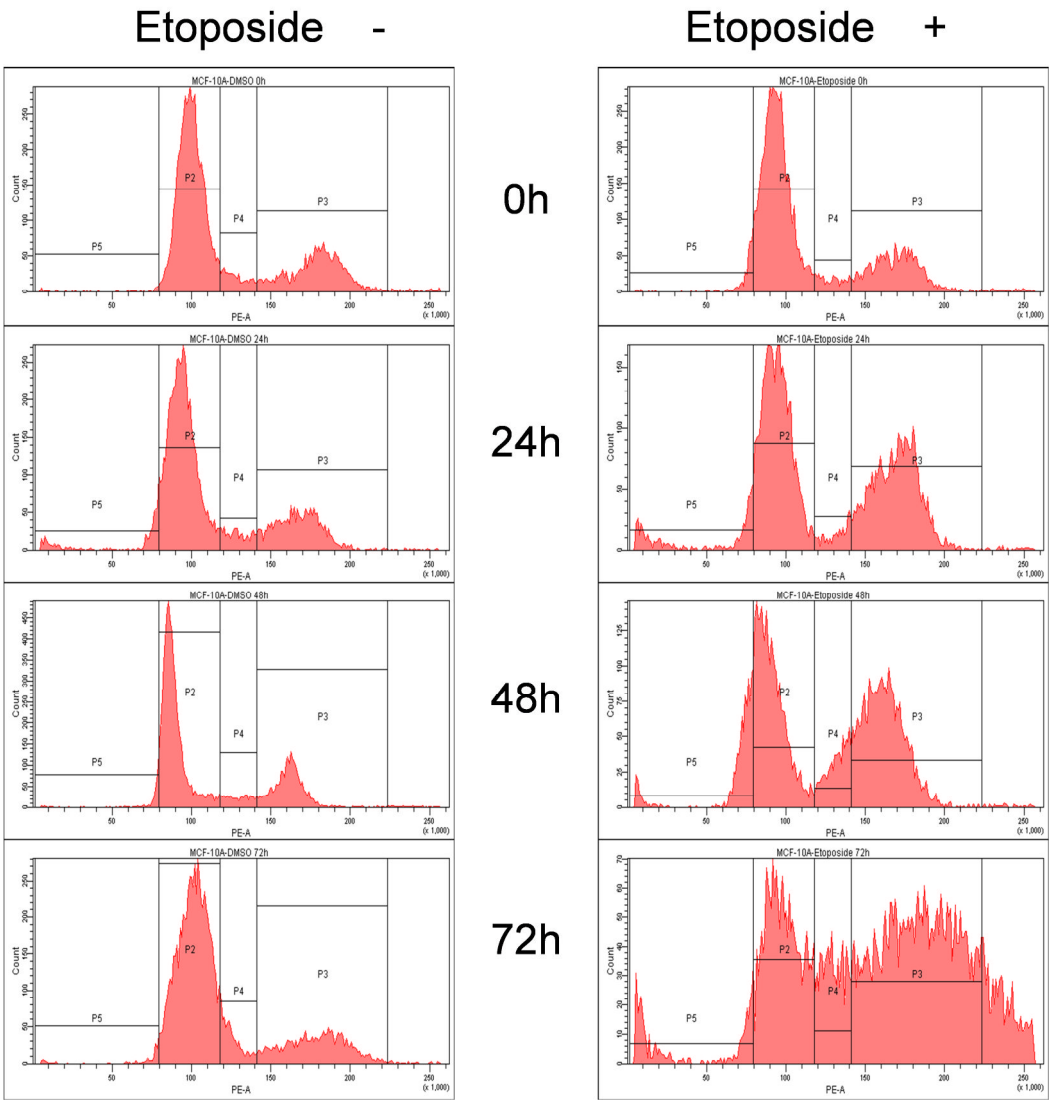

Figure 5.5 Effect of Etoposide on cell cycle profile of MCF-10A cells. Breast tissue cells MCF-10A were treated with or without Etoposide, harvested at 0h, 24h, 48h and 72h and dyed by Propidium Iodide (PI) Stain. Cells were analysed by FACS CANTO. The graphs show DNA changes in cell cycle. The relative DNA content is shown on the X axis and the number of cells containing that content on the Y axis. Cell with a G1 (P2), G2/M (P3) or apoptotic content of DNA are shown.

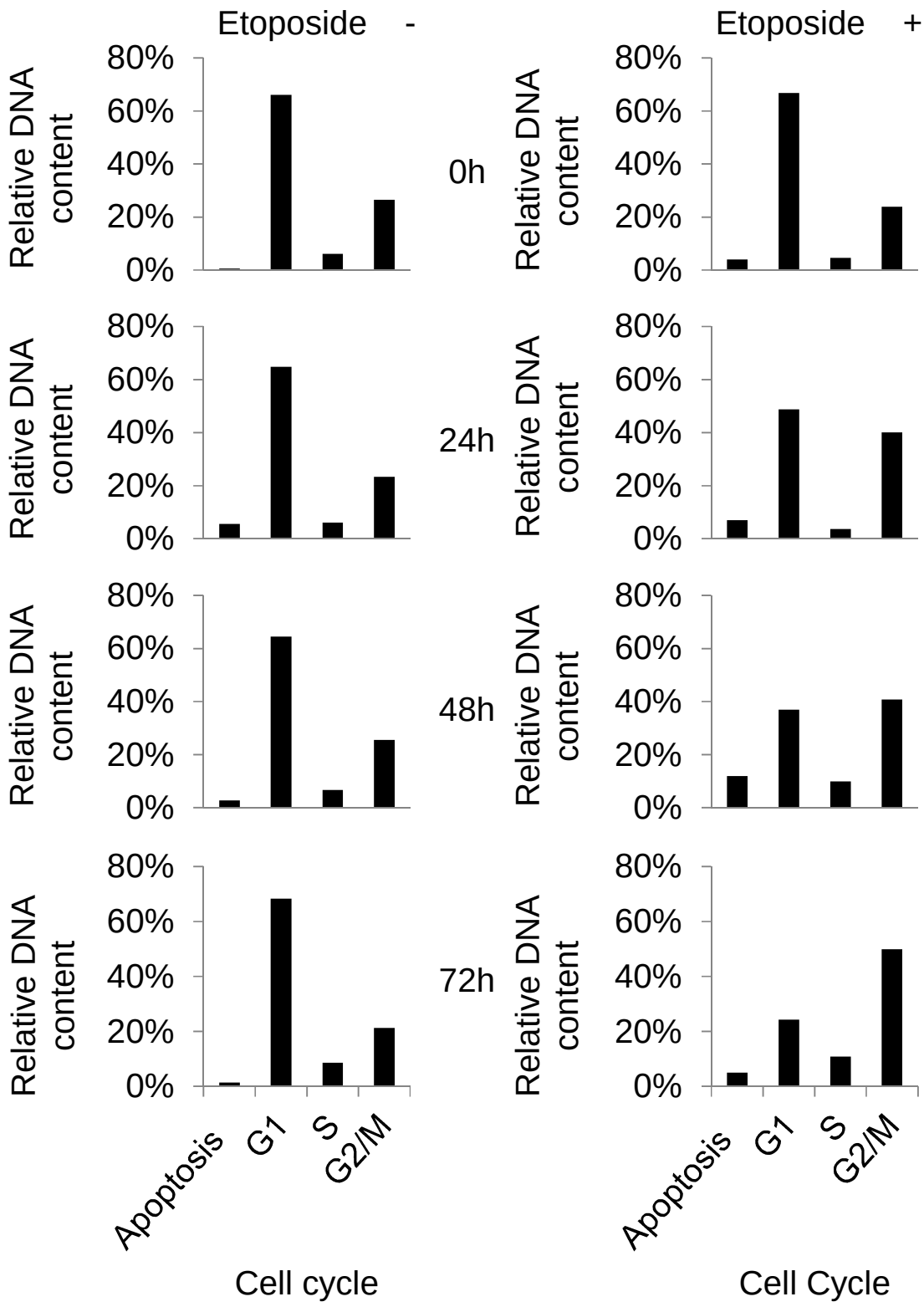

Figure 5.6 The histograms of FACS.results of MCF-10A. X axis is cell cycle and Y axis is the relative DNA content.

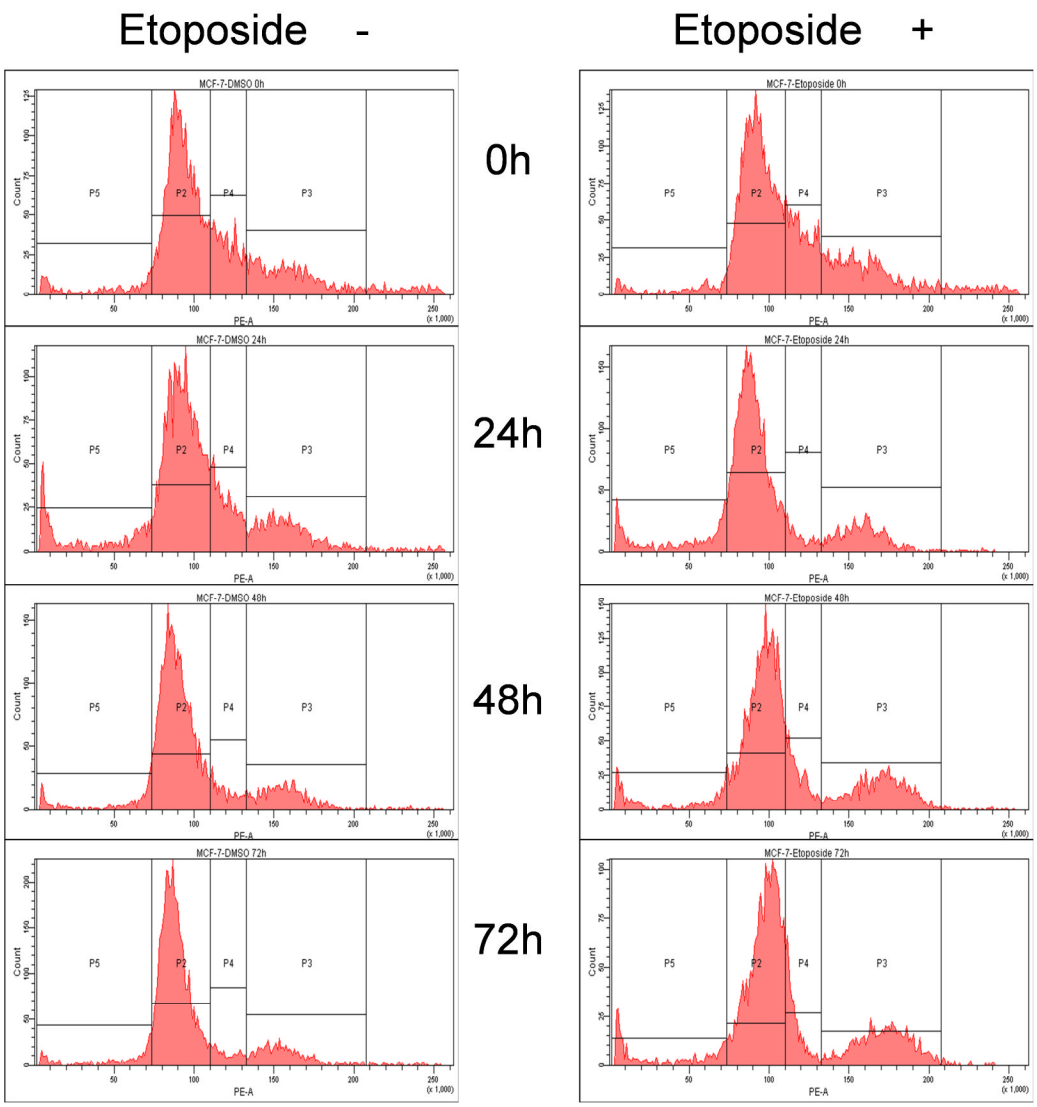

Figure 5.7 Effect of Etoposide on cell cycle profile of MCF-7 cells. Breast cancer cells MCF-7 were treated with or without Etoposide, harvested at 0h, 24h, 48h and 72h and dyed by Propidium Iodide (PI) Stain. Cells were analysed by FACS CANTO. The graphs show DNA changes in cell cycle. The relative DNA content is shown on the X axis and the number of cells containing that content on the Y axis. Cell with a G1 (P2), G2/M (P3) or apoptotic content of DNA are shown.

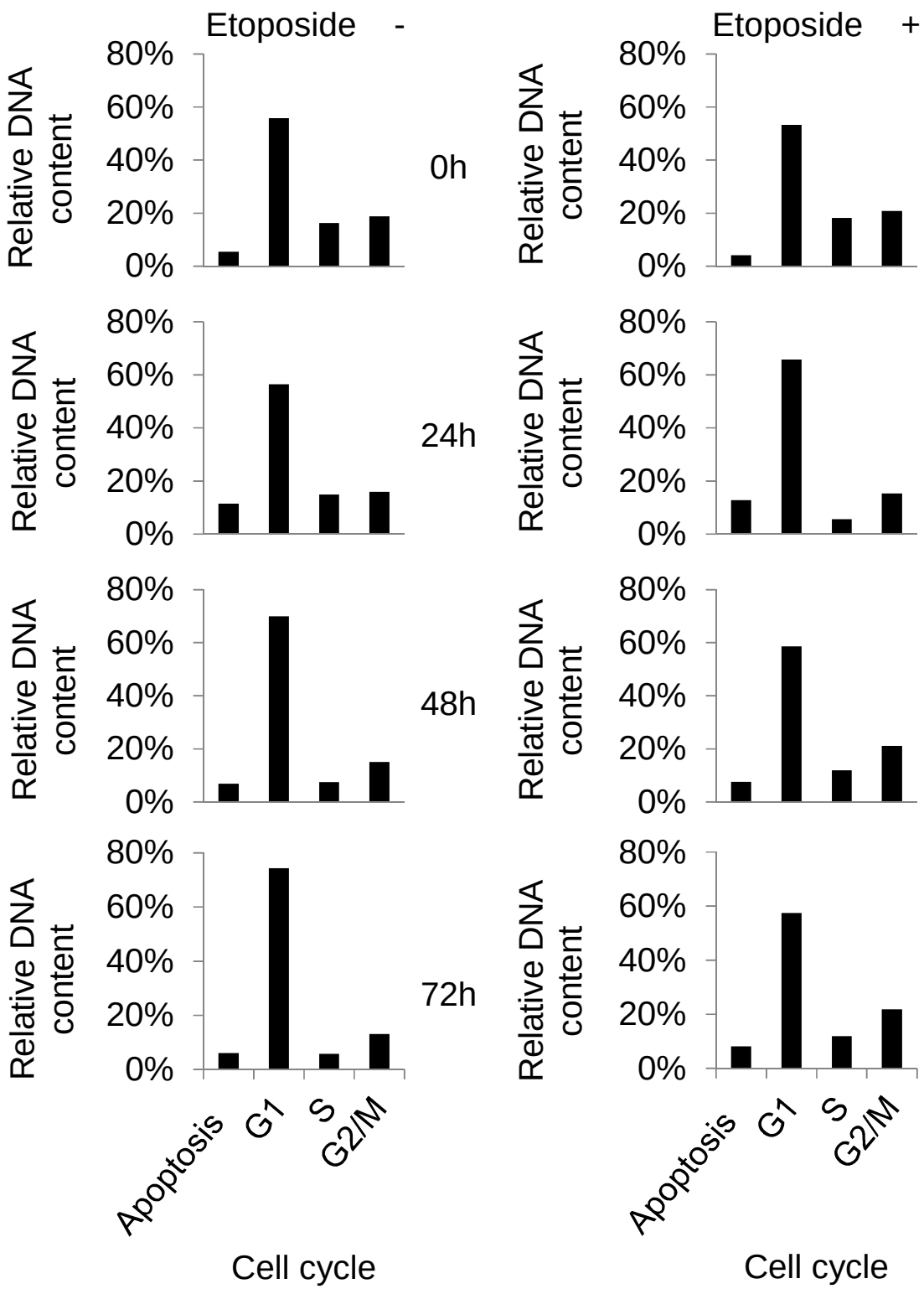

Figure 5.8 The histograms of FACS.results of MCF-7. X axis is cell cycle and Y axis is the relative DNA content.

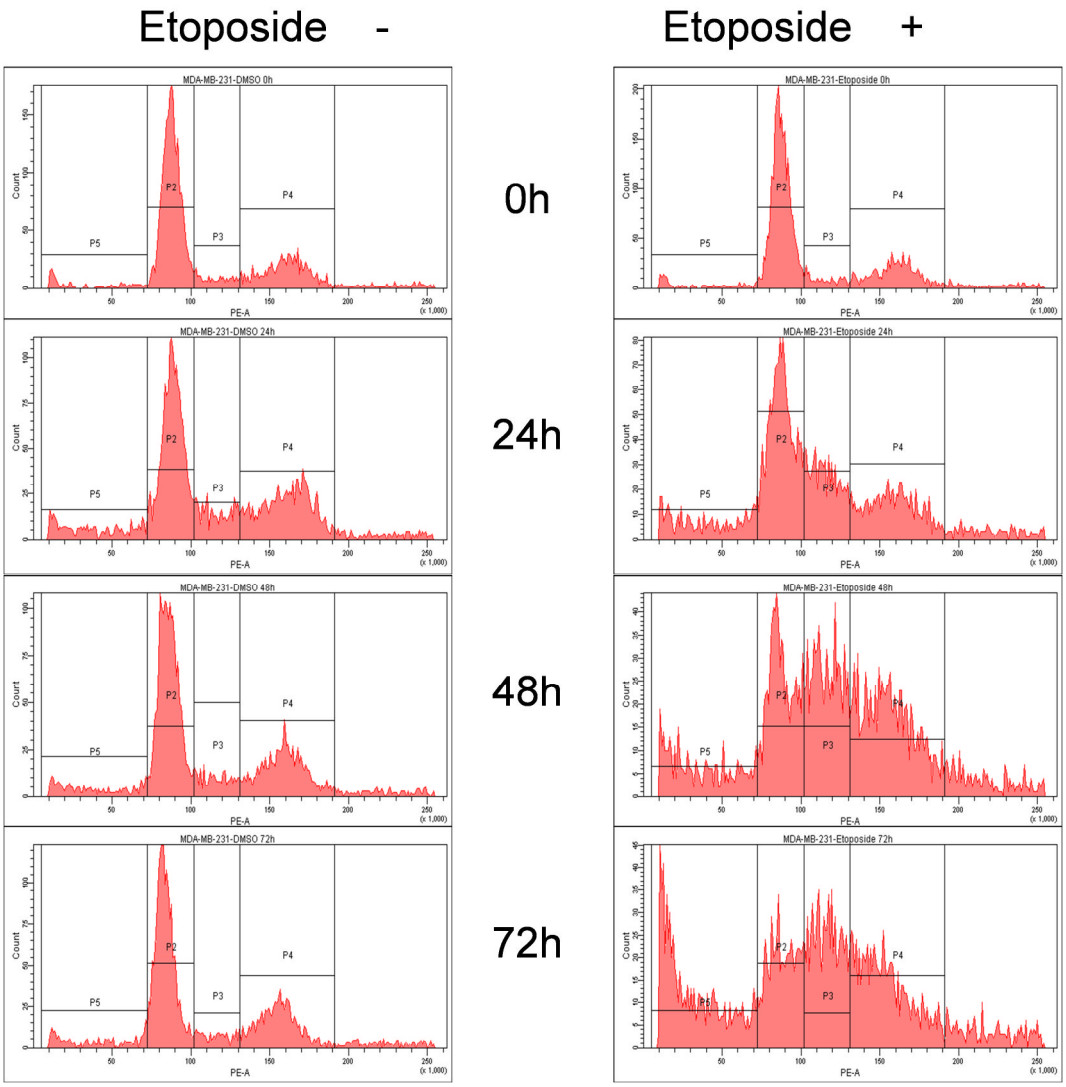

Figure 5.9 Effect of Etoposide on cell cycle profile of MDA-MB-231 cells. Breast cancer cells MDA-MB-231 were treated with or without Etoposide, harvested at 0h, 24h, 48h and 72h and dyed by Propidium Iodide (PI) Stain. Cells were analysed by FACS CANTO. The graphs show DNA changes in cell cycle. The relative DNA content is shown on the X axis and the number of cells containing that content on the Y axis. Cell with a G1 (P2), G2/M (P3) or apoptotic content of DNA are shown.

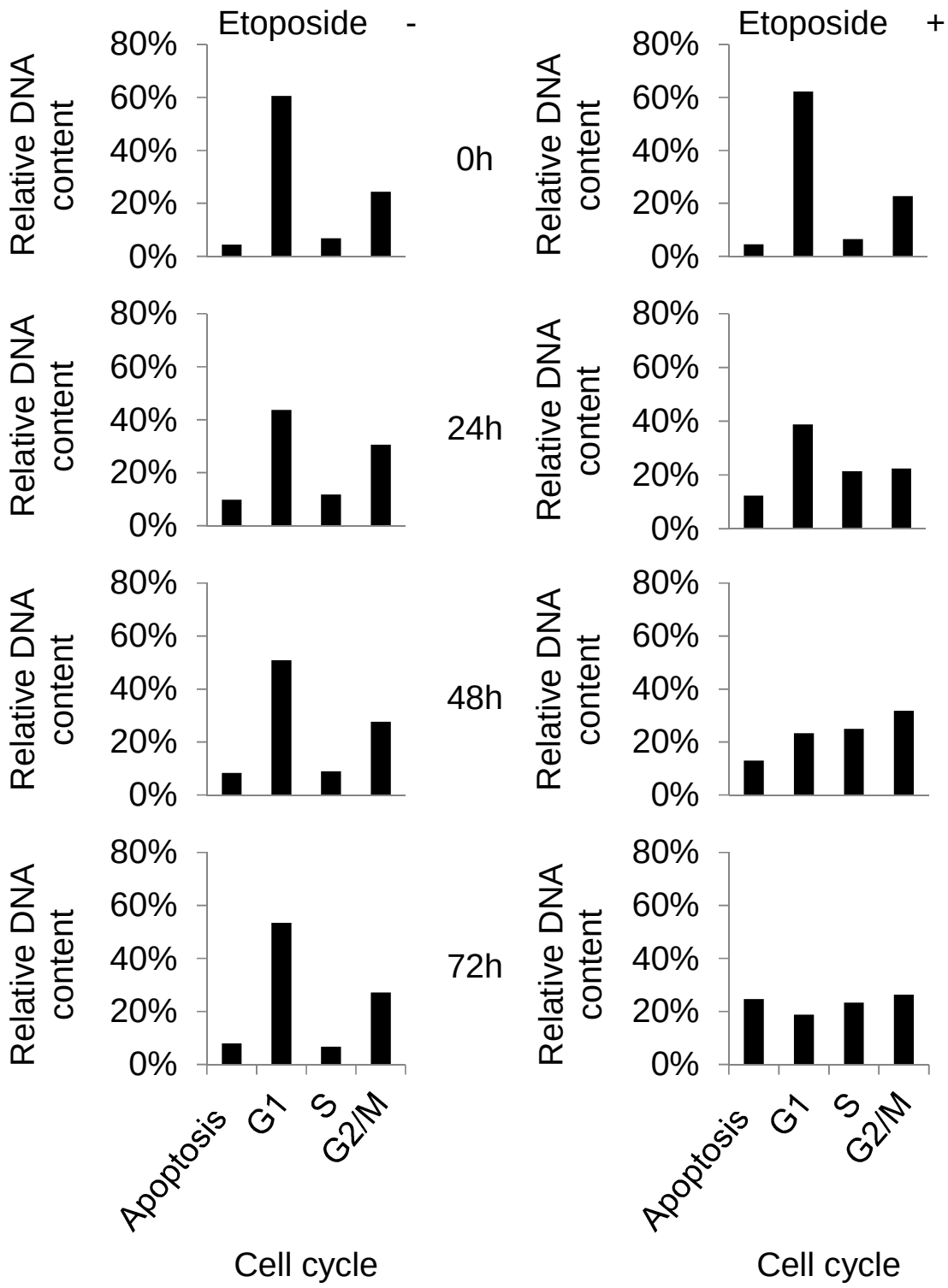

Figure 5.10 The histograms of FACS.results of MDA-MB-231. X axis is cell cycle and Y axis is the relative DNA content.

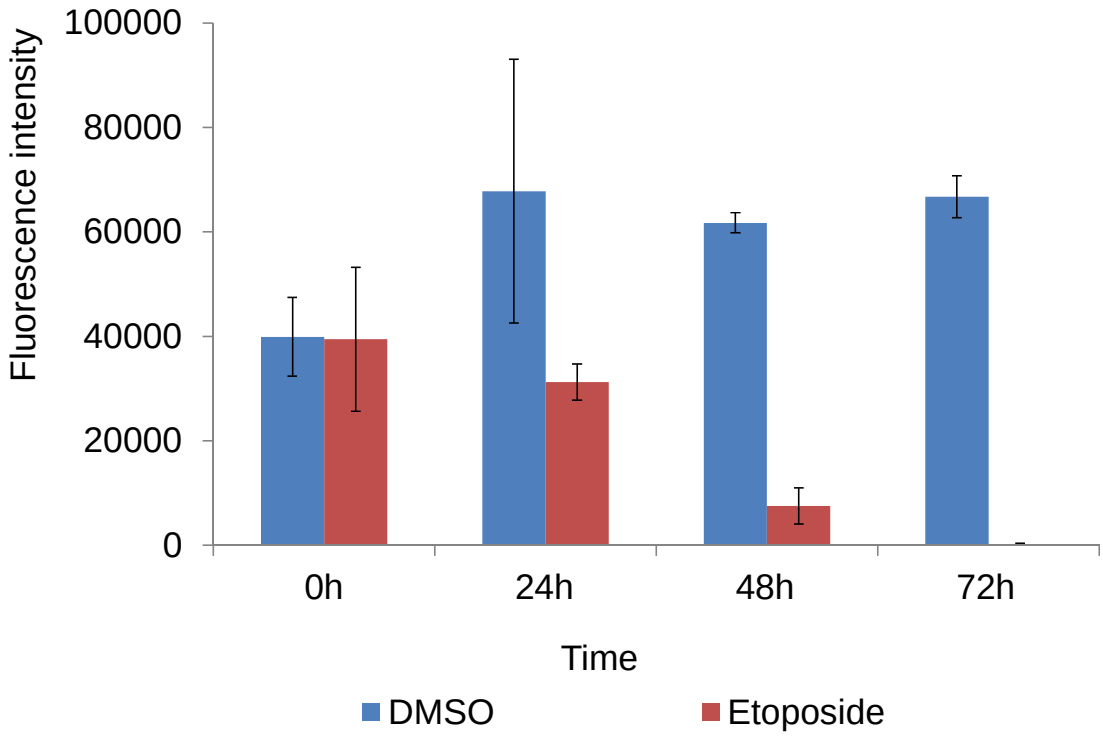

Figure 5.11 $3X10^5$ cells/ml of Jurkat 6 cells were either treated or untreated with Etoposide at 37°C. 100ml of cells were harvest at the indicate time point with 10μL of AlamarBlue incubated for 5 hours and then measured fluorescent intensity by using fluorometer with an excitation wavelength of 560nm and an emission wavelength of 590nm. The fluorescence intensity of blank control which was culture media with AlamarBlue was subtracted. Error bars represent standard deviation.

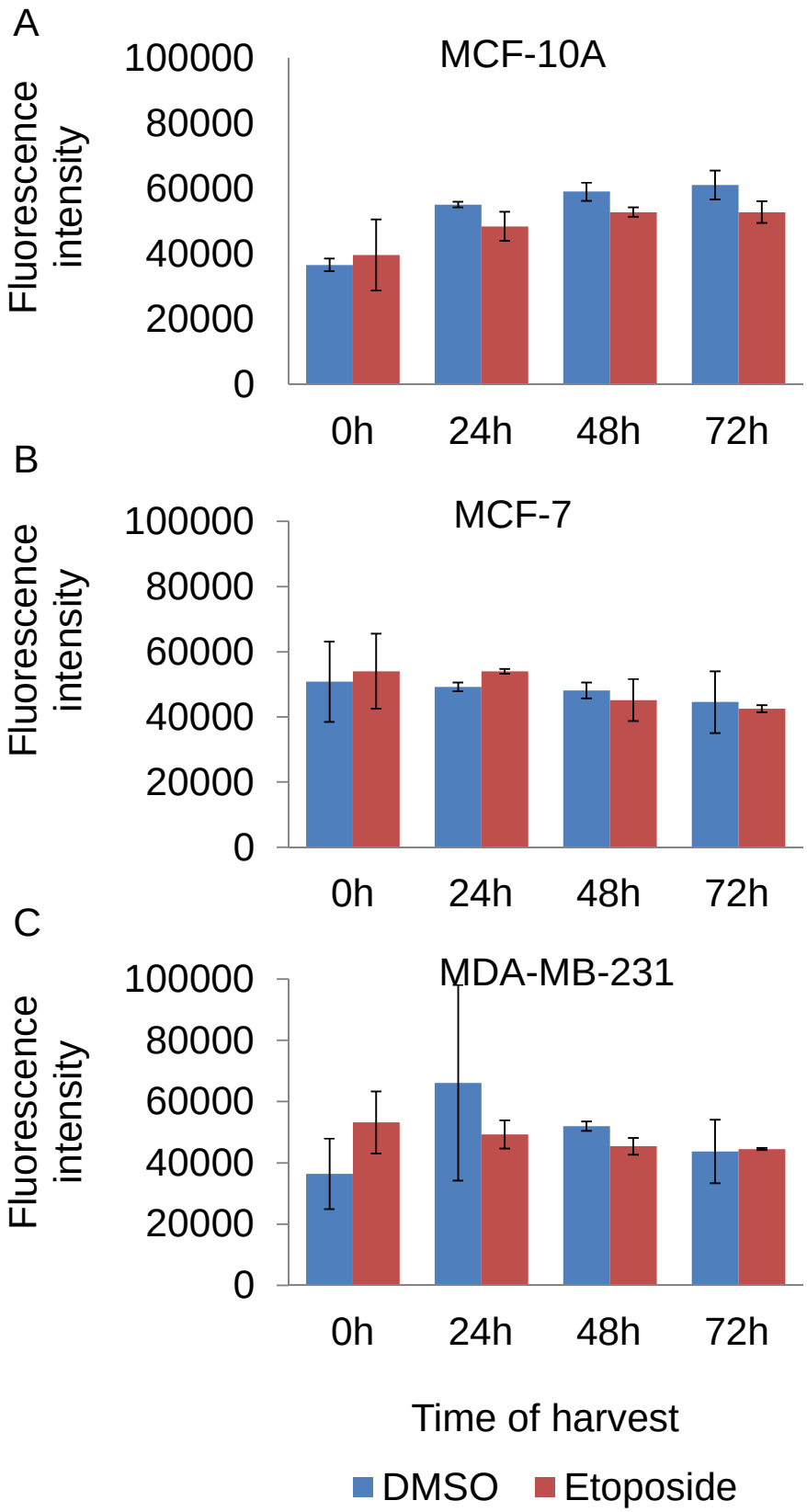

Figure 5.12 MCF-10A, MCF-7, and MDA-MB-231 cells were treated with trypsin. Cell suspensions were placed at 96-well plate at density of $2X10^5$ cells/ well with 10µL AlamarBlue incubated for 5 hours and then measured fluorescent intensity by using fluorometer with an excitation wavelength of 560nm and an emission wavelength of 590nm. Error bars represent standard deviation.

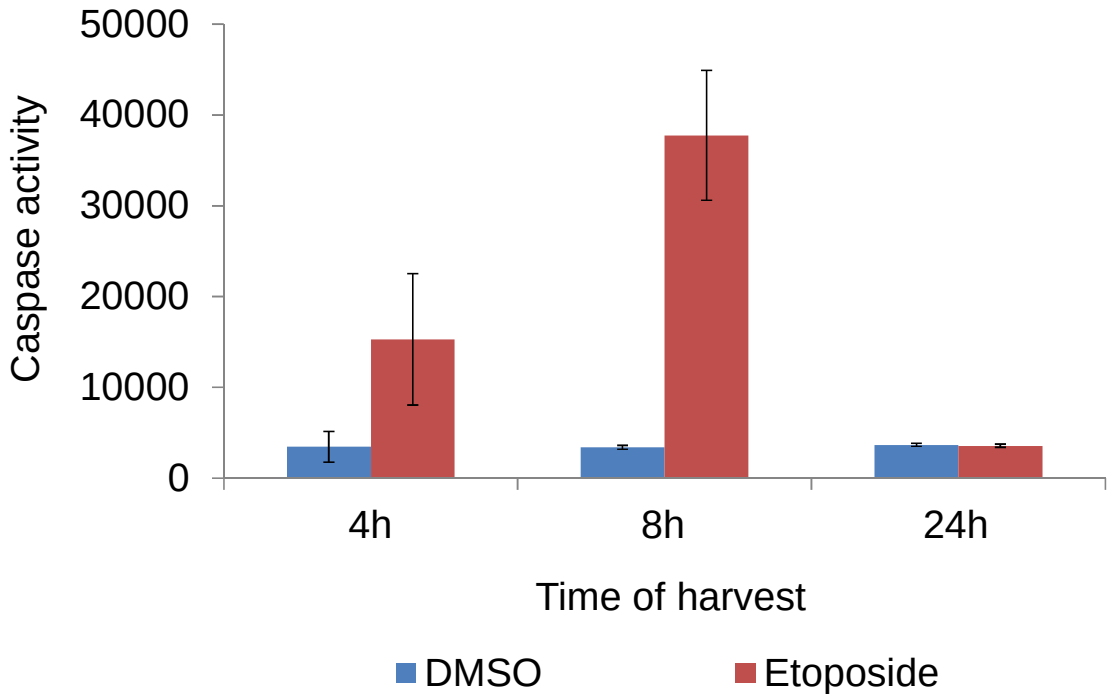

Figure 5.13 Lysates were prepared from Jurkat 6 cells which were either treated or untreated with Etoposide at each time point. Cell lysates were incubated with the Ac-DEVD-AMC Caspase-3 Fluorogenic Substrate in a 96-well plate for 120 minutes. The caspase activity was measured by fluorometer. Error bars represent standard deviation.

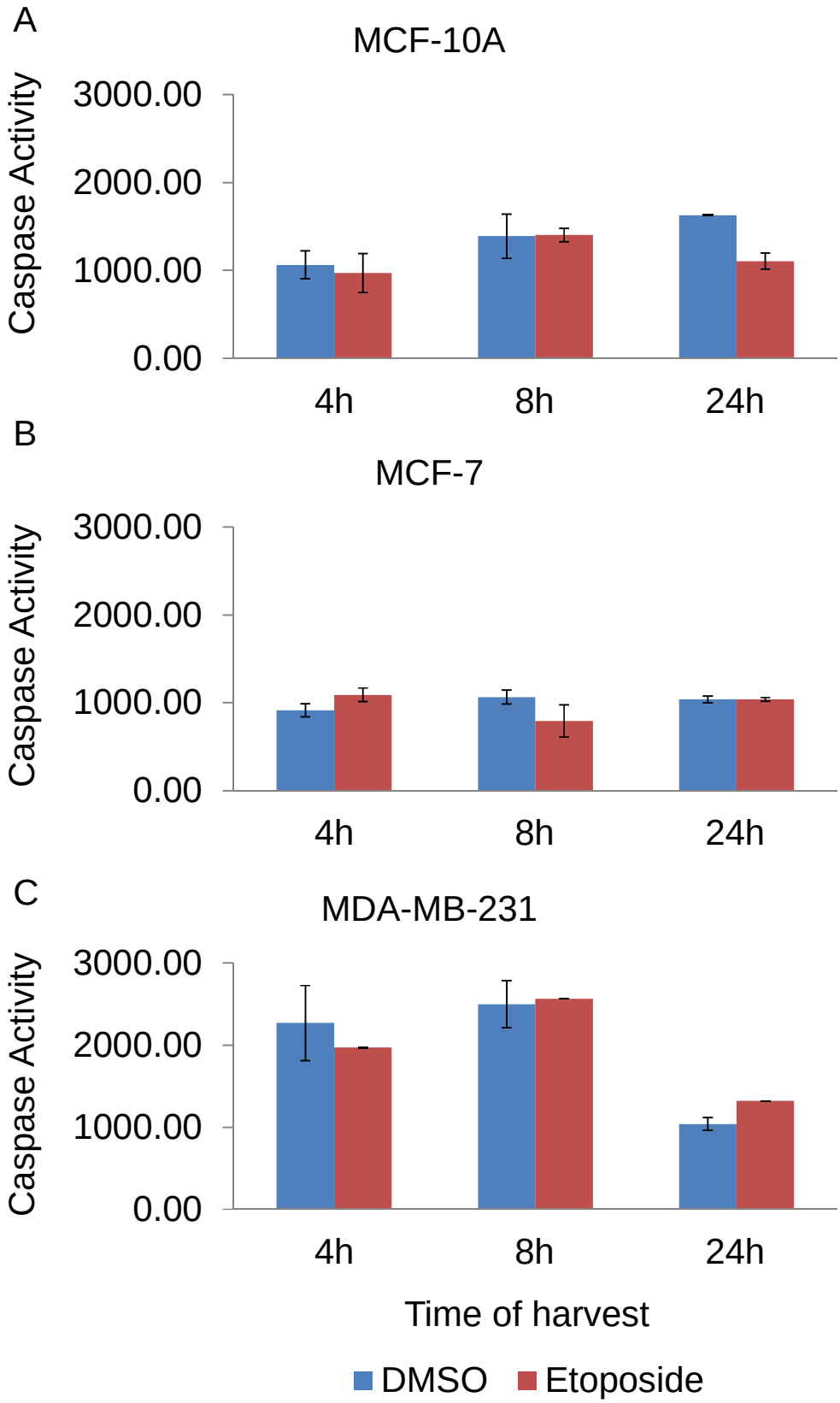

Figure 5.14 Lysates were prepared from MCF-10A, MCF-7 and MDA-MB-231 cells which were either treated or untreated with Etoposide at each time point. Cell lysates were incubated with the Ac-DEVD-AMC Caspase-3 Fluorogenic Substrate in a 96-well plate for 120 minutes. The caspase activity was measured by fluorometer with an excitation wavelength of 380nm and an emission wavelength of 440nm. Error bars represent standard deviation.

5.4 Using Caspase Assay to indicate apoptosis

Caspase proteins are very important in apoptosis. One major effector of apoptosis is caspase-3. It is a cysteine protease which exists in cells as an inactive precursor and can be activated by proteolytic processing. The activated caspases can cleave downstream caspase proteins, pass and amplify the death signals, and result in apoptosis (Cohen, 1997).

MCF-10A, MCF-7, and MDA-MB-231 cells after trypsinization and Jurkat 6 cells were lysed. The Ac-DEVD-AMC Caspase-3 assays were carried out in 96-well plate by mixing with lysed cells and then after incubated for 120 minutes. The caspase activity was measured by the fluorometer. With the increasing time, caspase 3 became active. Apoptosis was measured after 2 hours incubation. At 8 hours, Jurkat 6 cells apoptosis reached a peak as shown in Figure 5.13. But in breast cell lines, caspase activities of Etoposide group were the same as the control group with 24 hours treatment. No caspase activation was observed in breast cell lines (Figure 5.14).

Table 5.1The effect of treatment of Etoposide on 5 cell lines:

	DG75	Jurkat 6	MCF-10A	MCF-7	MDA-MB-231
FACS	Y	Y	Y	N	Y
AlamarBlue	N/A	Y	N	N	N
Caspase 3	N/A	Y	N	N	N

N/A: Not applicable.

Etoposide is clearly causing apoptosis in Jurkat 6 cells (Table 5.1). For the breast cells the data not so clear. Cell cycle changes have been observed but no reduction in cell viability and no increase in caspase activity. Therefore, analysis of apoptosis will be performed in Jurkat 6 cells.

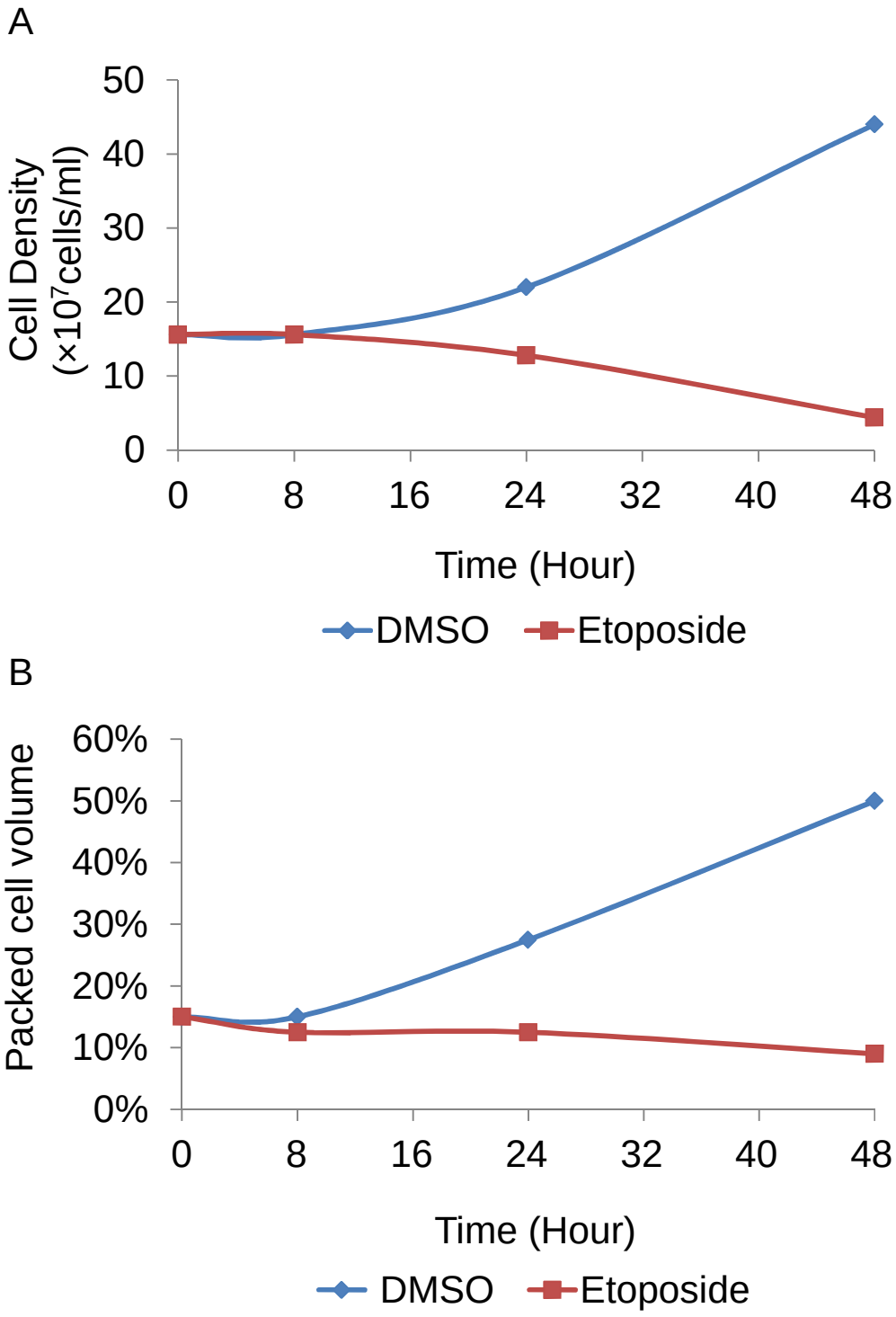

Figure 5.15 A shows that Jurkat 6 cells were either treated or untreated with Etoposide in time course up to 48 hours at 37°C. The cell density was determined by Trypan Blue Assay at indicated time point. B is the corresponding packed cell volume. 10µl of cell suspensions were loaded into a PCV tube and then centrifuged at 5000rpm for 1 minute. The packed cell volume in µl can be read from the PCV tubes.

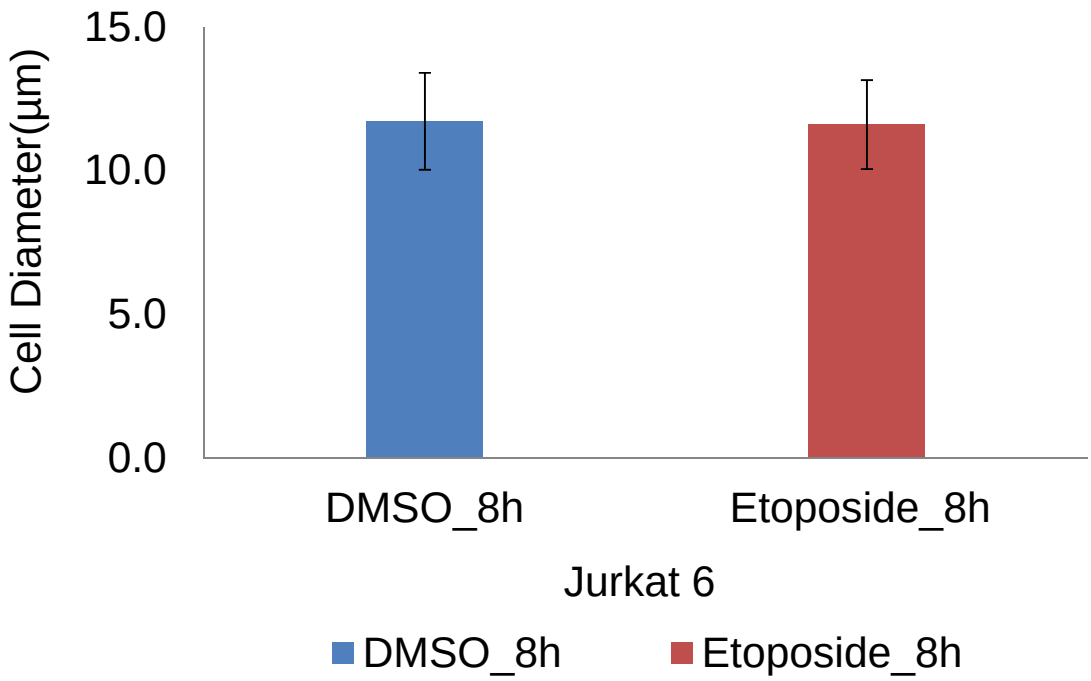

Figure 5.16 shows the average diameters of Jurkat 6 cells normal growing or undergoing apoptosis. Jurkat 6 cells were either treated or untreated with Etoposide for 8 hours at 37°C. The diameters of 25 cells of control or treatment were measured, respectively. Error bars represent standard deviation.

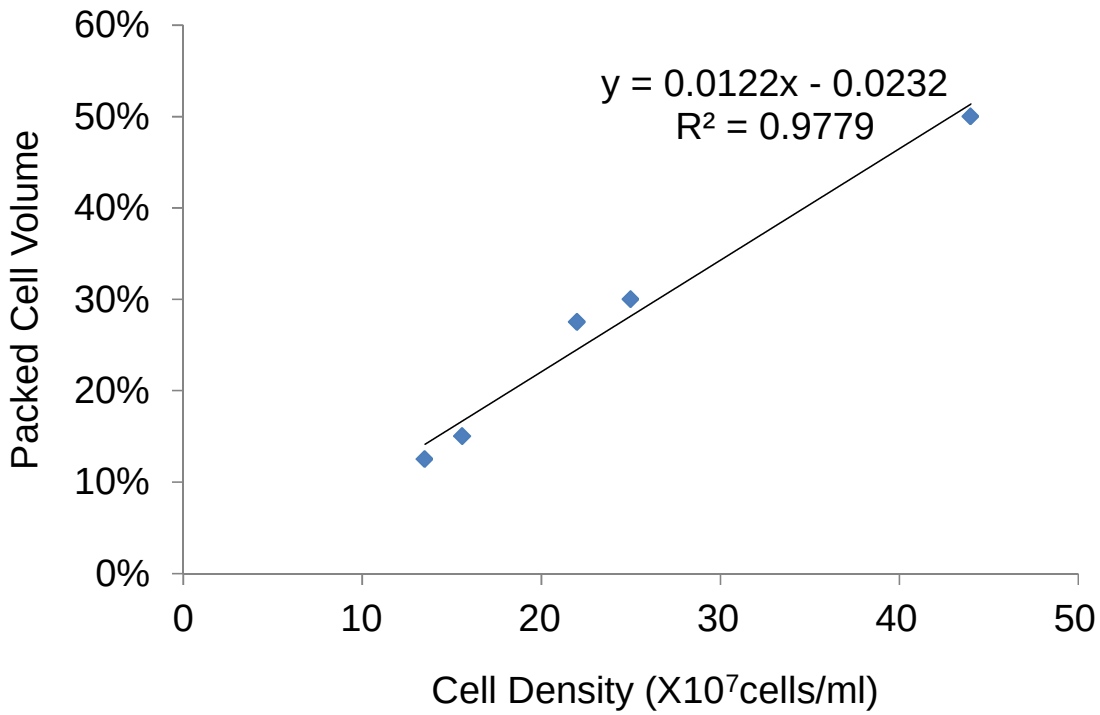

Figure 5.17 the standard curve of Jurkat 6 packed cell volume with corresponding cell density. The number of Jurkat 6 cells was determined by Trypan Blue Assay. 10µl of cell suspensions in culture media were loaded into a PCV tube and then centrifuged at 5000rpm for 1 minute. The packed cell volume in µl can be read from the PCV tubes. The X axis is cell density; the Y axis is packed cell volume.

5.5 Cell density and diameter

As discussed in Chapter Four, cell survival and packed cell volume are very important two factors in impedance measurement. But in apoptosis, cells shrink and die in the end. It is ideal to find a time point in which cells undergo apoptosis and cell size does not change a lot. As the caspase assay showed, with 8 hours the treatment with Etoposide, Jurkat 6 cells were undergoing apoptosis. Whether the cells are alive and whether cell size changes at 8 hours need to be determined.

Jurkat 6 cells treatment with Etoposide in a time course and the viable cells were determined with the Trypan blue assay. Figure 5.15A indicate that the density of Etoposide treated cells started to decrease from 8 hour. At 48 hours, Jurkat 6 cells with Etoposide treatment did not survive. In the meantime, cell volume was also measured by using PCV tubes. After 8 hours treatment, the PCV of DMSO treated was kept on increasing due to cell proliferation, but the PCV of Etoposide treated decreased as Figure 5.15B shown.

In order to know the cell diameters, 25 cells of each treatment were measured under microscope by using IC Imaging Control 3.0 software. Figure 5.16 shows that at 8 hours treatment, cell diameters were the same and not affected by the treatment. A series of packed cell volume at different density had been determined to draw a standard curve in which 20% PCV corresponding cell density can be read (Figure 5.17).

5.6 Bio-impedance of Jurkat 6 cells undergoing apoptosis

As described before, Jurkat 6 cells can survive in both modified buffer which is 50% DPBS and 50% sterile with serum replacement and isotonic media. It is still a question whether Jurkat 6 cells are able to survive after 8 hours treatment with DMSO or Etoposide in that media. Figure 5.18 represent that over 60 minutes, Jurkat 6 cells with both treatments can survive in modified buffer as well as isotonic media.

To prepare the impedance measurement, some samples of Jurkat 6 cell with both treatments had been saved to verify if cells undergo apoptosis or not.

As Figure 5.19 shown, the cells used to measure impedance were in undergoing apoptosis.

Jurkat 6 cells with DMSO or Etoposide treatment were washed with DPBS and removed. Cells were re-suspended with 50% DPBS and 50% sterile water with 2% serum replacement or isotonic media. Before and after measurement, viability, density testing and volume fraction were measured. Each time, 180µL of cells suspension were loaded into a chamber.

The cell density before and after each impedance measurement were also determined. Figure 5.20 shows that the cell density varies, because cells were difficult to be removed completely from the cylindrical chamber after impedance measurement.

In Figure 5.21, A shows cells were measured in modified buffer, the Jurkat 6 cells undergoing apoptosis had higher impedance than normal growing cells at all frequency and the dispersion appears from 0.5MHz to 1.5MHz. B shows the same trends as A. But in isotonic media, the impedance difference between cells undergoing apoptosis and normal was smaller.

Over low frequencies of Figure 5.21A and B, 1 kHz~30 kHz 10 values of each cell lines are used to calculate significance of the data. Both of the P Values are less than 0.05, which shows the significant (Table 5.2 and Table 5.4). Membrane capacitance of each cell line also was calculated as Table 5.3 and Table 5.5 shown (The equations were provided by Dr Guofeng Qiao). The control group, DMSO, has higher membrane capacitance than the Etoposide treated Jurkat 6 cells.

Table 5.2 Student Ttest of 10 impedance values at low frequency (in modified buffer at 20°C)

Test	P Value
DMSO against Etoposide	9.9E-14

Table 5.3 Membrane capacitance of Jurkat 6 cells from the equivalent circuit model (in modified buffer at 20°C)

	Cm (μF/ cm^2)	SD
DMSO	0.6	0.4
Etoposide	0.2	0.1

*The results were calculated from a series of equations which were provided by Dr Guofeng Qiao (Qiao, 2011).

Table 5.4 Student Ttest of 10 impedance values at low frequency (in isotonic media at 37°C)

Test	P Value
DMSO against Etoposide	8.5E-12

Table 5.5 Membrane capacitance of Jurkat 6 cells from the equivalent circuit model (in isotonic media at 37°C)

	Cm (μF/ cm^2)	SD
DMSO	0.8	0.1
Etoposide	0.6	0.02

*The results were calculated from a series of equations which were provided by Dr Guofeng Qiao (Qiao, 2011).

5.7 Transmission electron micrographs of Jurkat 6 cells

Transmission electron micrographs were taken to investigate what caused the impedance difference in undergoing apoptotic cells. After 8 hours, chromosome condensation, cytoplasm bubbling and irregular cell shape occurred in Etoposide treated Jurkat 6 cells in comparison with DMSO treatment (Figure 5.22). Thanks Dr Julian Thorpe for the TEM section and TEM photographing.

The nuclear circularity of TEM photos of cells were analysed using the Image J software. The nuclear circularity and cell circularity of Jurkat 6 with DMSO or Etoposide treatment for 8 hours had significant difference, respectively (Figure 5.23).

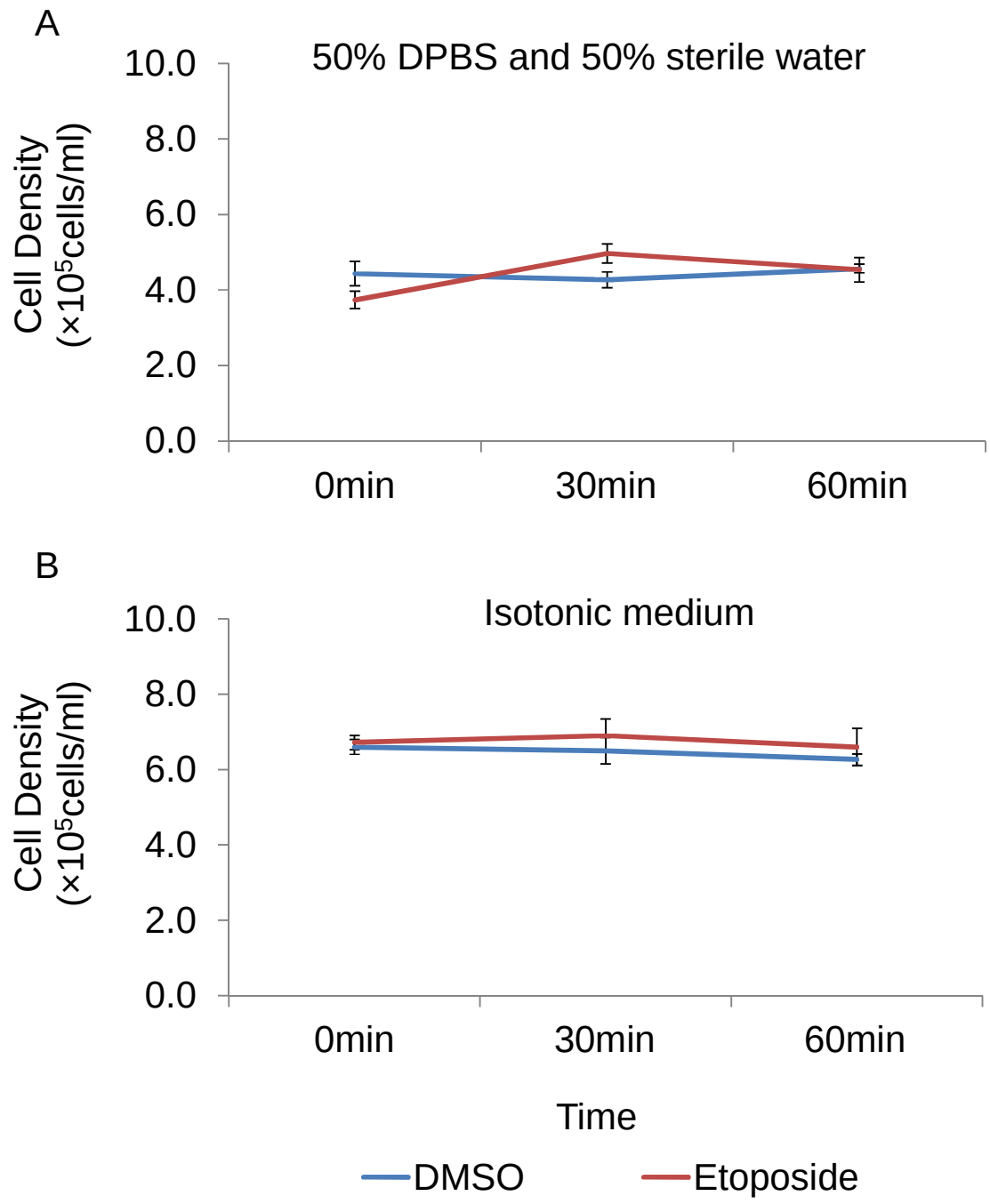

Figure 5.18 Jurkat 6 viability test. Lymphoma cells Jurkat 6 were either treated or untreated with Etoposide for 8 hours at 37°C and incubated in 50% DPBS and 50% sterile water with 2% Serum Replacement at 20°C (A) or 8mS isotonic media at 37°C (B) for 0~60 minutes. The number of viable cells was determined by Trypan Blue Assay in triplicate. Error bars represent standard deviation.

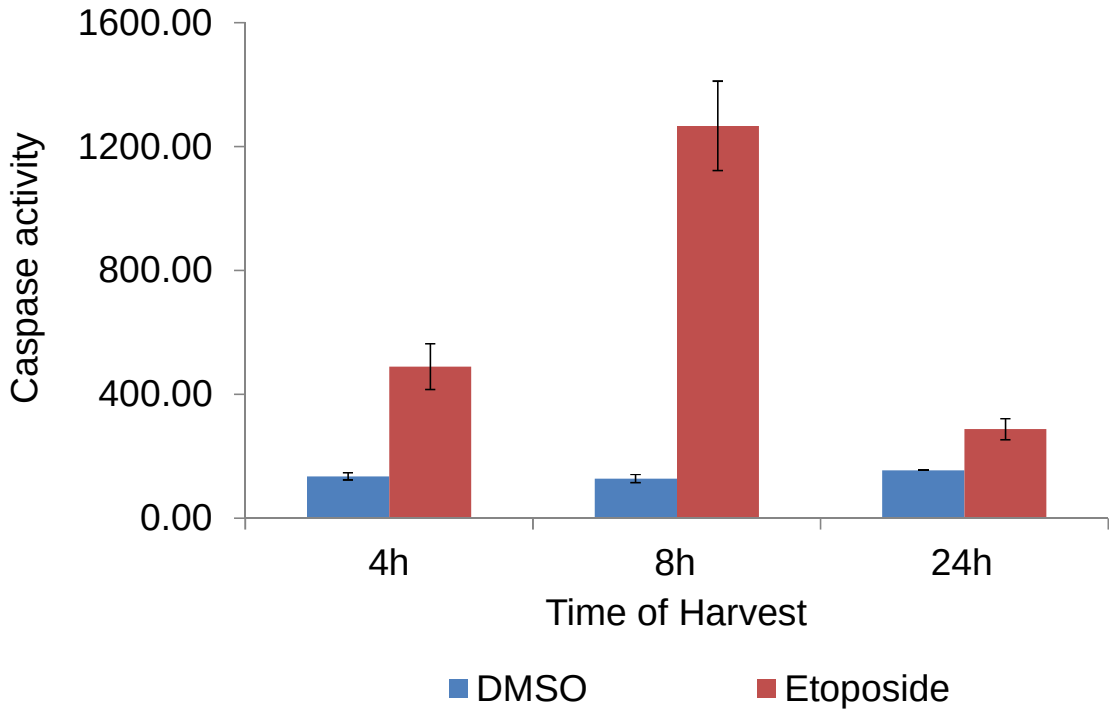

Figure 5.19 Lysates were prepared from Jurkat 6 cells which were either treated or untreated with Etoposide at each time point. Cell lysates were incubated with the Ac-DEVD-AMC Caspase-3 Fluorogenic Substrate in a 96-well plate for 120 minutes. The caspase activity was measured by fluorometer with an excitation wavelength of 380nm and an emission wavelength of 440nm. Error bars represent standard deviation.

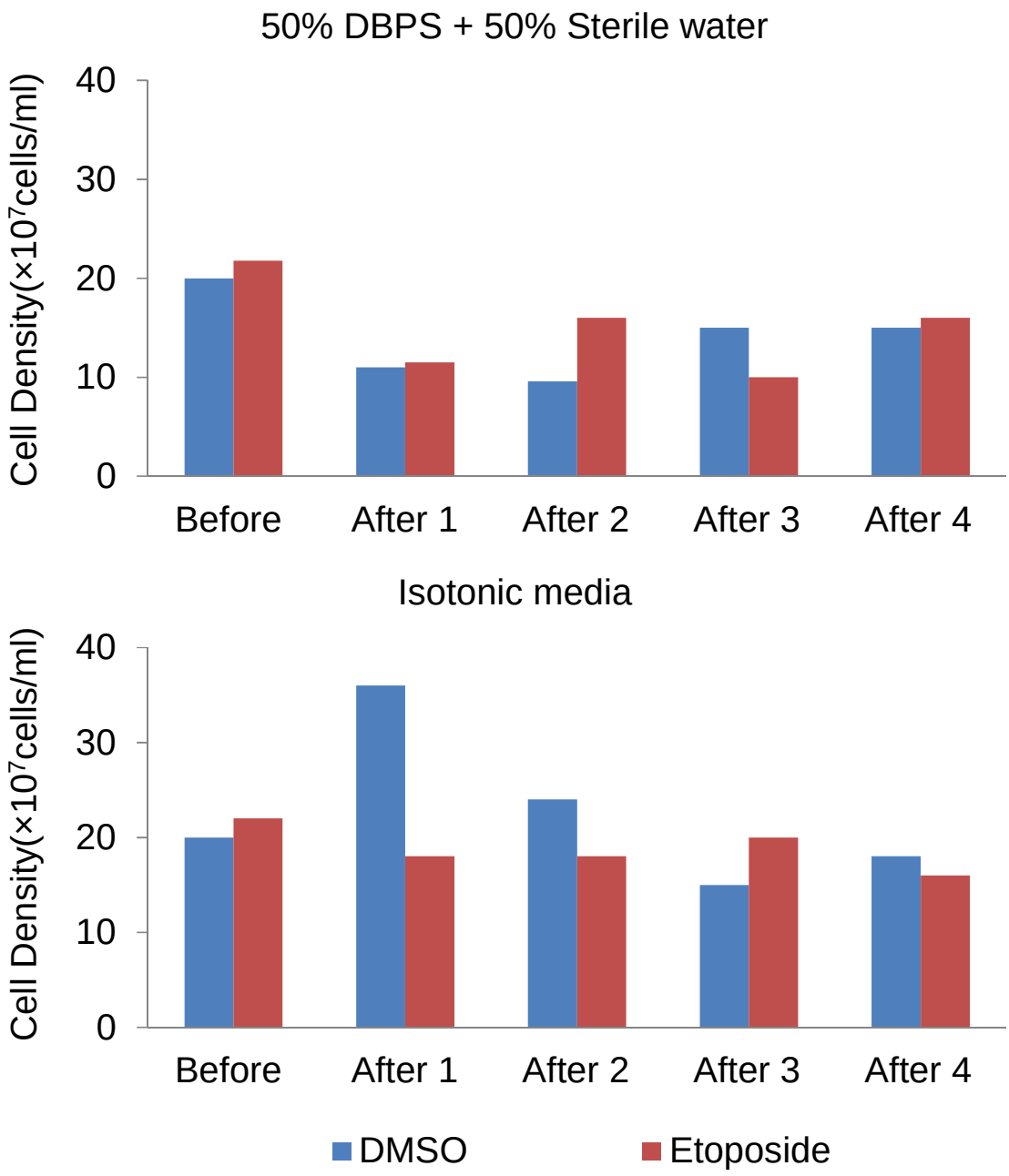

Figure 5.20 Cells viability test before or after impedance measurement. Cells were incubated in 50%DPBS+50% sterile water, or the isotonic media. Cell densities were measured after each impedance measurement

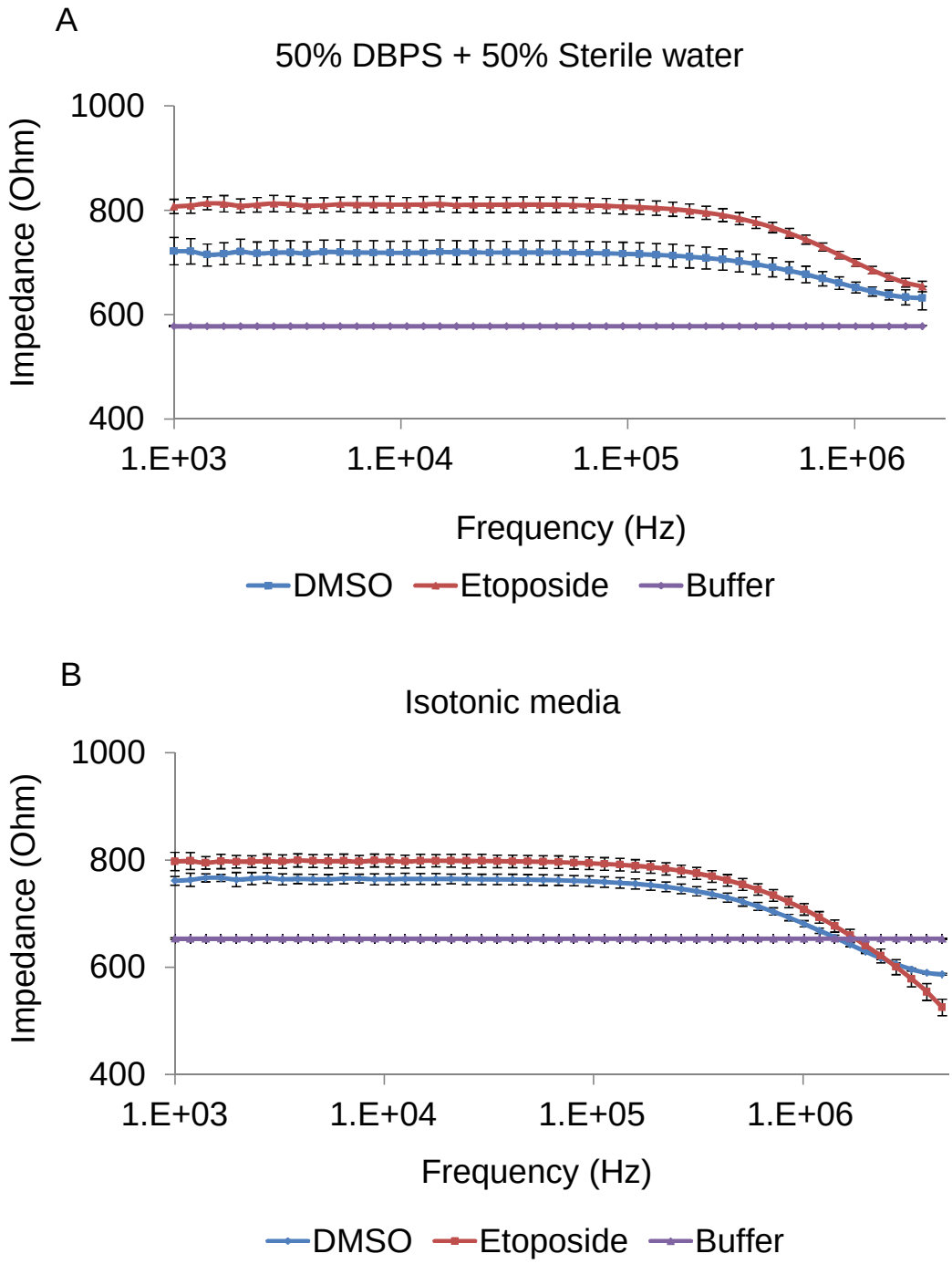

Figure 5.21 the impedance of Jurkat 6 cell undergoing apoptosis measured using an Impedance Analyser at same volume ratio 20%(v/v) at 20°C. Jurkat 6 cells were induced by Etoposide for 8 hours at 37°C. A The buffer is 50% sterile water and 50% DPBS with 2% serum replacement. The conductivity is 8 mS. B the buffer is isotonic media and the conductivity is around 8 mS. X axis is frequency and Y axis is impedance.

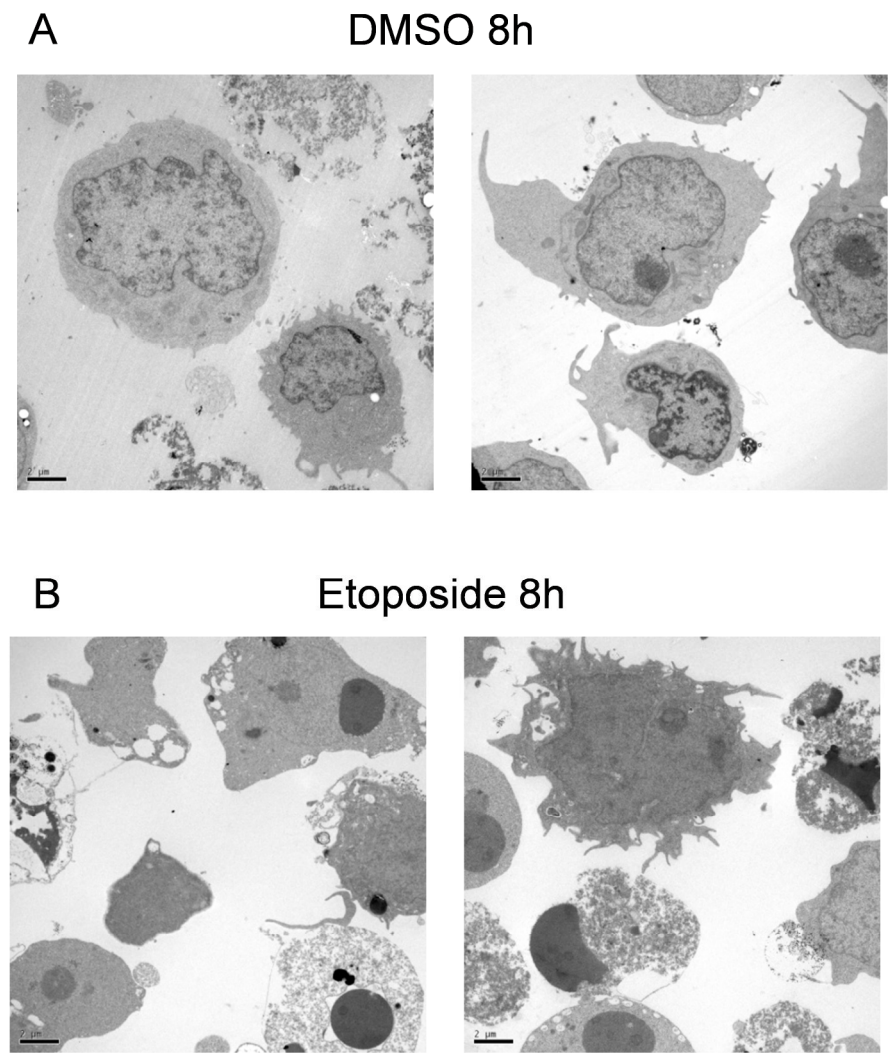

Figure 5.22 Jurkat 6 cells undergoing apoptosis. Jurkat 6 cells were either treated or untreated with Etoposide at 37°C. Transmission electron micrographs show the chromosome condensed and vacuoles in cytoplasm in undergoing apoptosis. Thanks Dr Julian Thorpe for the TEM section and TEM photographing.

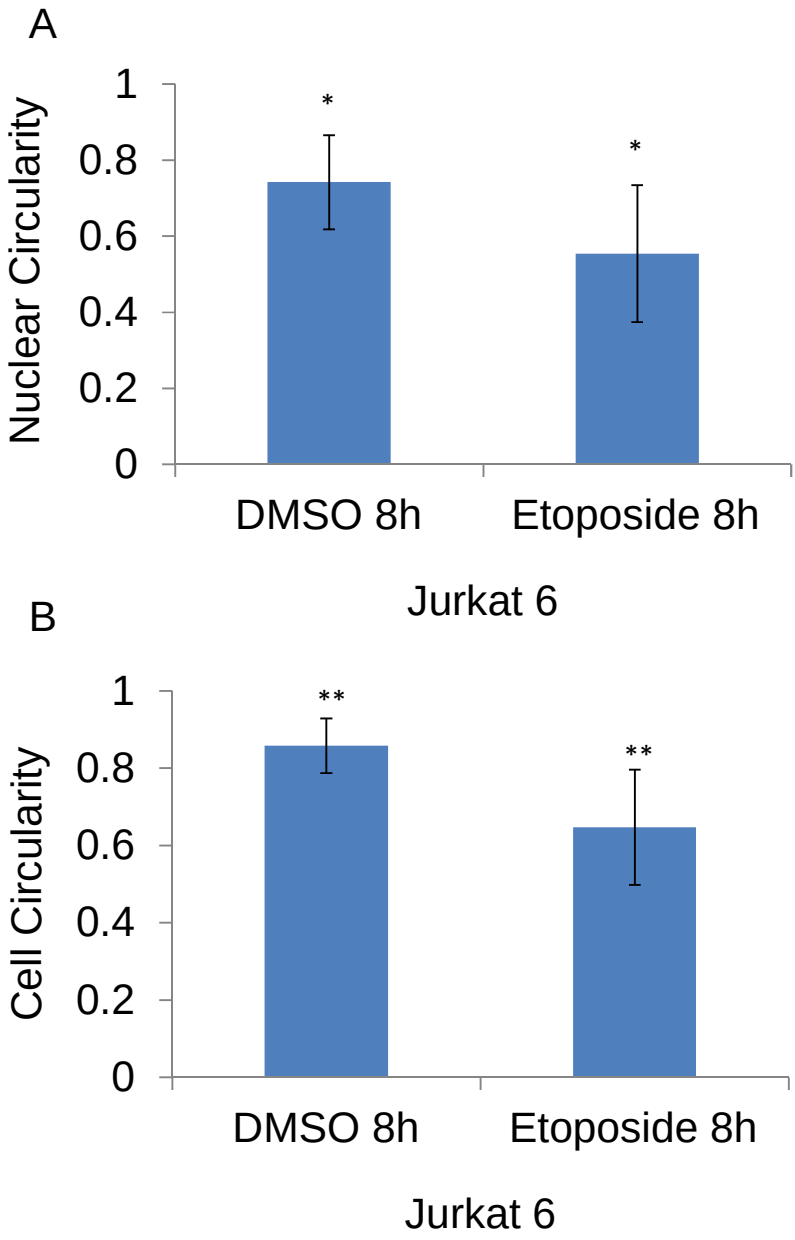

Figure 5.23 Nuclear circularity and cell circularity of Jurkat 6 cells. The TEM micrographs were analysed by using Image J. The circularity of a circle is 1. X axis is control and treated Jurkat 6 cells and Y axis is nuclear circularity or cell circularity. The student Ttest as indicated (*,**) shows p value <0.05. Error bars represent standard deviation.

6 Discussion

Bio-impedance is a non-invasive, label-free, fast, low-cost way to be applied to many fields as discussed before. In this study, with conditions controlled, Cell Impedance System (CIS) has been successfully used to distinguish the breast tissue cell line MCF-10A, the early-stage breast cancer cell line MCF-7 and the invasive breast cancer cell line MDA-MB-231, and also distinguish the lymphoma Jurkat 6 cells undergoing apoptosis and normal growing.

In order to ensure the accurate results of cell impedance, the measurement conditions were strictly controlled as discussed in Chapter Three. The cell viability, cell volume, temperature, buffer conductivity these were crucial factors which would affect the impedance measurement. In the meanwhile, the system errors were minimized by two means. The calibration solutions (Hanna Instruments, USA) with indicated conductivity were utilized to calibrate the system before impedance measurement. Also, the system errors generated by the impedance analyser can be eliminated by calculations (Qiao *et al.*, 2012).

There were two conditions we used to measure cell impedance, 50% DPBS and 50% sterile water with 2% serum replacement at 25°C, and isotonic media at 37°C. In both conditions, MCF-10A, MCF-7, MDA-MB-231, Jurkat 6 undergoing apoptosis, and Jurkat 6 cells all can survive over 120 minutes. This ensured that during the impedance measurement cells were alive. Besides, 25°C was thought to be an ideal temperature which can keep cell survival and prevent the over-heating generated by the flow of current. The research work of Rodrigo Franco *et al.* on electronic impedance analysis of Jurkat apoptosis was carried out at room temperature 20-25°C as well (Franco *et al.*, 2008). And yet the limitation is that it is not the temperature of native environment of cell growing. Another limitation is that 50% DPBS and 50% sterile water with 2% serum replacement is not isotonic media which may change the osmolality of cells, though cells survived in it. Considering these limitations, isotonic media at 37°C is a better condition to mimic cell native growing environment.

With respect to bio-impedance of cells, the work of Arum Han *et al.* on quantification of breast cancer impedance spectroscopy (Han *et al.*, 2007) shows in the same order of impedance decreased with MCF-10A, MCF-7 and MDA-MB-231. Also, the work of R. Pethig and M.S. Talary on dielectrophoretic detection of Jurkat cells in undergoing Etoposide-induced apoptosis (Pethig and Talary, 2007) shows the membrane capacitance of Jurkat undergoing apoptosis was lower than the control group which is in the same trends of our search.

In the future, another issue that can be addressed is whether cancerous cells surrounded with normal cells, will be apparent by CIS. This could be tackled by mixing cell populations or perhaps the impedance properties of the cancer cells could be modulated, for example by coating the cells with antibodies carrying electrical conductors such as gold nano-particles.

7 Bibliography

Acehan, D., Jiang, X., Morgan, D. G., Heuser, J. E., Wang, X. and Akey, C. W. (2002). "Three-dimensional structure of the apoptosome: implications for assembly, procaspase-9 binding, and activation." *Mol Cell* 9(2): 423-432.

Alberts, B. (2002). Molecular biology of the cell. New York, *Garland Science*.

Alberts, B. (2008). Molecular biology of the cell. New York, *Garland Science ; [London : Taylor & Francis, distributor]*.

Alberts, B. (2010). Essential cell biology. New York ; London, *Garland Science*.

Bauchot, A. D., Harker, F. R. and Arnold, W. M. (2000). "The use of electrical impedance spectroscopy to assess the physiological condition of kiwifruit." *Postharvest Biology and Technology* 18(1): 9-18.

Bermudez, Y., Erasso, D., Johnson, N. C., Alfonso, M. Y., Lowell, N. E. and Kruk, P. A. (2006). "Telomerase confers resistance to caspase-mediated apoptosis." *Clin Interv Aging* 1(2): 155-167.

Bouck, N., Stellmach, V. and Hsu, S. C. (1996). "How tumors become angiogenic." *Adv Cancer Res* 69: 135-174.

Bryan, T. M. and Cech, T. R. (1999). "Telomerase and the maintenance of chromosome ends." *Curr Opin Cell Biol* 11(3): 318-324.

Bryan, T. M., Englezou, A., Gupta, J., Bacchetti, S. and Reddel, R. R. (1995). "Telomere elongation in immortal human cells without detectable telomerase activity." *EMBO J* 14(17): 4240-4248.

Circu, M. L., Rodriguez, C., Maloney, R., Moyer, M. P. and Aw, T. Y. (2008). "Contribution of mitochondrial GSH transport to matrix GSH status and colonic epithelial cell apoptosis." *Free Radic Biol Med* 44(5): 768-778.

Cohen, G. M. (1997). "Caspases: the executioners of apoptosis." *Biochem J* 326 (Pt 1): 1-16.

Cole, K. S. and Cole, R. H. (1941). "Dispersion and Absorption in Dielectrics I. Alternating Current Characteristics." *The Journal of Chemical Physics* 9(4): 341-351.

Counter, C. M., Avilion, A. A., LeFeuvre, C. E., Stewart, N. G., Greider, C. W., Harley, C. B. and Bacchetti, S. (1992). "Telomere shortening associated with chromosome instability is arrested in immortal cells which express telomerase activity." *EMBO J* 11(5): 1921-1929.

Dean, D. A., Ramanathan, T., Machado, D. and Sundararajan, R. (2008). "Electrical Impedance Spectroscopy Study of Biological Tissues." *J Electrostat* 66(3-4): 165-177.

Denault, J. B. and Salvesen, G. S. (2002). "Caspases: keys in the ignition of cell death." *Chem Rev* 102(12): 4489-4500.

Earnshaw, W. C., Martins, L. M. and Kaufmann, S. H. (1999). "Mammalian caspases: structure, activation, substrates, and functions during apoptosis." *Annu Rev Biochem* 68: 383-424.

Edell, S. L. and Eisen, M. D. (1999). "Current imaging modalities for the diagnosis of breast cancer." *Del Med J* 71(9): 377-382.

Elmore, J. G., Barton, M. B., Moceri, V. M., Polk, S., Arena, P. J. and Fletcher, S. W. (1998). "Ten-year risk of false positive screening mammograms and clinical breast examinations." *N Engl J Med* 338(16): 1089-1096.

Elmore, S. (2007). "Apoptosis: a review of programmed cell death." *Toxicol Pathol* 35(4): 495-516.

Fadeel, B. and Orrenius, S. (2005). "Apoptosis: a basic biological phenomenon with wide-ranging implications in human disease." *J Intern Med* 258(6): 479-517.

Fadeel, B., Orrenius, S. and Zhivotovsky, B. (1999). "Apoptosis in human disease: a new skin for the old ceremony?" *Biochem Biophys Res Commun* 266(3): 699-717.

Fedi, P., Tronick, S. R. and Aaronson, S. A. (1997). Growth factors, *Cancer Research Campaign*: 41-64.

Fedi, P., Tronick, S.R., and Aaronson, S.A. (1997). Growth factors. In: Cancer Medicine.

Franco, R., DeHaven, W. I., Sifre, M. I., Bortner, C. D. and Cidlowski, J. A. (2008). "Glutathione depletion and disruption of intracellular ionic homeostasis regulate lymphoid cell apoptosis." *J Biol Chem* 283(52): 36071-36087.

Fricke H, M. S. (1926). "The electrical capacity of tumors of the breast." *Cancer Res* 10(340): 76.

Fulda, S. and Debatin, K. M. (2004). "Targeting apoptosis pathways in cancer therapy." *Curr Cancer Drug Targets* 4(7): 569-576.

Gascoyne, P. R., Wang, X. B., Huang, Y. and Becker, F. F. (1997). "Dielectrophoretic Separation of Cancer Cells from Blood." *IEEE Trans Ind Appl* 33(3): 670-678.

Gersing, E. (1998). "Impedance spectroscopy on living tissue for determination of the state of organs." *Bioelectrochemistry and Bioenergetics* 45(2): 145-149.

Gibson, L. J., Hery, C., Mitton, N., Gines-Bautista, A., Parkin, D. M., Ngelangel, C. and Pisani, P. (2010). "Risk factors for breast cancer among Filipino women in Manila." *International Journal of Cancer* 126(2): 515-521.

Grimnes, S. and Martinsen, Ø. G. (2008). Bioimpedance and bioelectricity basics. London, *Academic*.

Grimnes, S. and Martinsen, Ø. G. (2008). Bioimpedance and bioelectricity basics. London, *Academic*.

Halter, R. J., Hartov, A., Heaney, J. A., Paulsen, K. D. and Schned, A. R. (2007). "Electrical impedance spectroscopy of the human prostate." *IEEE Trans Biomed Eng* 54(7): 1321-1327.

Halter, R. J., Hartov, A., Heaney, J. A., Paulsen, K. D. and Schned, A. R. (2007). "Electrical impedance spectroscopy of the human prostate." *Ieee Transactions on Biomedical Engineering* 54(7): 1321-1327.

Han, A., Yang, L. and Frazier, A. B. (2007). "Quantification of the heterogeneity in breast cancer cell lines using whole-cell impedance spectroscopy." *Clin Cancer Res* 13(1): 139-143.

Hanahan, D. and Folkman, J. (1996). "Patterns and emerging mechanisms of the angiogenic switch during tumorigenesis." *Cell* 86(3): 353-364.

Hanahan, D. and Weinberg, R. A. (2000). "The hallmarks of cancer." *Cell* 100(1): 57-70.

Hannun, Y. A. (1997). "Apoptosis and the dilemma of cancer chemotherapy." *Blood* 89(6): 1845-1853.

Harrington, K. J. (2008). "Biology of cancer " *Cancer Biology and Imaging* 36(1): 1-4.

Hayflick, L. (1997). "Mortality and immortality at the cellular level. A review." *Biochemistry (Mosc)* 62(11): 1180-1190.

Hoffman, W. H., Biade, S., Zilfou, J. T., Chen, J. and Murphy, M. (2002). "Transcriptional repression of the anti-apoptotic survivin gene by wild type p53." *J Biol Chem* 277(5): 3247-3257.

Holland, J. F. and Frei, E. (2000). Cancer medicine-5 review : a companion to Holland-Frei Cancer Medicine-5. Hamilton, Ont. ; London, *B.C. Decker*.

Hoogstraten, B. and McDivitt, R. W. (1981). Breast cancer. Boca Raton, Fla., *CRC Press*.

Ishizaki, Y., Cheng, L., Mudge, A. W. and Raff, M. C. (1995). "Programmed cell death by default in embryonic cells, fibroblasts, and cancer cells." *Mol Biol Cell* 6(11): 1443-1458.

Jossinet, J., Lobel, A., Michoudet, C. and Schmitt, M. (1985). "Quantitative technique for bio-electrical spectroscopy." *J Biomed Eng* 7(4): 289-294.

Kastan, M. B. and Bartek, J. (2004). "Cell-cycle checkpoints and cancer." *Nature* 432(7015): 316-323.

Kaufmann, S. H. (1989). "Induction of endonucleolytic DNA cleavage in human acute myelogenous leukemia cells by etoposide, camptothecin, and other cytotoxic anticancer drugs: a cautionary note." *Cancer research* 49(21): 5870-5878.

Kellner, U., Sehested, M., Jensen, P. B., Gieseler, F. and Rudolph, P. (2002). "Culprit and victim -- DNA topoisomerase II." *The lancet oncology* 3(4): 235-243.

Kerner, T. E., Paulsen, K. D., Hartov, A., Soho, S. K. and Poplack, S. P. (2002). "Electrical impedance spectroscopy of the breast: Clinical imaging results in 26 subjects." *Ieee Transactions on Medical Imaging* 21(6): 638-645.

Kerr, J. F., Wyllie, A. H. and Currie, A. R. (1972). "Apoptosis: a basic biological phenomenon with wide-ranging implications in tissue kinetics." *Br J Cancer* 26(4): 239-257.

King, R. J. B. (2000). Cancer biology. Harlow, *Pearson Education*.

Kylarova, D., Prochazkova, J., Mad'arova, J., Bartos, J. and Lichnovsky, V. (2002). "Comparison of the TUNEL, lamin B and annexin V methods for the detection of apoptosis by flow cytometry." *Acta Histochem* 104(4): 367-370.

Labeed, F. H., Coley, H. M. and Hughes, M. P. (2006). "Differences in the biophysical properties of membrane and cytoplasm of apoptotic cells revealed using dielectrophoresis." *Biochim Biophys Acta* 1760(6): 922-929.

Leist, M. and Jaattela, M. (2001). "Four deaths and a funeral: from caspases to alternative mechanisms." *Nat Rev Mol Cell Biol* 2(8): 589-598.

LifeTechnologies. (2012). "alamarBlue®—Rapid & Accurate Cell Health Indicator." Retrieved 21 November 2012, *from http://www.invitrogen.com/site/us/en/home/brands/Molecular-Probes/Key-Molecular-Probes-Products/alamarBlue-Rapid-and-Accurate-Cell-Health-Indicator.html*.

LifeTechnologies. (2012, http://www.invitrogen.com/1/1/1569-propidium-iodide.html). "Propidium Iodide (Molecular Probes®)." Retrieved 21 November, 2012.

Lutz, W. K. and Fekete, T. (1996). "Endogenous and exogenous factors in carcinogenesis: limits to cancer prevention." *Int Arch Occup Environ Health* 68(2): 120-125.

McRae, D. A., Esrick, M. A. and Mueller, S. C. (1999). "Changes in the noninvasive, in vivo electrical impedance of three xenografts during the necrotic cell-response sequence." *International Journal of Radiation Oncology Biology Physics* 43(4): 849-857.

Medema, R. H. and Bos, J. L. (1993). "The role of p21ras in receptor tyrosine kinase signaling." *Crit Rev Oncog* 4(6): 615-661.

Mihara, M., Erster, S., Zaika, A., Petrenko, O., Chittenden, T., Pancoska, P. and Moll, U. M. (2003). "p53 has a direct apoptogenic role at the mitochondria." *Mol Cell* 11(3): 577-590.

Millipore. (2005, April 2005). "TRAPeze Telomerase Detection Kit - Data Sheet." Retrieved 28/06/2012, 2012, *from http://www.millipore.com/publications.nsf/a73664f9f981af8c852569b9005b4eee/bd15690a97aebd448525730600750599/$FILE/S7700.pdf*.

Millipore. (2012). "Caspase 3/7 Assay Kit (Ac-DEVD-AMC Substrate)." Retrieved 21 November, 2012, *from http://www.millipore.com/catalogue/item/17-367*.

NHS. (2011, 29/11/2011). "MRI scan " Retrieved 17 Dec, 2012, *from http://www.nhs.uk/conditions/MRI-scan/Pages/Introduction.aspx*.

Otsuki, Y., Li, Z. and Shibata, M. A. (2003). "Apoptotic detection methods--from morphology to gene." *Prog Histochem Cytochem* 38(3): 275-339.

Pethig, R. (1987). "Dielectric properties of body tissues." *Clin Phys Physiol Meas* 8 Suppl A: 5-12.

Pethig, R. and Talary, M. S. (2007). "Dielectrophoretic detection of membrane morphology changes in Jurkat T-cells undergoing etoposide-induced apoptosis." *IET Nanobiotechnol* 1(1): 2-9.

Qiao, G. (2011). "Bioimpedence analysis techniques for malignant tissue identification [electronic resource]." *from http://sro.sussex.ac.uk/7439/*.

Qiao, G., Wang, W., Duan, W., Zheng, F., Sinclair, A. J. and Chatwin, C. R. (2012). "Bioimpedance analysis for the characterization of breast cancer cells in suspension." *IEEE Trans Biomed Eng* 59(8): 2321-2329.

Reed, J. C. (2002). "Apoptosis-based therapies." *Nat Rev Drug Discov* 1(2): 111-121.

Rowinsky, E. K., Windle, J. J. and Von Hoff, D. D. (1999). "Ras protein farnesyltransferase: A strategic target for anticancer therapeutic development." *J Clin Oncol* 17(11): 3631-3652.

Saraste, A. and Pulkki, K. (2000). "Morphologic and biochemical hallmarks of apoptosis." *Cardiovasc Res* 45(3): 528-537.

Sariego, J., Zrada, S., Byrd, M. and Matsumoto, T. (1995). "Breast cancer in young patients." *Am J Surg* 170(3): 243-245.

Scarlett, J. L., Sheard, P. W., Hughes, G., Ledgerwood, E. C., Ku, H. H. and Murphy, M. P. (2000). "Changes in mitochondrial membrane potential during staurosporine-induced apoptosis in Jurkat cells." *FEBS Lett* 475(3): 267-272.

Scholz, B., Anderson, R. (2000). "On electrical impedance scanning—principles and simulations." *Electromedica* 68: 35–44.

Schwan, H. P. (1957). "Electrical properties of tissue and cell suspensions." *Adv Biol Med Phys* 5: 147-209.

Schwan, H. P. (1993). "Mechanisms responsible for electrical properties of tissues and cell suspensions." *Med Prog Technol* 19(4): 163-165.

Siegel, R., Naishadham, D. and Jemal, A. (2012). "Cancer statistics, 2012." *CA Cancer J Clin* 62(1): 10-29.

Sigma-Aldrich. (2010). "Serum Replacement 3 (50×)." Retrieved 04 October, 2010, *from http://www.sigmaaldrich.com/catalog/ProductDetail.do?lang=en&N4=S2640|SIGMA&N5=SEARCH_CONCAT_PNO|BRAND_KEY&F=SPEC*.

Simonetti, G., Cossu, E., Montanaro, M., Caschili, C. and Giuliani, V. (1998). "What's new in mammography." *Eur J Radiol* 27 Suppl 2: S234-241.

Slamon, D. J., Clark, G. M., Wong, S. G., Levin, W. J., Ullrich, A. and McGuire, W. L. (1987). "Human breast cancer: correlation of relapse and survival with amplification of the HER-2/neu oncogene." *Science* 235(4785): 177-182.

Soley, A., Lecina, M., Gamez, X., Cairo, J. J., Riu, P., Rosell, X., Bragos, R. and Godia, F. (2005). "On-line monitoring of yeast cell growth by impedance spectroscopy." *Journal of Biotechnology* 118(4): 398-405.

Sporn, M. B. (1996). "The war on cancer." *Lancet* 347(9012): 1377-1381.

Spreekens, K. J. A. and Stekelenburg, F. K. (1986). "Rapid estimation of the bacteriological quality of fresh fish by impedance measurements." *Applied Microbiology and Biotechnology* 24(1): 95-96.

Tacconi, P., Manca, D., Tamburini, G., Ferrigno, P., Cossu, G., Cannas, A. and Giagheddu, M. (2004). "Electroneurography index based on nerve conduction study data: method and findings in control subjects." *Muscle Nerve* 29(1): 89-96.

Terauchi, S., Yamamoto, T., Yamashita, K., Kataoka, M., Terada, H. and Shinohara, Y. (2005). "Molecular basis of morphological changes in mitochondrial membrane accompanying induction of permeability transition, as revealed by immuno-electron microscopy." *Mitochondrion* 5(4): 248-254.

Thornberry, N. A. and Lazebnik, Y. (1998). "Caspases: enemies within." *Science* 281(5381): 1312-1316.

Varshney, M. and Li, Y. (2008). "Double interdigitated array microelectrode-based impedance biosensor for detection of viable Escherichia coli O157:H7 in growth medium." *Talanta* 74(4): 518-525.

Vogel, V. G. (2000). "Breast cancer prevention: a review of current evidence." *CA Cancer J Clin* 50(3): 156-170.

Vousden, K. H. and Lu, X. (2002). "Live or let die: the cell's response to p53." *Nat Rev Cancer* 2(8): 594-604.

Wang, C. and Youle, R. J. (2009). "The role of mitochondria in apoptosis*." *Annu Rev Genet* 43: 95-118.

Watanabe, M., Hitomi, M., van der Wee, K., Rothenberg, F., Fisher, S. A., Zucker, R., Svoboda, K. K., Goldsmith, E. C., Heiskanen, K. M. and Nieminen, A. L. (2002). "The pros and cons of apoptosis assays for use in the study of cells, tissues, and organs." *Microsc Microanal* 8(5): 375-391.

Weil, M., Jacobson, M. D., Coles, H. S., Davies, T. J., Gardner, R. L., Raff, K. D. and Raff, M. C. (1996). "Constitutive expression of the machinery for programmed cell death." *J Cell Biol* 133(5): 1053-1059.

Weinberg, R. A. (1998). One renegade cell : the quest for the origins of cancer. London, *Phoenix, 1999*.

Wu, Y., Mehew, J. W., Heckman, C. A., Arcinas, M. and Boxer, L. M. (2001). "Negative regulation of bcl-2 expression by p53 in hematopoietic cells." *Oncogene* 20(2): 240-251.

Wyllie, A. H., Kerr, J. F. and Currie, A. R. (1980). "Cell death: the significance of apoptosis." *Int Rev Cytol* 68: 251-306.

Yarden, Y. and Ullrich, A. (1988). "Molecular analysis of signal transduction by growth factors." *Biochemistry* 27(9): 3113-3119.

Zou, Y. and Guo, Z. (2003). "A review of electrical impedance techniques for breast cancer detection." *Med Eng Phys* 25(2): 79-90.